A STATISTICAL STUDY OF THE SOLAR AND SEASONAL CONTROL OF E-LAYER CRITICAL FREQUENCY

by

Stamatios S. Kouris

EX BIBL UNIV. EDINBURGEN

Thesis presented for the Degree of Doctor of Philosophy of the University of Edinburgh in the Faculty of Science.

December, 1971.

ABSTRACT

The statistical investigation of the variation of f_oE with solar activity, solar zenith angle and season is treated in detail. The best mathematical models of the relationships between f_oE and each of the three solar indices, the Zurich relative sunspot number, R, the observed solar radio noise flux at 10.7 cm, $\Phi_{obs.}$, and the ionospheric index of solar activity, IF2, are first determined, and three numerical relationships are then derived:

$$(f_oE)^4 = a_R\,(1 + 0.0091\ R)$$

$$(f_oE)^4 = a_\Phi\,(1 + 0.0094\ \Phi)$$

$$f_oE \quad = a_I\,(1 + 0.00144\ IF2)$$

where f_oE is measured in MHz, and Φ, the relative solar flux, is $(\Phi_{obs.} - 66)$. The correlation coefficients of the variates in these expressions proved to be not significantly different from one another.

In the analysis of the diurnal variation of $(f_oE)^4$ the world-average value of the exponent of $\cos\chi$ is found to be $p = 1.20$ instead of the theoretical value $p = 1$. The important facts that the value of the exponent p does not vary systematically with season, and that it does not exhibit any regular variation with the latitude of the station, are demonstrated by means of statistical F tests.

The world morphology of the Appleton E-layer seasonal anomaly is investigated and it is shown that it depends on latitude, longitude and hemisphere. It is concluded that the anomaly could be the result of seasonal variations in the S_q current system.

To take account of the f_oE seasonal anomaly an analytical expression in terms of geographic or magnetic latitude is proposed.

The results of the whole investigation are synthesized to obtain a describing function of f_oE in terms of geographic latitude, 10.7 cm solar radio noise flux, and solar zenith angle, for the purpose of computer aided design of ionospheric transmission paths. The reliability of this describing function is assessed by comparing predicted and observed values at various stations, and the standard error of estimate is determined.

Finally suggestions are made concerning the direction of future work in this area.

CONTENTS

		Page
Chapter 1	Introduction	
1.1	The object of the investigation	1
1.2	Some relevant theoretical relationships	2
Chapter 2	Investigation of the variation of f_oE with solar activity	
2.1	Choice of the form of the appropriate relationship	7
2.2	Data and analysis	21
2.3	Results and discussion	28
Chapter 3	Investigation of the diurnal variation of f_oE	
3.1	Data	41
3.2	The treatment of the data	47
3.3	Results and discussion	59
Chapter 4	The Appleton E-layer seasonal anomaly	
4.1	Investigation of the world morphology of the anomaly	69
4.2	The latitude dependence of the anomaly	71
4.3	Discussion of results	91
Chapter 5	An analytical expression of f_oE for prediction purposes	
5.1	Assessment of the accuracy of the f_oE expression	98
5.2	Comparison of observed and estimated f_oE values	104
Chapter 6	Summary and conclusions	128
Appendix A	A review of the work done by previous investigators	
A.1	Variation of f_oE with solar activity	134
A.2	Variation of f_oE with $\cos\chi$	143
A.3	Anomalies in the E layer	152
A.4	On the Sq current system	161

Appendix B — Page

B.1 Comparison and pooling of the monthly diurnal exponents of $\cos\chi$ for each station 167

B.2 Comparison and pooling of the "individual pooled" slopes p_j 169

Appendix C List of stations used in the statistical analyses 173

Map of the stations 176

References 177

Acknowledgements

CHAPTER 1

INTRODUCTION

The ionospheric E layer, to a first approximation, behaves like a simple α-Chapman layer[1]. However, systematic deviations from this first-order theory have been identified by many investigators. Some of these discrepancies have been attributed to the inappropriateness of the assumptions in the Chapman theory [2]-[8], whereas some other of the most striking of these anomalies appear to be due to the influence of the S_q currents[5][8][9][10]. In addition the Appleton E-layer seasonal anomaly[11][13] has been considered as a distinct phenomenon[12].

1.1 THE OBJECT OF THE INVESTIGATION

The world morphology of most of the above anomalies, as well as their origin and the mechanism by which they are produced, are still the subject of detailed studies. It is evident that the actual interpretation and estimation of the non-Chapmanlike variations, on a world-wide basis, will greatly contribute to our knowledge of E-layer behaviour.

This thesis presents a report on the investigation of the world morphology of the Appleton E-layer seasonal anomaly, and of the variation of f_oE with solar activity and solar zenith angle, which are still subjects of considerable controversy. A result of this investigation is the synthesis of a formula, for Computer Aided Design methods using the ionosphere as a transmission medium, for calculating the value of f_oE at any given time of day, season, location and solar activity.

In Chapter 2 the relation between f_oE and each of the three solar indices, the Zurich relative sunspot number, R, the 10.7 cm solar radio noise flux, Φ, and the ionospheric index of solar activity, IF2, is examined, with the purpose to determine whether one of them may be superior to the others and eventually be used in the subsequent analysis.

In Chapter 3 the investigation of the diurnal exponent of $\cos\chi$ on the basis of world-wide measurements of f_oE is described.

Chapter 4 deals with the examination and the most reasonable interpretation of the Appleton seasonal anomaly.

In Chapter 5 the results of the investigation are gathered together and an analytical expression is obtained from which f_oE can be calculated. A comparison is then made with some formulae of this type previously obtained by other investigators[14]-[17].

Finally Chapter 6 summarizes the work and indicates the direction of future investigation.

In Appendix A a review is given of the work done by previous investigators on the various ionospheric factors that control f_oE.

The present chapter is concluded by highlighting those theoretical considerations which have an immediate bearing on this work.

1.2 SOME RELEVANT THEORETICAL RELATIONSHIPS

According to the classical Chapman theory[1] the continuity equation for electrons may be written:

$$\partial N/\partial t = q(h,\chi) - \alpha N^2 \qquad (1.1)$$

where N is the electron density at height h and time t; q is the rate of electron production per unit volume, and α is the recombination coefficient assumed independent of h and t[15][16][18][19].

The maximum electron production rate q_m is given by

$$q_m = q_o \cos\chi = (\eta S_\infty / H \exp 1)\cos\chi \tag{1.2}$$

and occurs at a height

$$h_m = h_o + H \ln \sec\chi \tag{1.3}$$

where χ is the solar zenith angle, q_o is the maximum electron production rate for overhead sun ($\chi = 0$) at the height h_o, H is the scale height of the atmosphere at the level concerned, η is the ionizing efficiency and S_∞ is the photon flux of the ionizing radiation outside the Earth's atmosphere.

Now it has been shown[4][5] that under quasi-stationary conditions the maximum electron concentration of the E layer, N_m, satisfies the equation:

$$dN_m/dt = q_o \cos\chi - \alpha N_m^2 \tag{1.4}$$

If, further, the layer conditions are completely stationary, then equation (1.4) becomes:

$$N_m^2 = (q_o/\alpha)\cos\chi \tag{1.5}$$

Expressing the peak electron density N_m in terms of f_oE (in MHz) by means of the relation[15][18]:

$$N_m = 1.24 \times 10^4 \times (f_oE)^2 \ [\text{electrons/cm}^3] \tag{1.6}$$

and combining equations (1.2), (1.5) and (1.6) we have:

$$(f_o E)^4 = K \cos\chi \tag{1.7}$$

where

$$K = (1.24 \times 10^4)^{-2}(\eta S_\infty / \alpha H \exp 1) \quad [MHz^4] \tag{1.8}$$

Equation (1.7) is the so-called Chapman relationship between the critical frequency and the solar zenith angle.

Various investigators have modified the simplified assumptions of Chapman's theory and have extended it [18][19][20].

For values of χ greater than about 80 degrees, i.e. near sunrise and sunset, $\sec\chi$ must be replaced by the Chapman[2] "grazing incidence function" $Ch(R + z, \chi)$, which has been tabulated by Wilkes[21]. Muggleton[22] has proposed an analytical expression equivalent to the Chapman function which is particularly useful for computer use.

Nicolet[3] and others[4][5][7] have examined the modification of Chapman's theory when the scale height varies with altitude. Direct measurements of H using rockets[23], and determinations of H in the E region from accurate measurements of the shape of the layer[24] have shown that H indeed increases with height. Assuming H to vary with height with a constant gradient μ, the above workers have shown that equation (1.7) becomes:

$$(f_o E)^4 = A(\cos\chi)^{1+\mu} \tag{1.9}$$

where A now is also a function of the height variation of the scale-height.

If the recombination coefficient α also varies with height the exponent of $\cos\chi$ in equation (1.7) will be similarly affected[4][5][8], and therefore it becomes difficult to distinguish between the effects of the two gradients on the exponent of $\cos\chi$.

The continuity equation (1.1) has also been modified by the introduction of an electron transport term. If only vertical movements of electrons are considered[18], then equation (1.1) becomes:

$$\partial N/\partial t = q - \alpha N^2 - \partial(Nv)/\partial h \qquad (1.10)$$

where v is the upward vertical drift velocity at height h.

Movements of ionization have important effects on the ionosphere. They lead to ionospheric currents if the mean drift velocities of the positive ions and of the electrons are unequal. Such currents, called dynamo currents, are concentrated mainly in the E region, as has been pointed out by Appleton and Piggott[25][26], and experimentally detected by rocket-borne magnetometers[27]-[37]. Moreover, movements of ionization affect the distribution of electron density in the E and F regions. (This effect is particularly important in the F_2 region where the lifetime of free electrons is measured in hours[38]-[43]). Vertical drifts in the E region are not as important as those in the F_2 region[44], because of the quick recombination of charged particles, which have a typical lifetime of only a few minutes[45], and also because of the greater drag of the neutral gas[46]. Nevertheless, certain anomalies, or deviations from the simple Chapman-like region behaviour, which many investigators have identified in the case of the E layer,

are attributed to such drifts, generated by the S_q currents produced by the dynamo action of solar tidal motions in the upper atmosphere[5][7][8][9][10][38][41],[47]-[57].

The theory of the effect of vertical drift in distorting a Chapman-like layer has been discussed by Martyn[38][41], Kirkpatrick[58], and Appleton and Lyon[4][5]. According to this theory the drift velocity itself will always reduce the peak electron density, whereas a vertical gradient in that drift may result in an increase or decrease in the peak density depending on the sense of the gradient. In fact, Appleton and Lyon have shown that in the case of the E layer the fractional change in the maximum electron density, N_m, due to vertical drifts, and the change in the height of the layer maximum, h_m, are given respectively by

$$\frac{\Delta N_m}{N_m} = -\frac{1}{2\alpha N_m}\frac{\partial v}{\partial h} - \frac{1}{4H^2}\left(\frac{v}{2\alpha N_m}\right)^2 \qquad (1.11)$$

and

$$\Delta h_m = v/2\alpha N_m \qquad (1.12)$$

where v is the vertical drift velocity, $\partial v/\partial h$ is its vertical gradient (both measured positive upwards), and H is the scale height. Therefore, the final result could be an increase or a decrease in N_m according to the sign of the gradient and the relative magnitudes of the two terms in equation (1.11), whereas the variation of h_m has the same sign as the drift velocity v .

With these considerations forming the background we now proceed to describe the investigation.

CHAPTER 2

INVESTIGATION OF THE VARIATION OF f_oE WITH SOLAR ACTIVITY

The purpose of this part of the investigation has been to provide average world-wide relationships between the critical frequency, f_oE, and each of the three most used indices of solar activity, the Zurich relative sunspot number, R, the 10.7 cm solar radio noise flux, Φ, and the ionospheric index of solar activity, IF2; and to determine whether any of the three above indices has a significantly greater correlation with f_oE, for the purpose of obtaining the most useful relationship for ionospheric predictions.

2.1 CHOICE OF THE FORM OF THE APPROPRIATE RELATIONSHIP

An extensive review of previously published work is given in section A.1 of Appendix A and the introductory remarks in this present section are therefore very condensed.

Some investigators, in studying the variation of f_oE with sunspot number, R, have used monthly median f_oE values and corresponding sunspot numbers in an assumed linear relationship (59)(60)(61). But Appleton(26)(62) and other workers(63) have correlated monthly-median noon values of $(f_oE)^2$ with corresponding monthly mean R values. Again, some others(64)(65) related the fourth power of the critical frequencies to the corresponding monthly sunspot numbers. Schwentek(66) has found that in summer a linear relationship between f_oE and R fits the data well, while in winter a linear relationship between $(f_oE)^4$ and R is better.

Thus, we see that different models have been considered by the various investigators; we may summarise these in the form:

$$(f_oE)^n = a(1 + bX) \qquad (2.1)$$

where X stands for R or Φ or IF2 as required, although no relationships between $(f_oE)^n$ and either Φ or IF2 appear to have been proposed by any authors.

All workers [for instance, references (14)(26), (59)-(76)] have stated that the relationship between $(f_oE)^n$ and X is approximately linear whatever the power to which f_oE is raised in equation (2.1); but there is considerable variation in the value obtained for the sensitivity, b, as can be seen from Table 2.0, where the findings of some investigators are summarised.

TABLE 2.0

Values of n and b in equation $(f_oE)^n = a(1 + bR)$ given by various investigators

	n	b x 10^3
Waldmeier[67]	3	9.3
Tremellen and Cox[68]	3.2	7.3
Allen[65]	4	9.7
Harnischmacher[14]*	3.7	8.1
Scott[69]	1	1.75
Saha[70]	1	1.72
Rao and Malhorta[61]	1	1.5
Davies[15] - Van Zandt[16]	4	8.0
Appleton and Beynon[77]	2	3.3
Schwentek[66]**	4	9.66
Schwentek[66]***	1	1.45
Muggleton[63]	2	3.34

* for the latitude of $\theta = 60^o$

** for winter

*** for summer

However, according to equations (1.7) and (1.8), deduced from Chapman's theory, the intensity of ionizing radiation is proportional to the fourth power of the critical frequency in the E region. Therefore, it should be expected that a better correlation exists between $(f_oE)^4$ and each of the three indices, R or Φ or IF2, rather than f_oE raised to any other power with each of the three indices.

In order to determine statistically whether any difference in merit exists between the various models it was decided to carry out a preliminary investigation to establish which model should be used for each index. For this purpose the following more general form of equation was used:

$$(f_oE)^n = a_o + a_1X + a_2X^2 + a_3X^3 \qquad (2.2)$$

where n = 1,2,3.3,4, and X stands for R or Φ or IF2.

To remove any seasonal, annual, and possible latitude influences, the regression analysis has been carried out separately for each month at a given station.

Two criteria for assessing the relative merits of the various models have been adopted; these are based on a) the number of second - and third-order terms in the regression with coefficients significantly different from zero at the 5 per cent level, and b) the linear correlation coefficients between $(f_oE)^n$ and X. For this purpose the monthly median f_oE values at noon, measured at eight stations with a long period of data available and providing a wide spread of latitude, have been used. Details of the stations and the periods of data used in the statistics are given in Table 2.1 .

TABLE 2.1

Stations and periods of data used in the statistics for the choice of the relationship between f_oE and either of the three solar indices, R, Φ, IF2

Station	Geog. Lat. θ°	Geog. Long. λ°	Period of Data (R, IF2)	Period of Data (Φ)
Slough	51.5	359.4	1938 - 1967	1947 - 1967
Lindau	51.6	10.1	1953 - 1963	1953 - 1963
Ottawa	45.4	284.1	1946 - 1967	1947 - 1967
Washington	38.7	282.9	1938 - 1967	1947 - 1967
Tokyo	35.7	139.5	1946 - 1967	1947 - 1967
Singapore	1.3	103.8	1954 - 1964	1954 - 1964
Watheroo	-30.3	115.9	1940 - 1958	1947 - 1958
P. Stanley	-51.7	302.2	1947 - 1967	1947 - 1967

Sunspot numbers and IF2 data are available from 1938 onwards, but Φ values are available only from 1947 onwards. The Φ observed values used in the present investigation are "relative" values, referred to a mean minimum value for the quiet Sun of 66 flux units[78], corresponding approximately to R = 0.

To handle the large amount of data and of regressions, not only in the present analysis but throughout the whole investigation described in this thesis, computer programmes have been employed.

The curvilinear regressions of higher-order terms (2.2) have been fitted, by the method of least squares, to the f_oE data of each month at each station and the corresponding monthly mean values of each of the three solar indices, R, Φ, and IF2. Thus, for each solar index and for each month at each station, we have four curvilinear regressions, one for each chosen value of n(n = 1,2,3.3,4).

We shall refer heareafter to three cases of four models each. For each model, the hierarchy of regressions:

$$(f_oE)^n = a_o + a_1X \tag{2.3}$$

$$(f_oE)^n = a_o + a_1X + a_2X^2 \tag{2.4}$$

$$(f_oE)^n = a_o + a_1X + a_2X^2 + a_3X^3 \tag{2.5}$$

was tested to see whether the coefficients a_2 and a_3 of the non-linear terms differed significantly from zero. This was done using an F-test[79]. The results are summarised in Table 2.2, in which the percentage of non-linear regressions over a total of 96 (12 months x 8 stations) curvilinear regressions for each of the models is given.

TABLE 2.2

Percentage of sets of data requiring a higher-order regression at the 5% significance level. (Total number of sets examined 96 i.e. 12 months x 8 stations)

Model	f_oE,R	$(f_oE)^2,R$	$(f_oE)^{3.3},R$	$(f_oE)^4,R$
Percentage	47	31	22	15
Model	f_oE,Φ	$(f_oE)^2,\Phi$	$(f_oE)^{3.3},\Phi$	$(f_oE)^4,\Phi$
Percentage	56	50	28	16
Model	f, IF2	f^2,IF2	$f^{3.3}$,IF2	f^4,IF2
Percentage	11	27	34	46

It is shown in Table 2.2 that at the 5 per cent significance level the need of the second- and/or third-order term for a significant improvement in the correlation existed only in 15 regressions out of 100 in the case of the model $(f_oE)^4/R$;

whereas, in the f_oE/R model, the second- and/or third-order term improved the correlation in 47 per cent of the regressions.

Again, in the $(f_oE)^4/\Phi$ model only in 16 per cent of the regressions the second- and/or third-order term were significant at the 5 per cent level, while in the f_oE/Φ model there was in 56 per cent of the regressions an improvement in the correlation by using a regression of higher-order.

On the contrary, the IF2 models present the opposite situation. The correlation in the $f_oE/IF2$ model is improved by using higher-order terms only in 11 per cent of the sets of data examined, while in the $(f_oE)^4/IF2$ in 46 per cent. It is interesting to note that at the 1 per cent significance level in the $(f_oE)^4/R$, $(f_oE)^4/\Phi$, and $f_oE/IF2$ models the contribution of higher-order terms was significant in less than 6 per cent of the 96 regressions examined.

As already mentioned, the other criterion on which is based the choice of the appropriate power to which f_oE should be raised in the relationship with each of the three indices, is the linear correlation coefficients in each of the three cases. Here again, the noon f_oE monthly median values for each month at each station and the corresponding monthly mean values of R or Φ or IF2 respectively, were fitted by the method of least squares to the linear regression:

$$(f_oE)^n = c_m + d_m X \qquad (2.6)$$

where the subscript m refers to the month of the year, X stands for R or Φ or IF2 respectively, and n takes the values of 1,2,3.3, and 4 in turn.

TABLE 2.3

Linear correlation coefficients for Slough, for each month and each model.

Number of data N_i(R or IF2) = 30; $N_i(\Phi)$ = 21

Month	f / R	f^2 / R	$f^{3.3}$/ R	f^4 / R	f / Φ	f^2 / Φ	$f^{3.3}$/ Φ	f^4 / Φ	f / I	f^2 / I	$f^{3.3}$/ I	f^4 / I
Jan.	0.960	0.964	0.968	0.968	0.972	0.977	0.982	0.984	0.966	0.963	0.956	0.951
Feb.	0.963	0.963	0.962	0.961	0.972	0.975	0.977	0.977	0.973	0.973	0.971	0.969
Mar.	0.966	0.968	0.970	0.971	0.951	0.956	0.961	0.964	0.982	0.979	0.974	0.971
Apr.	0.961	0.964	0.967	0.968	0.949	0.952	0.954	0.954	0.968	0.967	0.964	0.960
May	0.944	0.947	0.949	0.950	0.916	0.920	0.922	0.923	0.951	0.951	0.948	0.946
June	0.957	0.958	0.958	0.957	0.930	0.934	0.936	0.937	0.933	0.930	0.925	0.920
July	0.948	0.950	0.951	0.951	0.950	0.954	0.957	0.958	0.953	0.952	0.949	0.946
Aug.	0.965	0.966	0.966	0.964	0.969	0.969	0.968	0.967	0.971	0.967	0.960	0.956
Sept.	0.948	0.953	0.959	0.960	0.961	0.966	0.975	0.976	0.945	0.946	0.936	0.937
Oct.	0.961	0.966	0.970	0.971	0.984	0.987	0.988	0.987	0.956	0.950	0.939	0.931
Nov.	0.969	0.972	0.975	0.975	0.976	0.979	0.982	0.983	0.968	0.964	0.958	0.953
Dec.	0.927	0.930	0.933	0.933	0.973	0.978	0.982	0.983	0.969	0.964	0.955	0.949

As an example Table 2.3 shows the linear correlation coefficients for each month, for each of the three solar indices and for each of the four models for the station of Slough. Similar results were obtained for the other seven ionospheric stations chosen.

In order to compare the linear correlation coefficients of the different models of equation (2.6), it is necessary to combine the obtained 96 linear correlation coefficients (12 months x 8 stations) of each model. Since the correlation coefficients are very high, and their distributions very skew (see for example Fig. 2.1), it is necessary to use Fisher's z-transformation of r, which is very nearly normally distributed with variance, $1/(N - 3)$, where N is the number of pairs of observations of the sample. Hence, the usual tests of significance for a normal distribution could be applied. The homogeneity of the 96 values of r was tested by means of a χ^2 test[80], and the result showed that the 96 samples of each model of each of the three cases may be regarded as drawn from the same normal population. Therefore, it is permissible to average the 96 correlation coefficients. In Table 2.4 are listed the combined correlation coefficients for each station and model. In Table 2.5 are given the combined correlation coefficients for the four models of equation (2.6) for each of the three cases obtained by means of z-transformation, and also their standard errors.

An inspection of the results of Table 2.5 reveals that the $(f_oE)^4$ model of equation (2.6) for both R and Φ indices, gave somewhat higher correlation coefficients than the models using lower values of n.

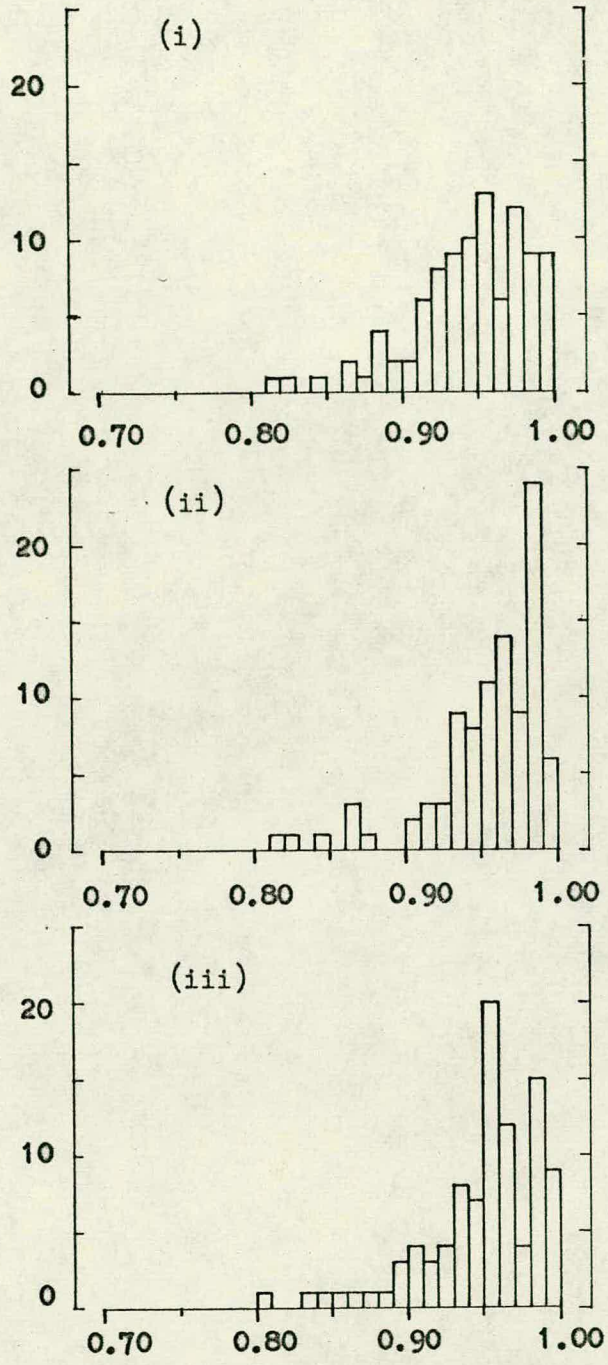

Fig. 2.1

The distributions of the 96 linear correlation coefficients for the 8 stations.
(i) $(f_oE)^4/R$, (ii) $(f_oE)^4/\Phi$, (iii) $f_oE/IF2$

TABLE 2.4

Combined linear correlation coefficients for each station and model

Station	f/R	f^2/R	$f^{3.3}/R$	f^4/R	f/Φ	f^2/Φ	$f^{3.3}/\Phi$	f^4/Φ	$f/IF2$	$f^2/IF2$	$f^{3.3}/IF2$	$f^4/IF2$
Slough	0.957	0.960	0.962	0.962	0.963	0.967	0.970	0.971	0.963	0.961	0.955	0.951
Lindau	0.981	0.984	0.987	0.988	0.976	0.984	0.988	0.989	0.985	0.984	0.982	0.980
Ottawa	0.911	0.909	0.904	0.901	0.931	0.933	0.932	0.931	0.906	0.900	0.891	0.885
Washington	0.921	0.925	0.929	0.931	0.961	0.964	0.967	0.969	0.954	0.953	0.951	0.948
Tokyo	0.943	0.946	0.949	0.949	0.947	0.953	0.958	0.960	0.956	0.955	0.953	0.950
Singapore	0.982	0.986	0.988	0.989	0.980	0.984	0.987	0.988	0.991	0.990	0.988	0.985
Watheroo	0.919	0.920	0.919	0.918	0.915	0.916	0.915	0.914	0.907	0.904	0.900	0.896
P. Stanley	0.954	0.956	0.958	0.959	0.951	0.954	0.957	0.959	0.959	0.958	0.954	0.951

TABLE 2.5

Combined linear correlation coefficients for the different models, obtained from 96 linear correlation coefficients (12 months x 8 stations)

Models	r	r ± S.E.
f_oE/R	0.945	0.943 - 0.948
$(f_oE)^2/R$	0.949	0.946 - 0.951
$(f_oE)^{3.3}/R$	0.951	0.949 - 0.953
$(f_oE)^4/R$	0.951	0.949 - 0.954
f_oE/Φ	0.955	0.953 - 0.957
$(f_oE)^2/\Phi$	0.960	0.958 - 0.962
$(f_oE)^{3.3}/\Phi$	0.963	0.961 - 0.965
$(f_oE)^4/\Phi$	0.965	0.963 - 0.966
$f_oE/IF2$	0.956	0.954 - 0.958
$(f_oE)^2/IF2$	0.954	0.952 - 0.956
$(f_oE)^{3.3}/IF2$	0.950	0.947 - 0.952
$(f_oE)^4/IF2$	0.946	0.944 - 0.949

The opposite is shown in the case of the IF2 index; the $f_oE/IF2$ model gave a greater correlation coefficient than the other models. It is also obvious from Table 2.5, column r ± S.E., that there is probably no significant difference between the correlation coefficients of the four models of equation (2.6) for $X \equiv R$, but the difference of the correlation coefficients may be significant in the case of $X \equiv \Phi$ and $X \equiv IF2$, respectively, in equation (2.6).

Therefore, the usual test of significance of the difference of two correlation coefficients[81] was applied and the results of these comparisons are reported below:

Case $X \equiv R$.

$$(f_o E)^n = c_m + d_m R \text{ , where } n = 1,\ 2,\ 3.3,\ 4.$$

The difference to be tested is $| r(f_o E^4, R) - r(f_o E, R) |$, which in simplified form can be written as $|r_4 - r_1|$, where the subscript refers to the power to which $f_o E$ is raised in the corresponding model. We have to compare the difference between the corresponding values of z with the standard error of that difference:

$$\text{S.E. } (z_4 - z_1) = [2/\Sigma (N_i - 3)]^{\frac{1}{2}}$$

where ΣN_i, the total number of pairs of observations, is equal to 1956 in this case. Then,

$$| z_4 - z_1 | = | 1.846 - 1.787 | = 0.059 ;$$

$$\text{S.E. } (z_4 - z_1) = 0.0346 ;\ u = | z_4 - z_1 | / \text{S.E. } (z_4 - z_1) = 1.72$$

Since the difference of z is less than twice the S.E. of that difference, the difference between r_4 and r_1 is not significant at the 5 per cent level. Therefore, the correlation between $(f_o E)^4$ and R is not significantly better than the correlation between $f_o E$ and R. Similar results have been obtained in the case of all the other differences for the R index.

Case $X \equiv \Phi$.

$$(f_o E)^n = c_m + d_m \Phi \text{ , where } n = 1,\ 2,\ 3.3,\ 4.$$

The total number of pairs of observations of the 8 stations is in this case equal to 1632.

1) Difference tested $|r_4 - r_1|$:

$$|z_4 - z_1| = |2.007 - 1.887| = 0.120 ;$$

$$\text{S.E.}(z_4 - z_1) = 0.0386 ; \quad u = |z_4 - z_1| / \text{S.E.}(z_4 - z_1) = 3.10$$

Therefore the difference is highly significant and it is concluded that the correlation between $(f_oE)^4$ and Φ is significantly greater than the correlation between f_oE and Φ.

2) Difference tested $|r_{3.3} - r_1|$:

$$|z_{3.3} - z_1| = 0.104 ; \quad \text{S.E.}(z_{3.3} - z_1) = 0.0386$$

$$u = |z_{3.3} - z_1| / \text{S.E.}(z_{3.3} - z_1) = 2.69$$

Again the difference is highly significant indicating that the correlation between $(f_oE)^{3.3}$ and Φ is significantly greater than that between f_oE and Φ. The tests applied to all the other pairs of correlation coefficients showed that there was no significant difference between the correlation coefficients of any other pair.

Case $X \equiv IF2$

$$(f_oE)^n = c_m + d_m.IF2, \text{ where } n = 1, 2, 3.3, 4.$$

The total number of pairs of observations of the 8 stations is in this case equal to 1956.

1) Difference tested $|r_1 - r_4|$:

$$|z_1 - z_4| = |1.896 - 1.795| = 0.101$$

$$\text{S.E.}(z_1 - z_4) = 0.0346 ; \quad u = 2.92$$

The difference is highly significant and it is concluded that the correlation between $f_o E$ and IF2 is significantly greater than that between $(f_o E)^4$ and IF2.

2) Difference tested $|r_1 - r_{3.3}|$:

$$|z_1 - z_{3.3}| = 0.069 \; ; \; \text{S.E.}(z_1 - z_{3.3}) = 0.0346 \; ; \; u = 1.99$$

The difference is just significant at the 5 per cent level but not at the 1 per cent level. The two correlation coefficients are significantly different at the 5 per cent level.

3) Difference tested $|r_2 - r_4|$:

$$|z_2 - z_4| = 0.079 \; ; \; \text{S.E.}\,(z_2 - z_4) = 0.0346 \; ; \; u = 2.29$$

The difference is significant at the 5 per cent level but not at the 1 per cent level. Therefore, at the 5 per cent level the correlation between $(f_o E)^2$ and IF2 is significantly better than that between $(f_o E)^4$ and IF2. For all other differences of r's the tests showed that they were not significant.

The results obtained in this section (Tables 2.2 and 2.5) enable us, therefore, to deduce that the following relationships should be used in order to obtain the best linear correlations:

$$(f_o E)^4 = a_m (1 + b_m R) \tag{2.7}$$

$$(f_o E)^4 = a_m (1 + b_m \Phi) \tag{2.8}$$

$$f_o E = a_m (1 + b_m \text{IF2}) \tag{2.9}$$

Having established a suitable model for each index the next requirement was to determine, by examining the data of 47 stations, whether any pair of variates in each of the three equations (2.7), (2.8) and (2.9), has a significantly greater correlation than the others. This work is reported in the next sections.

2.2 DATA AND ANALYSIS

The f_oE data used in the present analysis are taken from 47 ionospheric observatories, covering a wide range of latitudes, which are collected in Table C.1 and illustrated in Fig. C.1 of Appendix C. The data used are monthly median f_oE noon values of one or possibly two solar cycles. The actual period of the data used in the statistics for each station is given in Table C.1. The f_oE data were obtained primarily from the tabulated ionospheric data of the National Bureau of Standards, C.R.P.L.[82], as well as from ionospheric data published by the R.S.R.S., Slough[83]. The sunspot-number data were those given by Waldmeier[84] in "The Sunspot-Activity in the years 1610 - 1960" and in the "Quarterly Bulletin on Solar Activity"[85], whereas the data of 10.7 cm solar radio noise flux were kindly supplied by Dr. Covington (Ottawa, Canada), and the IF2 ionospheric index data by the R.S.R.S., Slough.

In order to compare the correlation coefficients of the regressions (2.7), (2.8) and (2.9), it is important to examine the available f_oE data over the same period of years for each of the three indices R, Φ, IF2, at each station. Since Φ data are available only from February 1947 onwards, all available data used in the analysis are taken over periods from 1947 onwards. Moreover, it seems, from a comparison between Φ and either R or IF2 data, that the Φ data of the few first months of 1947 are "suspect". Therefore, data are taken only from June 1947 onwards. The Φ values used in the statistical analysis are the observed values, uncorrected for varying Sun-Earth distance[91], but referred to a mean minimum value for the quiet Sun of 66 flux units[78] corresponding approximately to R = 0.

That is,

$$\Phi_{used} = \Phi_{obs.\ tabulated} - 66 \qquad (2.10)$$

The monthly mean R and IF2 values were used as published, and the published f_oE values were accepted at their face value.

The analysis has been carried out individually for each month at each station, fitting the equations (2.7),(2.8) and (2.9) to the corresponding pairs of data by the method of least squares. Thus, for each month at each station the values of b_m (ratio of the corresponding regression coefficient and intercept, $a_m b_m / a_m$) in equations (2.7), (2.8) and (2.9), and the linear correlation coefficients were determined. In Fig. 2.2 are shown the monthly values of b_m in each of the three equations (2.7), (2.8) and (2.9), that is, for each solar index employed, at some typical stations. Fig. 2.3 shows the frequency distributions of 545 linear correlation coefficients for 47 ionospheric stations, related to R, Φ and IF2 respectively. It should be noted that for stations at very high geographic latitudes (higher than 60 degrees) the number of months examined was between 6 and 10, instead of 12; this reduced the number of linear regressions to 545, instead of 564 for each solar index.

We may note from Fig. 2.2 that the sensitivity of the E-layer critical frequency to changes in solar activity is almost the same from month to month throughout the year and its random variation very nearly the same for any of the three indices.

From Fig. 2.3 we can see that the correlation coefficients for each of the three groups are very high and their distribution very skew.

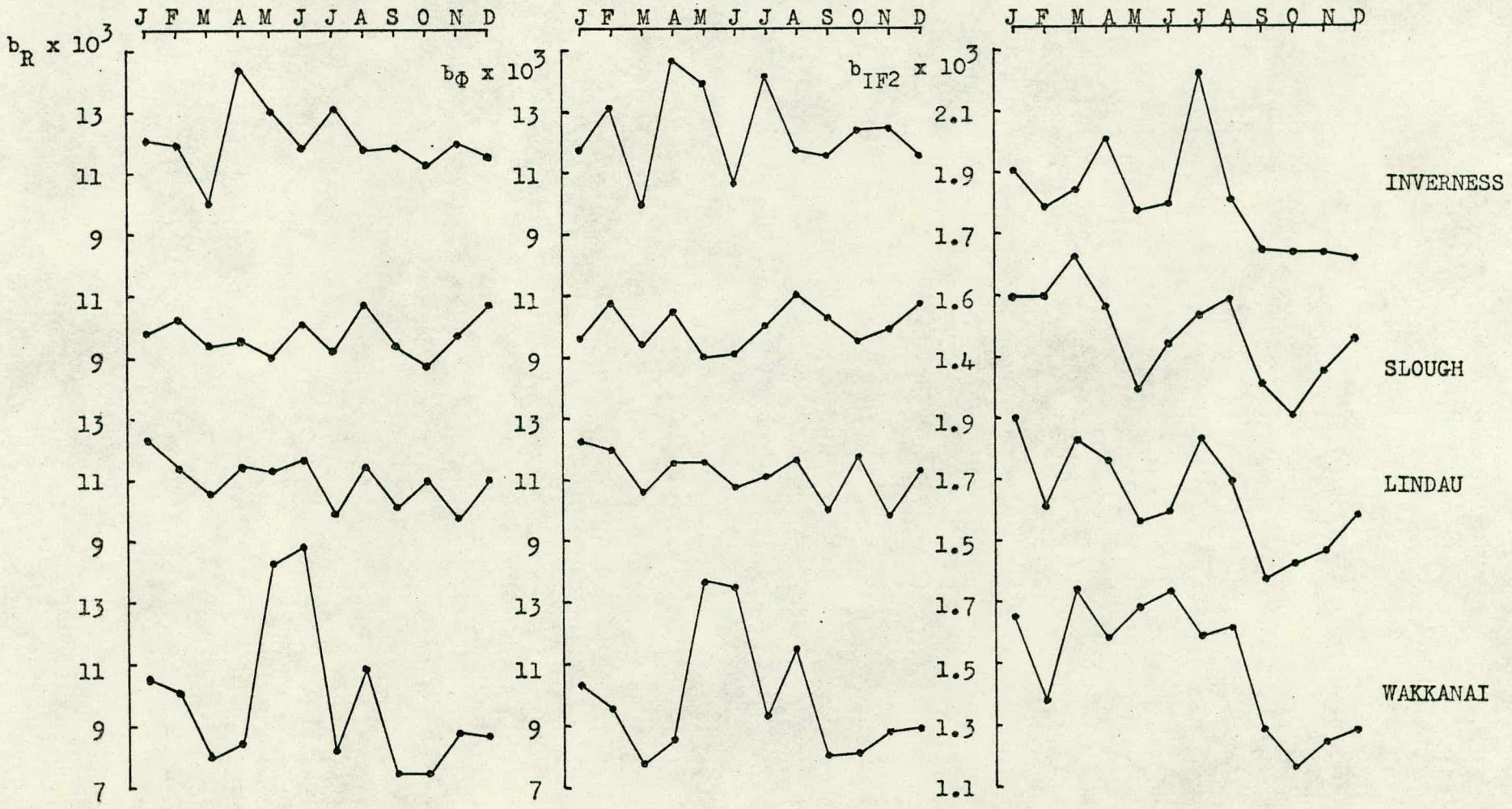

Fig. 2.2(a) Seasonal variation of the monthly values of b_R, b_Φ, b_{IF2} in equations $(f_oE)^4 = a_R(1 + b_R R)$, $(f_oE)^4 = a_\Phi(1 + b_\Phi \Phi)$, $f_oE = a_I(1 + b_I \cdot IF2)$, at some typical stations.

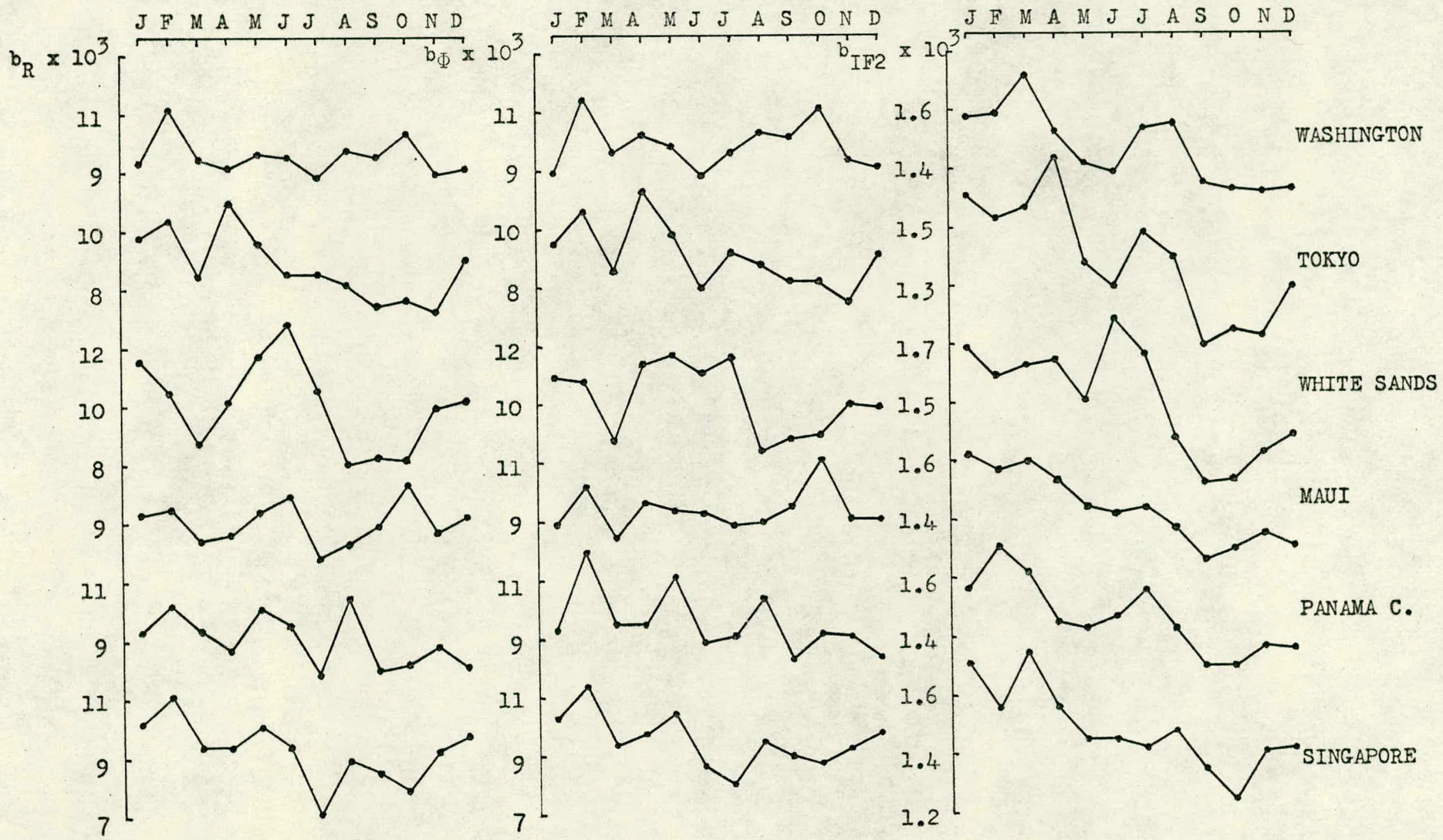

Fig. 2.2(b) Seasonal variation of the monthly values of b_R, b_Φ, b_{IF2}, at some typical stations.

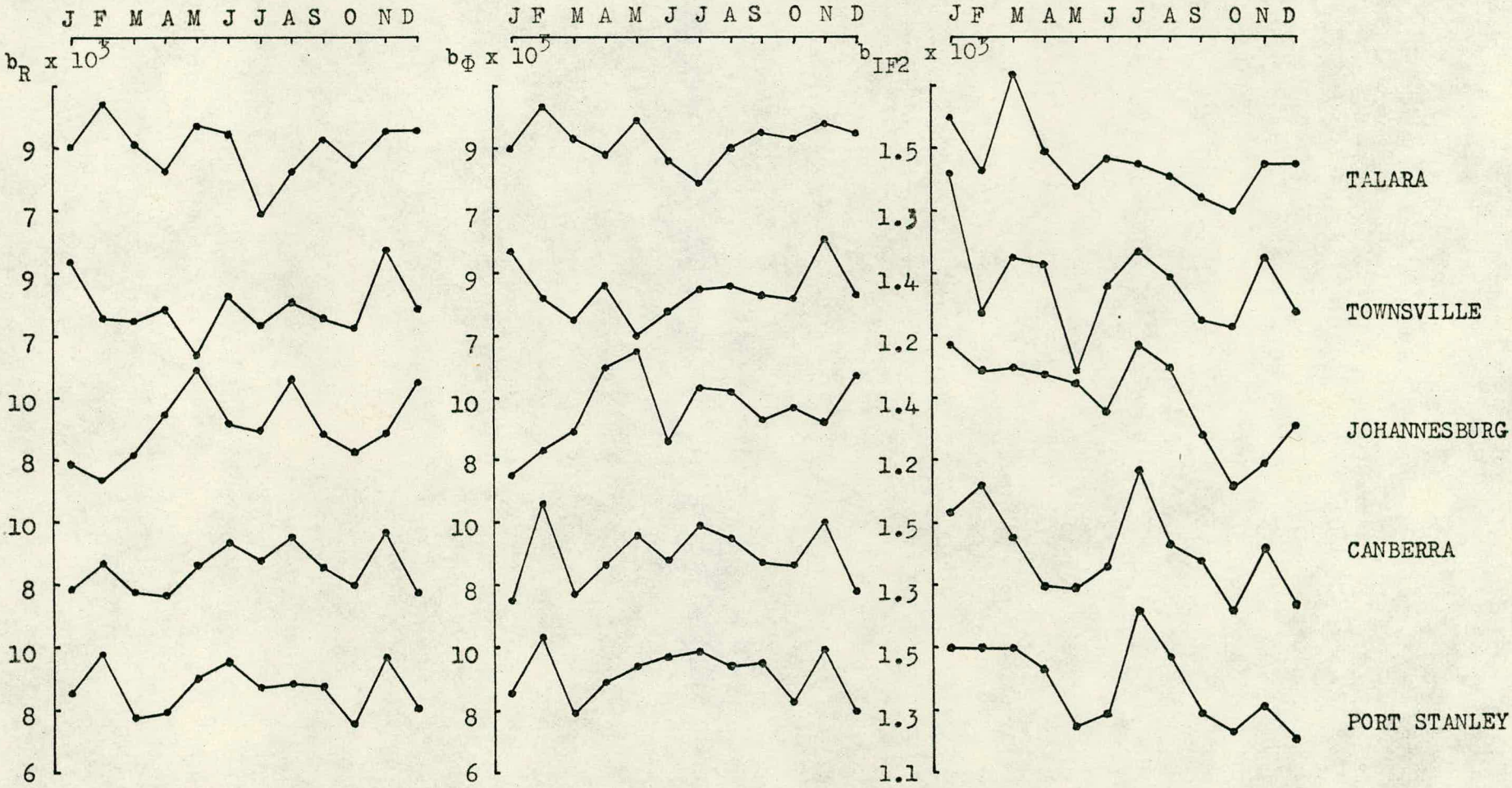

Fig. 2.2(c) Seasonal variation of the monthly values of b_R, b_Φ , b_{IF2}, at some typical stations.

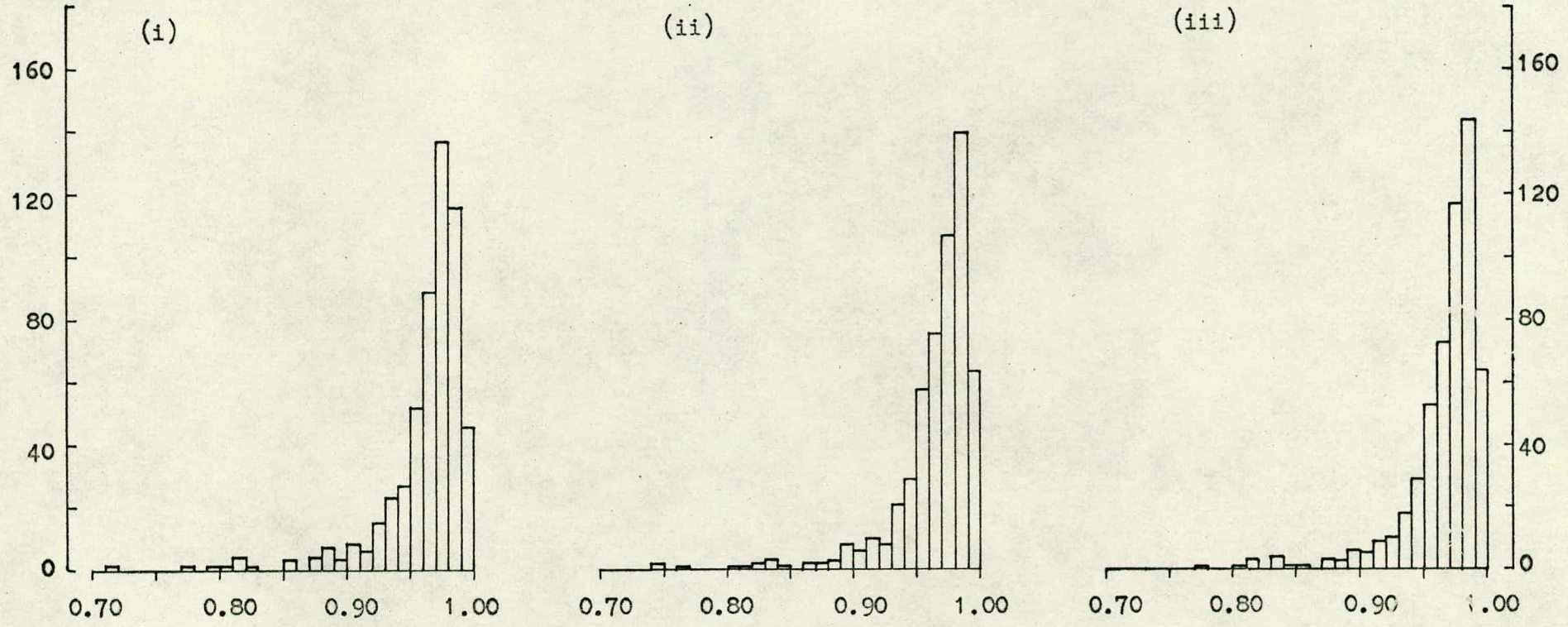

Fig. 2.3

Frequency distributions of linear correlation coefficients for 47 stations.
(i) $(f_oE)^4/R$, (ii) $(f_oE)^4/\Phi$, (iii) $f_oE/IF2$

Hence, in order to obtain an average correlation coefficient for each group, it is necessary to use Fisher's z-transformation of r,

$$z = (1/2)\,[\ln(1 + r) - \ln(1 - r)] \tag{2.11}$$

which is very nearly normally distributed[80][81] with variance $1/(N - 3)$, where N is the size of the sample. To combine the correlation coefficients, r_i, of the K samples of each group it should be examined whether they may be regarded as homogeneous, that is, the K samples as drawn from the same normal population. To test the homogeneity of the correlation coefficients, r_i, we use the χ^2 test[80]: the quantity

$$\Sigma(N_i - 3)(z_i - \bar{z})^2 = \Sigma n_i z_i^2 - (\Sigma n_i z_i)^2 / \Sigma n_i \tag{2.12}$$

is distributed approximately as χ^2 with $(K - 1)$ degrees of freedom under the null hypothesis of homogeneity. Hence, the significance of departures from homogeneity can be ascertained from χ^2 tables in the usual way. In the expression (2.12) $n_i = N_i - 3$, and $\bar{z}$ is the estimated weighted mean corresponding to the required mean correlation coefficient, which is given by the expression:

$$\bar{z} = \Sigma(n_i z_i) / \Sigma n_i \tag{2.13}$$

and its standard error by

$$\text{S.E.}\ (\bar{z}) = 1/(\Sigma n_i)^{\frac{1}{2}} \tag{2.14}$$

If the expression (2.12) does not give a significant value then the r_i correlation coefficients may be regarded as homogeneous and the samples as taken from a single normal population.

In that case, the required average correlation coefficient is given by

$$\bar{r} = (e^{2\bar{z}} - 1)/(e^{2\bar{z}} + 1)$$

or

$$\bar{r} = \tanh \bar{z} \qquad (2.15)$$

The value of the expression (2.12) has been calculated for the twelve correlation coefficients of each station in each of the three cases (R, Φ, IF2), and it was found to lie between 4 and 10, which for 11 degrees of freedom is not at all significant. Thus, the twelve monthly correlation coefficients of each station and "solar index" were regarded as homogeneous and therefore they could be combined. Next, the homogeneity of the 47 combined correlation coefficients of each of the three indices R,Φ and IF2, has been ascertained by means of the expression (2.12). The calculated values of this expression were:

$$\chi^2 (f_oE^4, R) = 20.87$$

$$\chi^2 (f_oE^4, \Phi) = 25.73 \qquad (2.16)$$

$$\chi^2 (f_oE, IF2) = 26.11$$

For 46 degrees of freedom these values are not at all significant, and hence it is legitimate, for each of the three groups, to regard the samples as drawn from a single normal population.

2.3 RESULTS AND DISCUSSION

Fig. 2.2 shows the twelve monthly b_m values in each of the equations (2.7), (2.8) and (2.9) obtained for each station by the least squares method from an examination over one or two solar cycles of monthly median noon f_oE values and corresponding monthly mean values of R or Φ or IF2.

A glance at Fig. 2.2 shows that the b_m values for each station, in each of the three cases, do not alter appreciably from month to month. According to Appleton and Piggott[86] the sensitivity b of the f_oF_2 critical frequency to changes in solar activity was found to be greater in local winter than in local summer in both hemispheres. To examine whether the present b_m values undergo a seasonal variation like those of f_oF_2, the average values for November, December and January, and for May, June and July, have been calculated for each station from 60° to about 18° of north and south latitudes. These values are shown in Fig. 2.4. Next, the difference between b-local winter and b-local summer was evaluated and the mean value of these 33 differences, in each of the three cases, has been found to be:

$$\overline{\Delta b}_R = - 0.124 \times 10^{-3} \; ; \; \overline{\Delta b}_\Phi = - 0.182 \times 10^{-3} \; ;$$

$$\overline{\Delta b}_{IF2} = - 0.0348 \times 10^{-3}.$$

Their standard errors have also been calculated using Bessel's formula[87]:

$$\text{Standard Error} = [\Sigma(x - \bar{x})^2/N(N - 1)]^{\frac{1}{2}} \qquad (2.17)$$

and found to be

$$\text{S.E.}(\overline{\Delta b}_R) = 0.258 \times 10^{-3} \; ; \; \text{S.E.}(\overline{\Delta b}_\Phi) = 0.256 \times 10^{-3} \; ;$$

$$\text{S.E.}(\overline{\Delta b}_{IF2}) = 0.0249 \times 10^{-3}.$$

From these results we may deduce that the means of the differences between b-winter and b-summer values are not significantly different from zero as can be shown by applying a t-test.

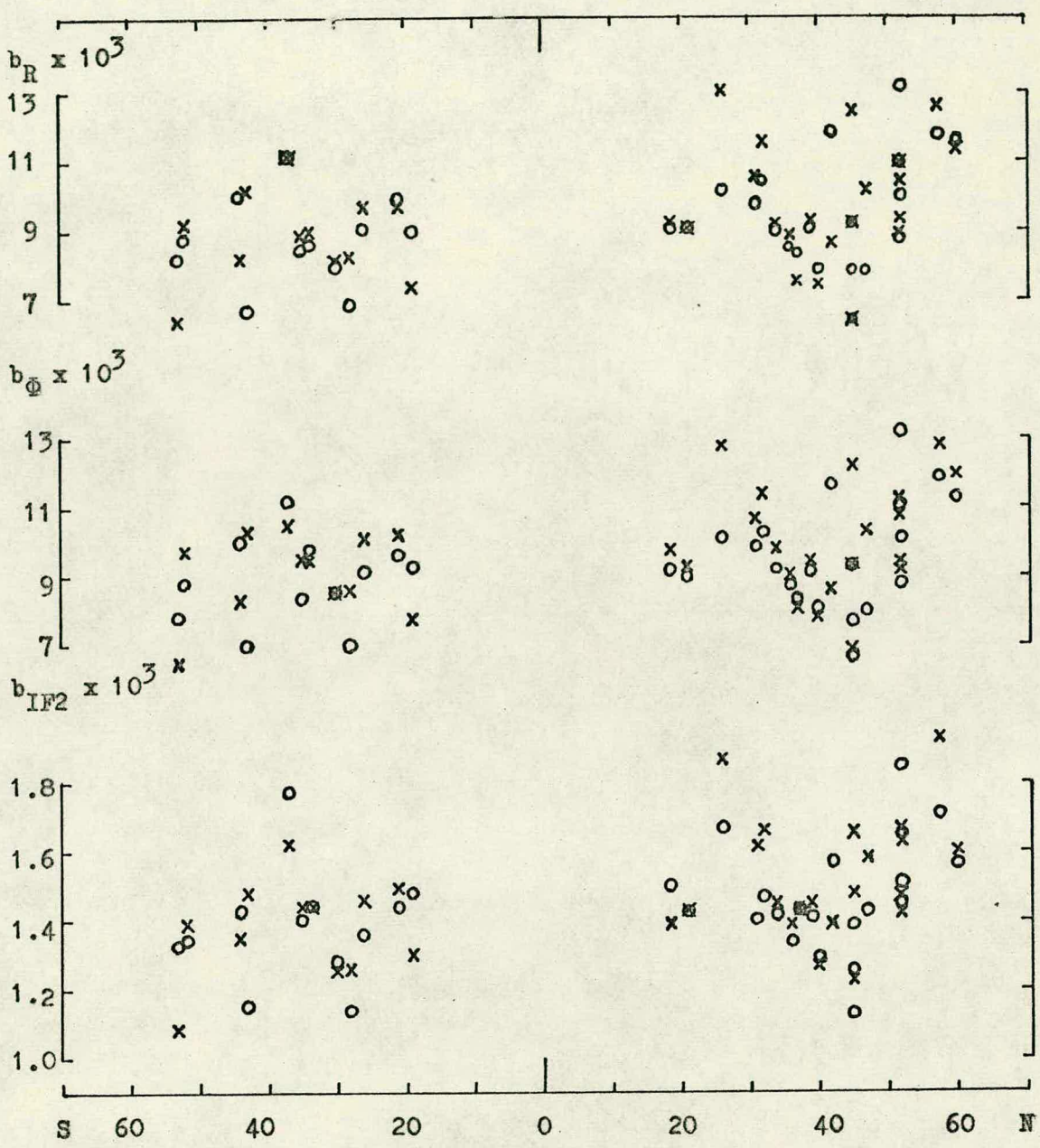

Geographic latitude in degrees

Fig. 2.4 Latitudinal distribution of sensitivities b.

o average November, December, January

x average May, June, July

Thus, the twelve monthly b_m values for each station were considered to be approximately constant throughout the year and the twelve-month average value may be taken as representative for the station.

The twelve-month average values are set out in Table 2.6 and plotted in Fig. 2.5 against geographic latitude. These plots show that b_R, b_Φ and b_{IF2} are practically independent of latitude. In Fig. 2.5 the b values are plotted against geographic latitude, but very similar trends are obtained if geomagnetic or magnetic latitudes are used. A careful inspection of Fig. 2.5, however, reveals that the b values are somewhat smaller on the whole in the southern hemisphere than in the northern hemisphere.

Next, the over-all average values of b_R, b_Φ and b_{IF2} have been calculated for each of the three groups of 47 values, as well as their standard errors by means of Bessel's formula (2.17). The results are as follows:

$$b_R = 9.1 \times 10^{-3} \pm 0.2 \times 10^{-3} \tag{2.18}$$

$$b_\Phi = 9.4 \times 10^{-3} \pm 0.2 \times 10^{-3} \tag{2.19}$$

$$b_{IF2} = 1.44 \times 10^{-3} \pm 0.02 \times 10^{-3} \tag{2.20}$$

Also median values and weighted means, using as weights the number of data of each set at each station, were evaluated and it was found that within the errors, these were equal to the values given in (2.18), (2.19) and (2.20).

A comparison between the value of b_R given in (2.18) and values found by other workers (see Appendix A.1 and Table 2.0) shows that this value is very close to the value given by Tremellen and Cox[68], provided that f_oE in their formula is first raised to the fourth power; but it differs from the values found by the other workers.

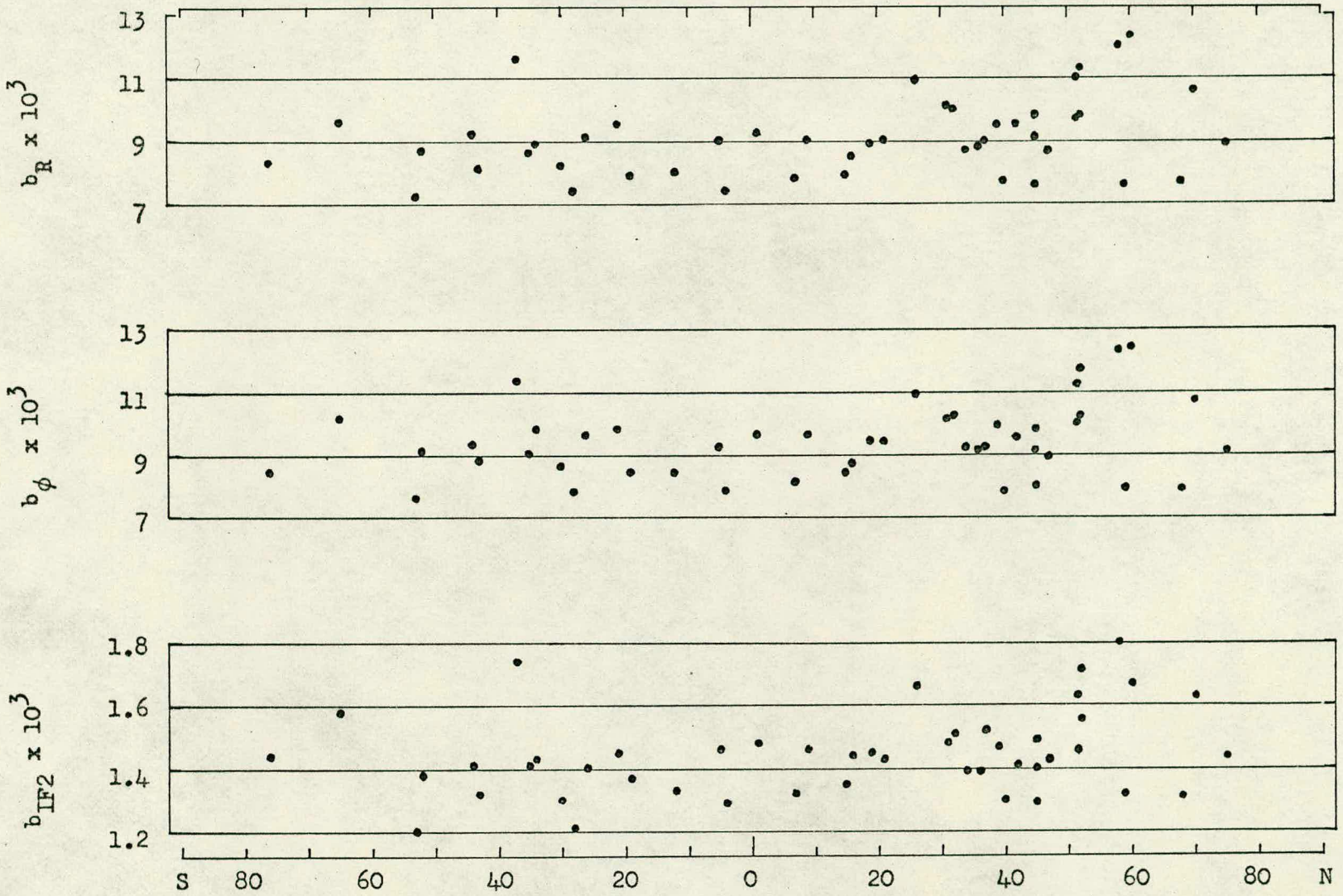

Fig. 2.5 Distribution with geographic latitude of the 12-month average b in equations (2.7), (2.8), (2.9).

TABLE 2.6

Average coefficients of sensitivity to solar activity (b), and combined linear correlation coefficients for each station (47 stations) for the cases:

$(i)(f_oE)^4 = a_R(1 + b_R.R)$; $(ii)(f_oE)^4 = a_\Phi(1 + b_\Phi.\Phi)$;

$(iii)f_oE = a_I(1 + b_I.IF2)$

Station	θ°	$b_R \times 10^3$	r_R	$b_\Phi \times 10^3$	r_Φ	$b_{IF2} \times 10^3$	r_{IF2}
Resolute Bay	74.7	8.85	0.965	9.08	0.967	1.44	0.962
Tromso	69.7	10.56	0.967	10.73	0.968	1.63	0.975
Kiruna	67.8	7.70	0.961	7.91	0.954	1.31	0.946
Oslo	60.0	12.26	0.976	12.35	0.979	1.67	0.972
Churchill	58.8	7.60	0.950	7.90	0.952	1.32	0.960
Inverness	57.5	12.02	0.976	12.29	0.978	1.80	0.980
De Bilt	52.1	11.31	0.968	11.66	0.973	1.71	0.970
Adak	51.9	9.80	0.977	10.15	0.978	1.56	0.979
Lindau	51.6	11.01	0.988	11.21	0.989	1.63	0.985
Slough	51.5	9.66	0.969	9.97	0.973	1.46	0.969
Sottens	46.7	8.66	0.971	8.89	0.971	1.43	0.978
Ottawa	45.4	7.58	0.963	7.95	0.962	1.29	0.965
Wakkanai	45.4	9.82	0.971	9.83	0.978	1.49	0.976
Genova	44.6	9.06	0.977	9.09	0.977	1.40	0.975
Rome	41.9	9.51	0.979	9.46	0.984	1.41	0.976
Akita	39.7	7.67	0.976	7.84	0.977	1.30	0.976
Washington	38.7	9.53	0.969	9.86	0.969	1.47	0.973
S. Francisco	37.4	9.03	0.951	9.21	0.929	1.52	0.969
Tokyo	35.7	8.78	0.960	9.08	0.961	1.39	0.958
Casablanca	33.6	8.67	0.977	9.24	0.978	1.39	0.975
White Sands	32.3	9.98	0.968	10.19	0.968	1.51	0.970

cont.

TABLE 2.6 Continued

Station	θ°	$b_R \times 10^3$	r_R	$b_\Phi \times 10^3$	r_Φ	$b_{IF2} \times 10^3$	r_{IF2}
Yamagawa	31.2	10.05	0.976	10.07	0.982	1.48	0.982
Okinawa	26.3	10.89	0.980	10.93	0.983	1.66	0.986
Maui	20.8	9.02	0.973	9.39	0.975	1.43	0.981
Puerto Rico	18.5	8.93	0.979	9.44	0.979	1.45	0.986
Baguio	16.4	8.47	0.978	8.74	0.976	1.44	0.984
Dakar	14.7	7.93	0.974	8.42	0.979	1.35	0.977
Panama Canal	9.4	9.02	0.992	9.57	0.993	1.46	0.993
Ibadan	7.4	7.75	0.977	8.12	0.977	1.32	0.976
Singapore	1.3	9.23	0.989	9.55	0.989	1.48	0.991
Leopoldville	-4.4	7.39	0.981	7.81	0.982	1.29	0.985
Talara	-4.6	9.04	0.990	9.24	0.992	1.46	0.989
Huancayo	-12.0	8.04	0.983	8.35	0.982	1.33	0.977
Townsville	-19.3	7.92	0.979	8.39	0.981	1.37	0.986
Rarotonga	-21.2	9.46	0.964	9.77	0.965	1.45	0.971
Johannesburg	-26.2	9.10	0.977	9.59	0.980	1.40	0.983
Brisbane	-27.5	7.44	0.954	7.76	0.955	1.21	0.962
Watheroo	-30.3	8.16	0.912	8.55	0.917	1.30	0.892
Cape-town	-34.1	8.92	0.978	9.79	0.980	1.43	0.986
Canberra	-35.3	8.56	0.968	8.95	0.969	1.41	0.980
Conception	-36.6	11.60	0.985	11.33	0.984	1.74	0.984
Hobart	-42.9	8.07	0.938	8.77	0.924	1.32	0.934
Godley-Head	-43.6	9.21	0.978	9.30	0.979	1.41	0.977
Port Stanley	-51.7	8.73	0.959	9.14	0.959	1.38	0.959
Campbell Is.	-52.5	7.15	0.918	7.55	0.918	1.20	0.911
Port Lockroy	-64.8	9.64	0.936	10.13	0.940	1.58	0.942
Halley Bay	-75.5	8.33	0.975	8.42	0.977	1.44	0.981

Comparisons of the values of b_Φ and of b_{IF2}, given in (2.19) and (2.20) respectively, are not possible, for no corresponding values have been found in the literature.

The over-all average values for the northern hemisphere stations and for the southern hemisphere stations were also calculated and found to be:

$$(b_R)_N = 9.3 \times 10^{-3}; \quad (b_\Phi)_N = 9.6 \times 10^{-3}; \quad (b_{IF2})_N = 1.47 \times 10^{-3};$$

$$(b_R)_S = 8.6 \times 10^{-3}; \quad (b_\Phi)_S = 9.0 \times 10^{-3}; \quad (b_{IF2})_S = 1.40 \times 10^{-3}.$$

It is noted that the southern hemisphere mean values are slightly smaller than the corresponding northern mean values but the differences are not significant, as can be shown. Indeed, the t statistic[79] to test the difference between two means is given by

$$t = |\bar{x} - \bar{y}| / S(1/n_1 + 1/n_2)^{\frac{1}{2}} \tag{2.21}$$

where $\bar{x}$ and $\bar{y}$ are the two means to be compared and n_1 and n_2 the size of samples of which $\bar{x}$ and $\bar{y}$ are the means. S is the pooled estimate of standard deviation which is given by the following equation:

$$S = \left[\frac{\Sigma(x - \bar{x})^2 + \Sigma(y - \bar{y})^2}{n_1 + n_2 - 2} \right]^{\frac{1}{2}} \tag{2.22}$$

Thus by applying expressions (2.21) and (2.22) to each of the three cases, we obtain:

$$t_R = \frac{0.71 \times 10^{-3}}{0.364 \times 10^{-3}} = 1.956 \quad ; \quad t_\Phi = \frac{0.61 \times 10^{-3}}{0.346 \times 10^{-3}} = 1.774 \; ;$$

$$t_{IF2} = \frac{0.076 \times 10^{-3}}{0.0391 \times 10^{-3}} = 1.975 \; ;$$

which for $n_1 + n_2 - 2 = 45$ degrees of freedom at the 5 per cent level are not significant. Thus, the difference between north and south mean values may have arisen by chance due to the fluctuation in the calculated values of the sensitivity b.

These results are in general agreement with the findings of Appleton and Beynon[77], and others [59][63] reviewed in Appendix A.1. It should be noted here that no attempt has been made to distinguish between years of rising and years of falling activity [60][61][88]. Neither have we taken account of the effect of the secular variation of the R/IF2 relationship, of period about four solar cycles, in which Muggleton[89][90] has shown that R is at a disadvantage to Φ and IF2 as a prediction index, because the f_oE/R relationship varies with the solar cycle considered[63].

In Table 2.6 are also set out the average correlation coefficients for each station evaluated by means of expression (2.15), which implies the use of Fisher's z - transformation (2.11). These correlation coefficients have been plotted in Fig. 2.6 against geographic latitude, which illustrates their homogeneity and uniformity with latitude. Their homogeneity has been tested using the χ^2 expression (2.12). The tests [see (2.16)] showed that the twelve-month average correlation coefficients of the 47 stations for R, Φ, or IF2 could be regarded as a sample taken from a single normal population. Therefore it was legitimate to calculate the over-all combined correlation coefficients for the populations represented by the three histograms of Fig. 2.3, by means of equations (2.11), (2.13) and (2.15). The standard errors of the combined correlation coefficients were also calculated using equation (2.14). The results are summarised in Table 2.7.

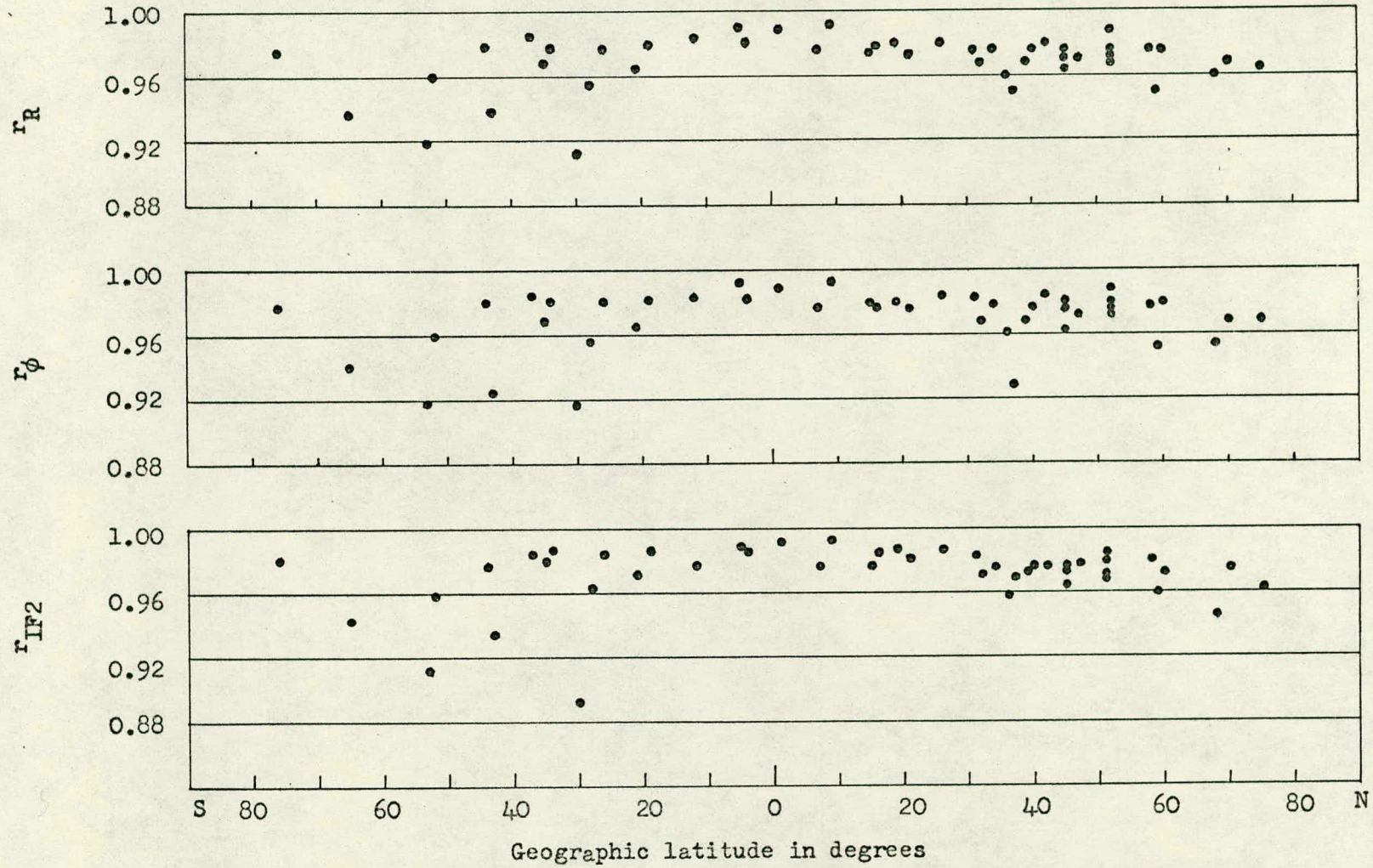

Fig. 2.6 Latitudinal distribution of the 47 combined linear correlation coefficients.

TABLE 2.7

Combined correlation coefficients, r, each one obtained from 545 linear correlation coefficients.

VARIATES	r	r ± S.E.
$(f_oE)^4$, R	0.971	0.972 - 0.9706
$(f_oE)^4$, Φ	0.973	0.974 - 0.972
(f_oE), IF2	0.974	0.975 - 0.973

It is obvious from this Table that if any difference exists between the over-all average correlation coefficients, it is very small. To ascertain by means of a statistical method whether there was a significantly greater correlation between f_oE, as used in equations (2.7), (2.8) and (2.9), and either R, Φ or IF2, the usual test of significance[81] was applied to the results given in Table 2.7, that is, the standard errors of the differences $|r_\Phi - r_R|$, $|r_\Phi - r_{IF2}|$ and $|r_{IF2} - r_R|$, have been calculated and compared to the corresponding differences of z values of the corresponding correlation coefficients. The results may be summarised as follows:

$$S.E.(z_\Phi - z_R) = S.E.(z_\Phi - z_{IF2}) = S.E.(z_{IF2} - z_R) =$$

$$= [2/\Sigma(N_i - 3)]^{\frac{1}{2}} = [2/4521]^{\frac{1}{2}} = 0.02103$$

$$u_{\Phi,R} = |z_\Phi - z_R|/S.E.(z_\Phi - z_R) = 0.0253/0.02103 = 1.20;$$

$$u_{\Phi,IF2} = 1.19 \quad ; \quad u_{IF2,R} = 2.40.$$

Since $u_{\Phi,R}$ and $u_{\Phi,IF2}$ are much less than 2, the corresponding differences are not significant at the 5 per cent level[80]. Thus, the samples may be regarded as drawn from the same parent population or from equally correlated ones.

On the other hand $u_{IF2,R}$ lies between 1.96 and 2.57, which means that the difference $|r_{IF2} - r_R|$ is significant at the 5 per cent level but it is not significant at the 1 per cent significance level[80][81]. Therefore, it is concluded that the correlation between f_oE and IF2 is significantly greater than that between $(f_oE)^4$ and R at the 5% level, but it is not at the 1% significance level. Thus, we may deduce from the preceding discussion that there is very little difference in the degree of correlation between the variates in each of the three equations (2.7), (2.8) and (2.9).

The results of this chapter enable us to conclude that in order to obtain the best linear correlations in the relations between f_oE and each of the three solar indices, R, Φ, or IF2, the models (2.7), (2.8) and (2.9) respectively should be used.

It would appear that equations (2.8), (2.19), and (2. 9),(2.20) provide the only f_oE/Φ and $f_oE/IF2$ numerical relationships contained in the ionospheric literature whilst equations (2.7) and (2.18) provide the first fourth-power relationship for f_oE and R based on such an extensive number of data, although a similar relationship has already been proposed by Allen[65].

Since there is little difference in the degree of correlation between the variates of each of the three equations (2.7), (2.8) and (2.9), the decision as to which to use for any particular purpose should be based on considerations such as secular variations[90], availability of data, convenience, and so on.

Having established a model for the solar-activity control of f_oE in this chapter the next is concerned with the diurnal variation.

CHAPTER 3

INVESTIGATION OF THE DIURNAL VARIATION OF f_oE

In the present chapter we describe the investigation of the relationship between the observed f_oE and the solar zenith angle χ on the basis of diurnal observations at 45 ionospheric stations.

It has been shown that according to Chapman theory the critical frequency f_oE is related to χ by the equation (1.7), which for convenience is rewritten here:

$$(f_oE)^4 = K \cos \chi \tag{3.1}$$

where K is given by equation (1.8). Now, if the scale height varies with constant gradient μ, equation (3.1) takes the modified form (1.9), which we write here as follows:

$$(f_oE)^4 = A(\cos\chi)^p \tag{3.2}$$

where $p = 1 + \mu$. Equation (3.2) can also be written in the more convenient logarithmic form:

$$\log(f_oE)^4 = \log A + p \log(\cos\chi) \tag{3.3}$$

since a regression analysis is used to provide the values of the slope p and the intercept $\log A$ of the straight line fitted to the observed data.

However, it should be noted here that the above equations are strictly valid only near noon when the term dN_m/dt of equation (1.4):

$$dN_m/dt = q_o \cos \chi - \alpha N_m^2 \tag{3.4}$$

is virtually zero.

If, therefore, conditions substantially away from noon are considered, corrections for the dN_m/dt term, which is neglected in equations (3.1), (3.2), (3.3), should be made. A way of doing this[5][10] is to use instead of f_oE, the average, $\overline{f_oE}$, of the morning and afternoon values at those times when χ has the same numerical value. On the other hand an estimate[7][52] of the value of the dN_m/dt term shows that this value is only 1% of each term of the right-hand side of equation (3.4) at 0900 and 1500 hours, and it becomes zero near noon.

3.1 DATA

The f_oE data employed in the present investigation are taken from 45 ionospheric stations all over the world; they are listed in Table C.1 and illustrated in Fig. C.1 of Appendix C, excluding the two stations of Maui (20.8^oN) and Rarotonga (21.2^oS). The data used are the monthly median values of f_oE for each hour mainly between 09.00 and 15.00 hours. For the above-mentioned reason regarding the validity of equations (3.2) and (3.3) the period has been limited to the hours stated. Care has also been taken to consider f_oE values in the morning and afternoon respectively corresponding to nearly the same numerical values of $\cos\chi$; so for certain months or stations the f_oE values used were those corresponding to the 0900 hrs. to 1600 hrs. period or to the 0800 hrs. to 1500 hrs. period as required. All f_oE values for which χ exceeds 78 degrees were excluded from the analysis because at high values of χ the model will be in error owing to the effect of grazing incidence. Thus, in some winter months the data are limited to four values only. When there were less than four values available the month in question was excluded from the analysis.

In addition, in order to obtain a more accurate evaluation of the parameters p and A in equation (3.2) or (3.3), the average value of $(f_oE)^4$ for the eleven years of a solar cycle was taken as the representative value for a given hour of the day in a given month, instead of the $(f_oE)^4$ value of a single year. When the values of f_oE were lacking at some hours of a given month in a given year, the data for the whole year, for the month in question in the given station, were omitted. The actual period of years used in the present statistical study is the same as that indicated in Table C.1 except for the stations listed in Table 3.1, where the appropriate period is given.

TABLE 3.1

Stations where the period of data used is different from Table C.1 of Appendix C.

STATION	Geogr. Lat.	Geogr. Long.	Period of Data
Slough	51.5°	359.4°	1954 - 1964
Washington	38.7°	282.9°	1954 - 1964
Tokyo	35.7°	139.5°	1951 - 1961
White Sands	32.3°	253.5°	1949 - 1959
Port Stanley	-51.7°	302.2°	1954 - 1964

At this point it is important to note that we are dealing with routine published data accepted at their face value, and using them to determine small departures from Chapman theory behaviour in the E-region. Therefore some questions may arise regarding the accuracy and uniformity of the values of f_oE. Daily values of f_oE are usually measured only to the nearest 0.10 or 0.05 MHz, depending on the station, and the monthly median values are tabulated to the same order of accuracy. The world-wide average error in f_oE is about $\pm$ 0.12 MHz[129].

It is also known that the characteristics of the ionospheric recorders and the accuracy of measurements may differ considerably from station to station. Moreover it is possible that tabulated values may not always refer to precisely the same "critical frequency" of the E layer[18]. Indeed, stratification in the E-region is a very frequent phenomenon[6] and could lead to some ambiguity in determination of the f_oE critical frequency. Bibl[130] has proposed a definition for f_oE which, when applied, reduces considerably the scatter of the daily measurements. This definition is somewhat arbitrary and not always accepted. Particular difficulties may arise when traces due to sporadic-E ionization are present, or when there is absorption near the critical frequency. In such cases scalings of the cusp-frequency as f_oE may lead to a lower value than the true value. These facts could have a significant effect on the value obtained for p from equation (3.3), especially when summer diurnal variation is considered. However, Beynon and Brown[9] have examined the influence of sporadic-E ionization on values of f_oE for temperate stations and found that, even in the presence of the most intense sporadic-E ionization, it is possible for the f_oE values to be practically unaffected.

In view of the above considerations, it is evidently an advantage to use a large amount of data in the analysis to eliminate random variations in f_oE. This has been followed throughout the whole investigation described in this thesis.

The f_oE data employed were taken from tabulated ionospheric data published by the National Bureau of Standards[82] and from data published by R.S.R.S., Slough[83]. The corresponding $\cos\chi$ values were obtained from the Ionospheric Stations Manual of U.R.S.I [129][131].

3.2 THE TREATMENT OF THE DATA

As already mentioned, hourly monthly median f_oE values of one solar cycle, mainly from 0900 to 1500 hours, have been examined for each of the 45 ionospheric stations named in Table C.1. In order to reduce random fluctuations in the f_oE values, the eleven-year average values of $(f_oE)^4$ have been calculated and used as the representative values at the corresponding hours of the day in each month. Then these eleven-year average values of $(f_oE)^4$ have been correlated with the corresponding $\cos\chi$ values. The analysis has been carried out individually for each month at each station, fitting equation (3.3) by the method of least squares to the corresponding pairs of data. Thus, for each month at each station the values of p_i and A_i have been determined. The subscript i refers to the month of the year. In Table 3.2 are set out for some typical stations, the monthly values of the diurnal exponent p_i of $\cos\chi$ and the values of the standard error in p_i, $s(p_i)$, which have been obtained by the least squares method. In the same Table, as an example, are also tabulated the corresponding correlation coefficients; these are very high, showing that the correlation between the two variates is highly significant. In Figs. 3.1(a),(b) and (c) is shown the variation of diurnal exponent with month of the year at some stations, typical of those used in the statistical analysis. From these figures we can see that the exponent p_i shows no apparent regular seasonal variations. In order to establish whether these monthly values of the diurnal exponent for each station are significantly different from each other, the statistical method outlined in Appendix B.1 has been applied.

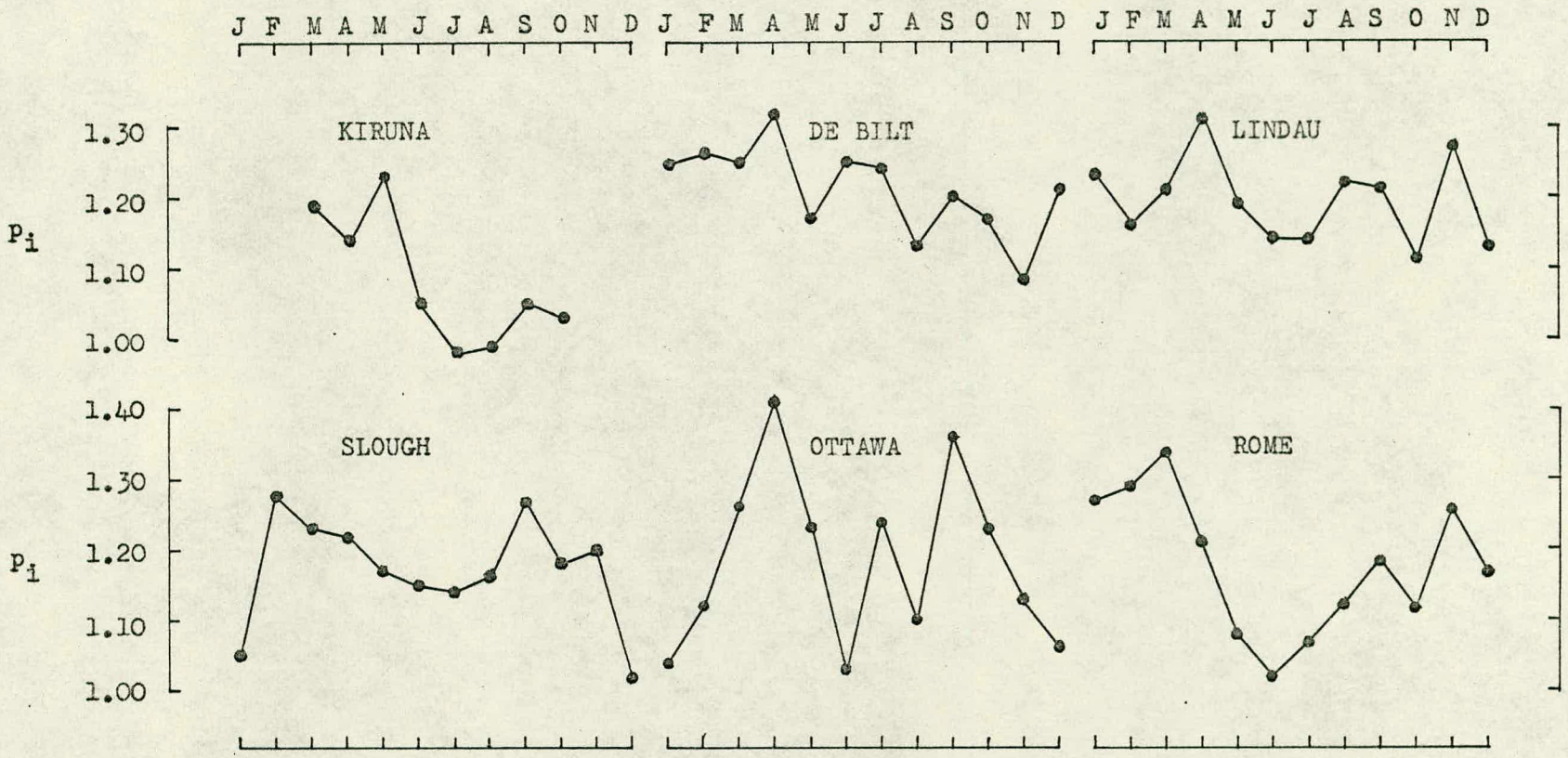

Fig. 3.1(a) Variation with month of the year of the diurnal exponent p_i in equation $(f_o E)^4 = A\,(\cos\chi)^P$ at some of the stations typical of those used in the statistical analysis.

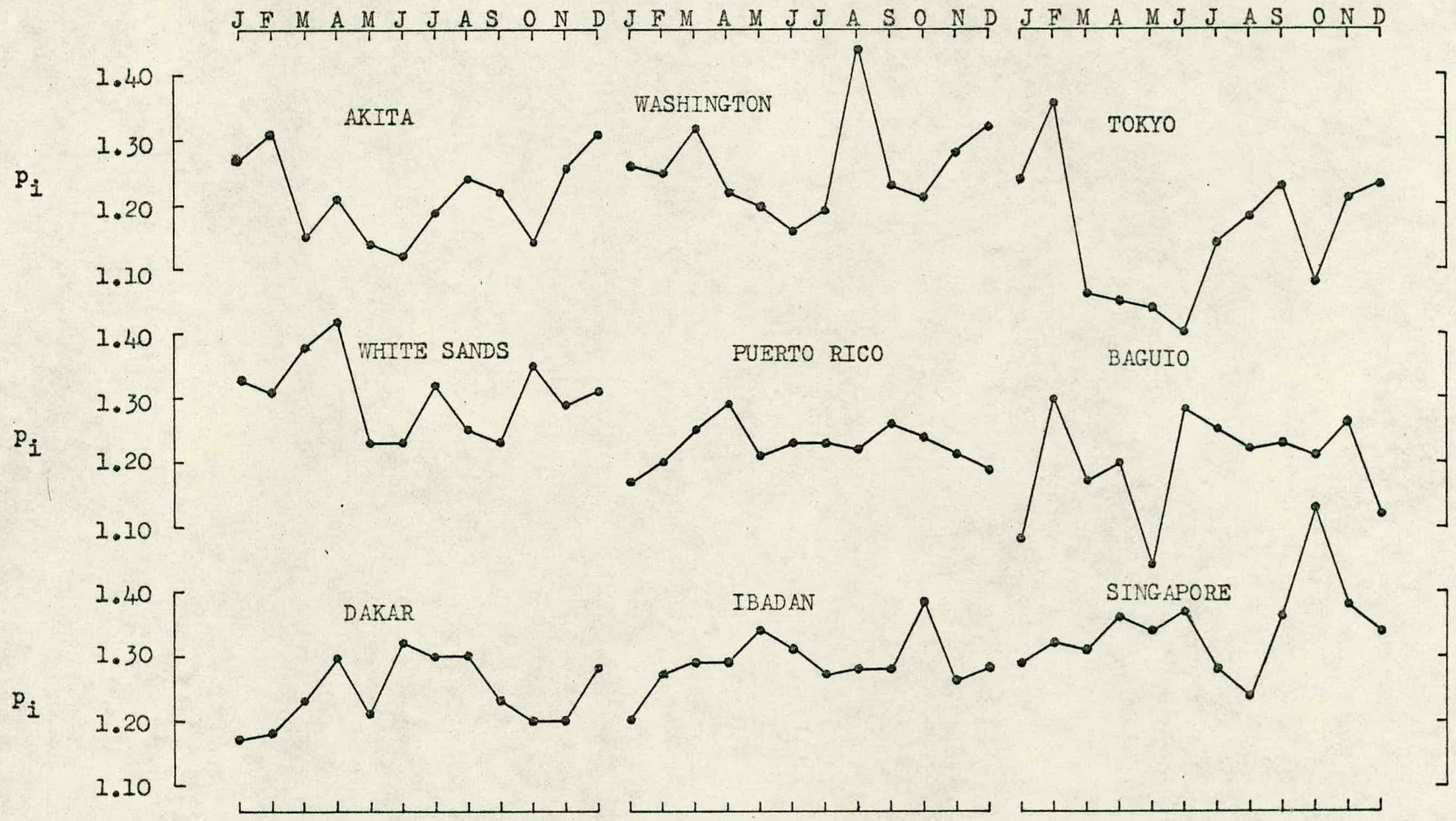

Fig. 3.1(b) Variation with month of the year of the diurnal exponent p_i.

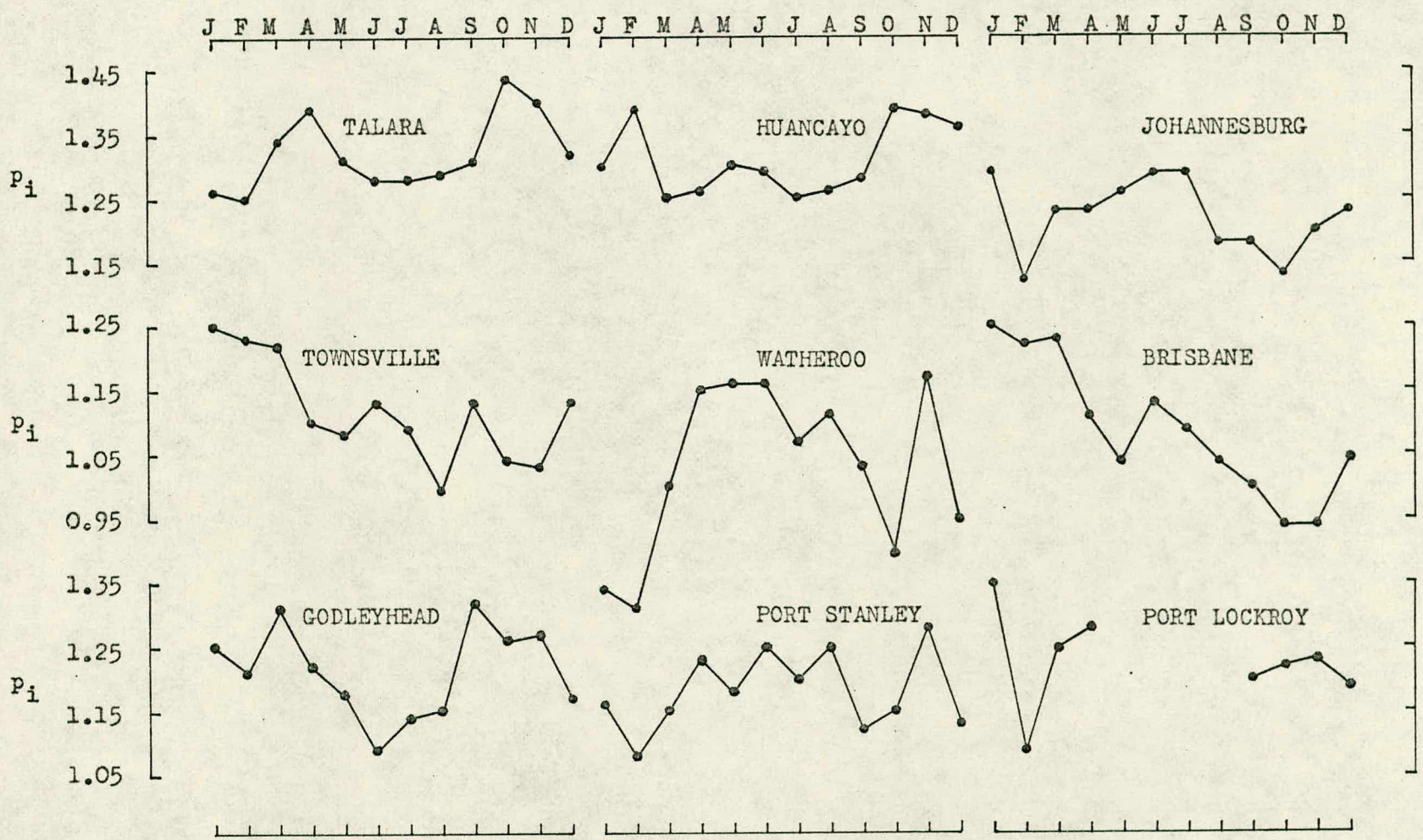

Fig. 3.1(c) Variation with month of the year of the diurnal exponent p_i.

TABLE 3.2

Monthly values of the diurnal exponent, p_i, in equation $(f_o E)^4 = A(\cos\chi)^p$ and their standard errors, $s(p_i)$, together with monthly linear correlation coefficients, r_i, and number of data, N_i, at a few stations.

	Slough (52°N)				Port Stanley (52°S)			
Month	p_i	$s(p_i)$	r_i	N_i	p_i	$s(p_i)$	r_i	N_i
Jan.	1.05	0.06	0.995	5	1.16	0.05	0.995	7
Feb.	1.28	0.04	0.998	7	1.08	0.05	0.995	7
Mar.	1.23	0.10	0.984	7	1.15	0.03	0.999	7
Apr.	1.22	0.08	0.990	7	1.23	0.07	0.992	7
May	1.17	0.06	0.990	9	1.18	0.15	0.976	5
June	1.15	0.05	0.994	9	1.25	0.23	0.968	4
July	1.14	0.06	0.990	9	1.20	0.13	0.983	5
Aug.	1.16	0.09	0.981	9	1.25	0.06	0.995	7
Sept.	1.27	0.10	0.985	7	1.12	0.07	0.990	7
Oct.	1.18	0.08	0.988	7	1.15	0.05	0.995	7
Nov.	1.20	0.07	0.993	6	1.28	0.07	0.991	8
Dec.	1.02	0.04	0.998	5	1.13	0.06	0.992	8

	Akita (40°N)				Godleyhead (44°S)			
Month	p_i	$s(p_i)$	r_i	N_i	p_i	$s(p_i)$	r_i	N_i
Jan.	1.27	0.03	0.999	7	1.25	0.07	0.991	8
Feb.	1.31	0.04	0.998	7	1.21	0.06	0.992	8
Mar.	1.15	0.16	0.956	7	1.31	0.02	0.999	8
Apr.	1.21	0.07	0.989	8	1.22	0.04	0.997	8
May	1.14	0.11	0.971	8	1.18	0.02	0.999	6
June	1.12	0.06	0.991	8	1.09	0.04	0.998	6
July	1.19	0.05	0.994	8	1.14	0.06	0.995	6
Aug.	1.24	0.13	0.969	8	1.15	0.02	0.999	8
Sept.	1.22	0.09	0.985	8	1.32	0.05	0.996	8
Oct.	1.14	0.05	0.995	8	1.26	0.04	0.997	8
Nov.	1.25	0.04	0.997	8	1.27	0.09	0.985	8
Dec.	1.31	0.04	0.998	6	1.17	0.06	0.993	8

Cont.

TABLE 3.2 Continued

	Ibadan (7°N)				Huancayo (12°S)			
Month	p_i	$s(p_i)$	r_i	N_i	p_i	$s(p_i)$	r_i	N_i
Jan.	1.20	0.04	0.997	7	1.30	0.10	0.986	7
Feb.	1.27	0.07	0.992	7	1.39	0.05	0.997	7
Mar.	1.29	0.05	0.996	7	1.25	0.07	0.993	7
Apr.	1.29	0.04	0.998	7	1.26	0.06	0.995	7
May	1.34	0.04	0.998	7	1.30	0.04	0.998	7
June	1.31	0.06	0.994	7	1.29	0.01	0.9998	7
July	1.27	0.06	0.994	7	1.25	0.02	0.999	7
Aug.	1.28	0.05	0.997	7	1.26	0.04	0.998	7
Sept.	1.28	0.04	0.998	7	1.28	0.06	0.995	7
Oct.	1.38	0.01	0.9998	7	1.39	0.06	0.996	7
Nov.	1.26	0.03	0.998	7	1.38	0.06	0.996	7
Dec.	1.28	0.02	0.999	7	1.36	0.05	0.996	7

The procedure for testing whether the individual slopes p_i of equation (3.3) are significantly different from one another is to test by means of the F test, whether the difference between the deviations using the pooled slope, and using individual slopes, is significant. If this difference is not significant the individual slopes may be pooled to obtain a better estimate of the exponent of $\cos\chi$.

In Fig. 3.2(a) are plotted the values of the variance about the regression against the mean values of the monthly sample of $\ln(\cos\chi)$ and of $\ln(f_0E)^4$ respectively. In Figs. 3.2(b) and (c) are shown plots of the variance about the regression with month of the year, and with corresponding slope, respectively. These figures illustrate that the condition that the variance of estimate be independent and uniform is satisfied, and therefore the F test can be applied[132].

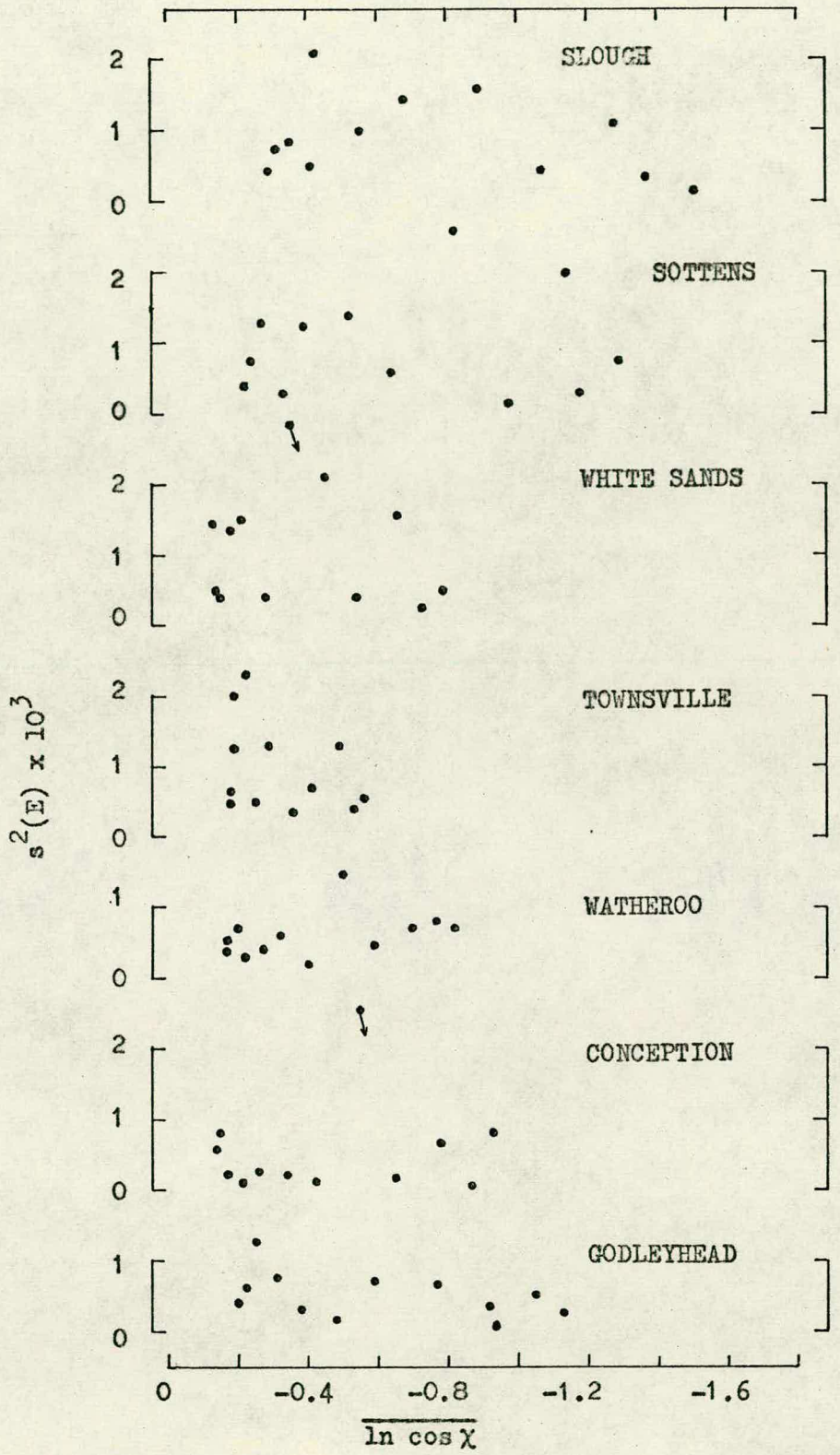

Fig. 3.2(a') Plots of the variance about the regression against the mean value $\overline{\ln \cos \chi}$ of the monthly sample for some stations. The independence and uniformity of the variance about the regression $s^2(E)$ is evident.

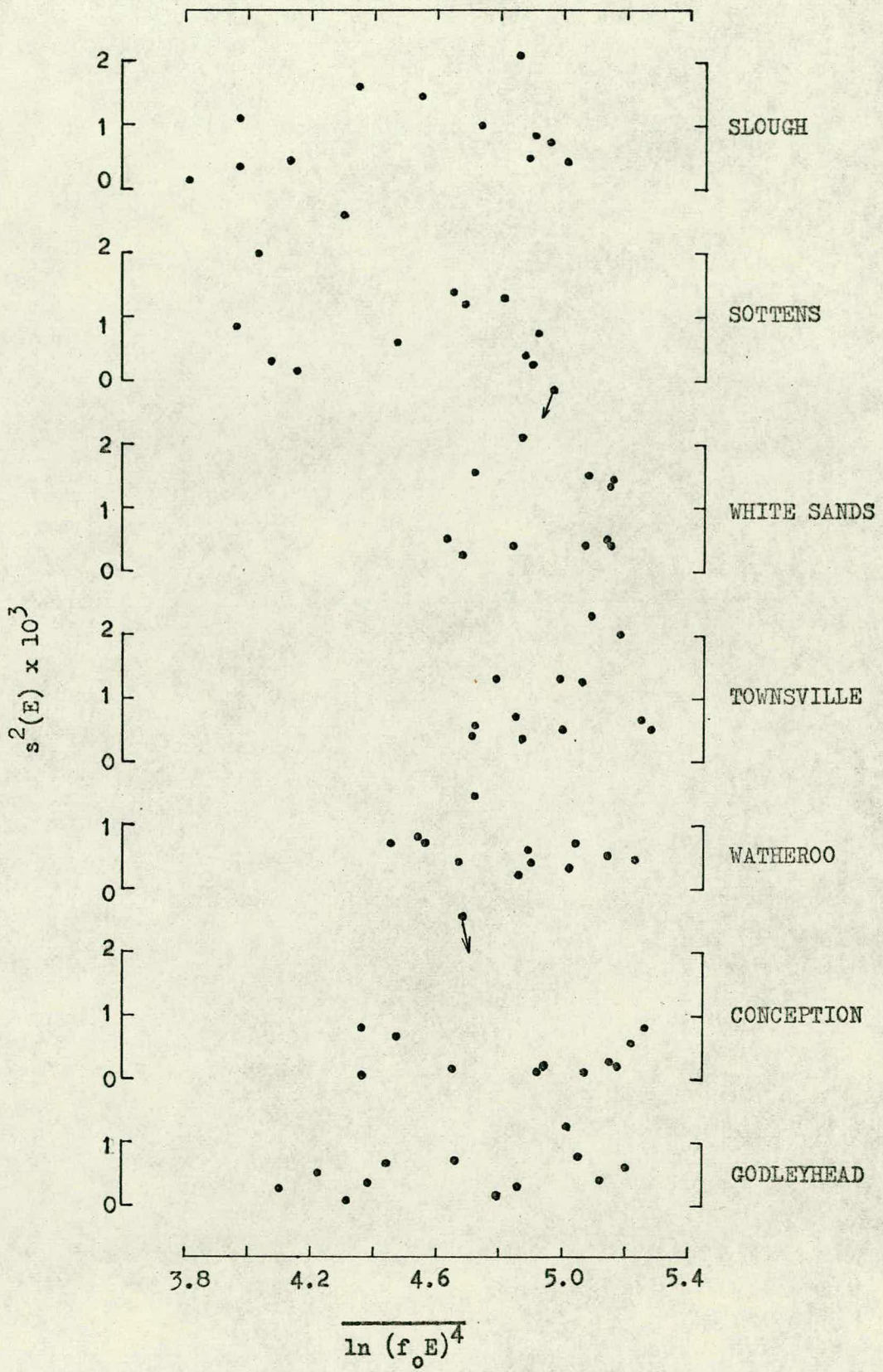

Fig. 3.2(a") Plots of variance about the regression against the mean value $\overline{\ln(f_o E)^4}$ of the monthly sample for some stations. The independence and uniformity of the variance about the regression $s^2(E)$ is evident.

EX BIBL UNIV. EDINBURGEN

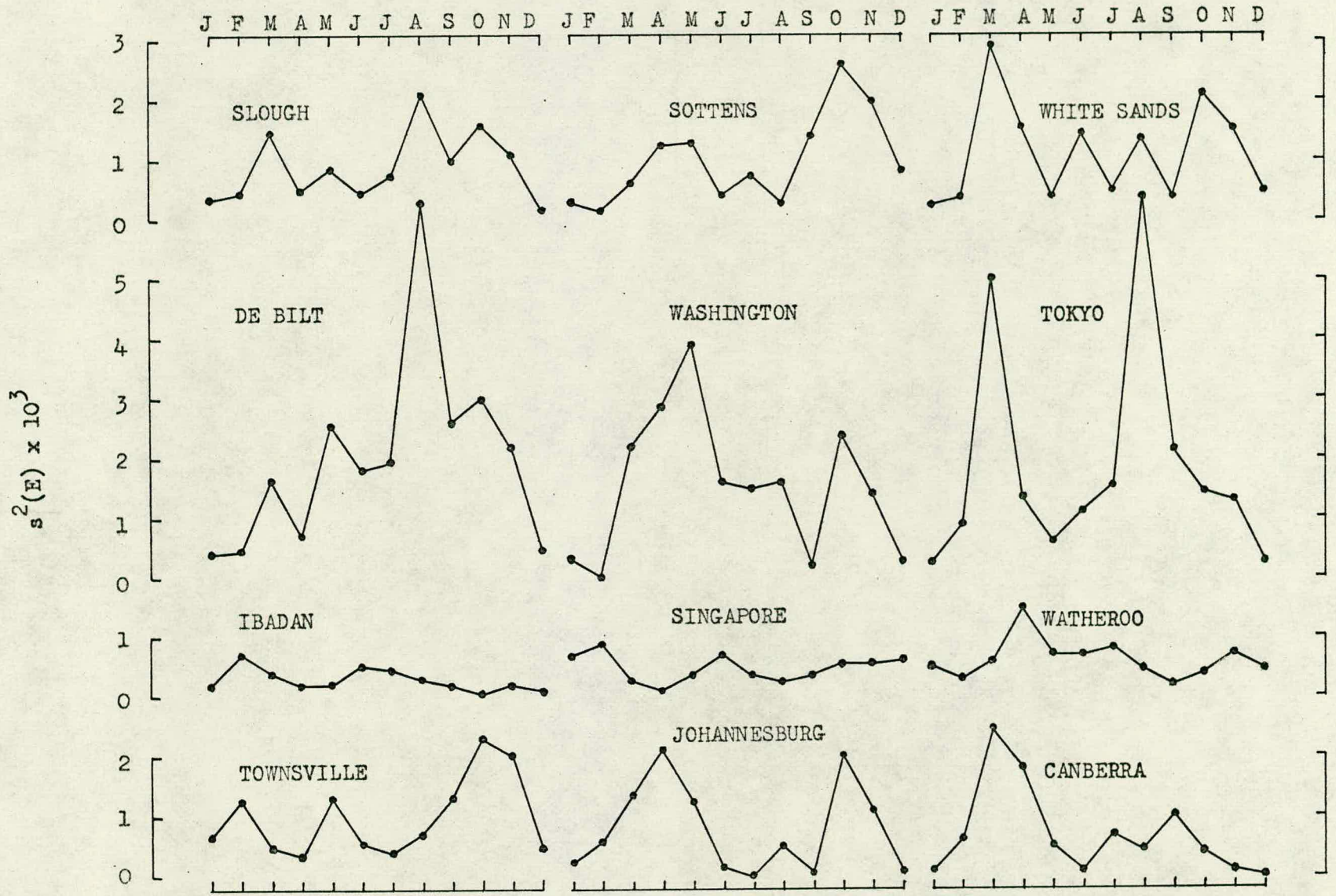

Fig. 3.2(b) Plots of the variance of estimate with month of the year.

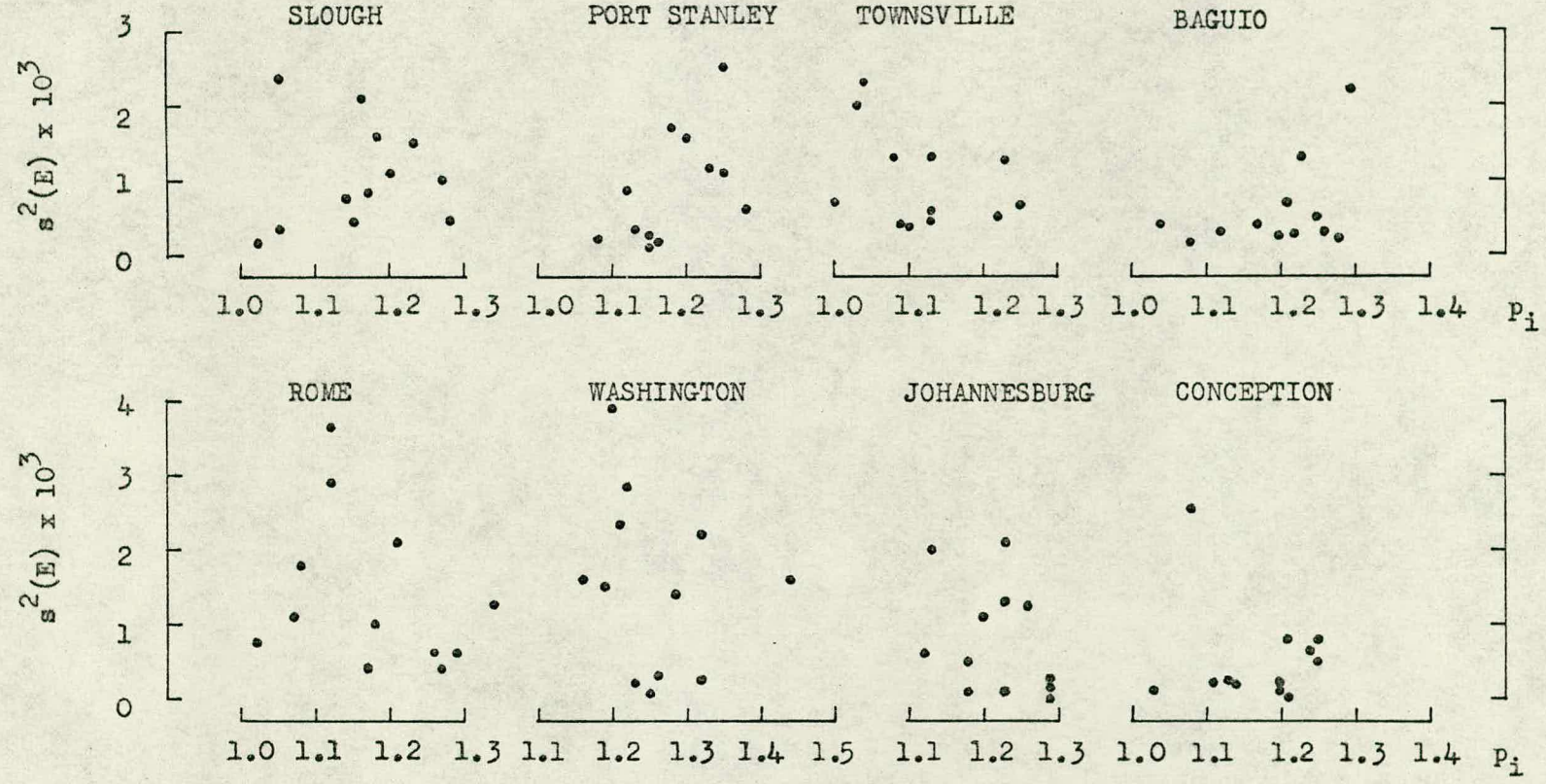

Fig. 3.2(c) Plots of variance of estimate with regression coefficient p_i at a few stations, showing the independence and uniformity of $s^2(E)$.

TABLE 3.3

Pooled slopes, p, and their standard errors, s(p), for each station, together with the corresponding F-ratio values at $\nu_1 = (K - 1)$ and $\nu_2 = (N - 2K)$ degrees of freedom. The F values indicate that within each station the monthly p_i values may be pooled for a better estimate of the slope.

Station	θ°	p	s(p)	F	ν_1	ν_2
Resolute Bay	74.7	1.24	0.040	3.16	6	37
Tromso	69.7	1.05	0.038	1.54	7	37
Kiruna	67.8	1.11	0.029	1.18	7	37
Oslo	60.0	1.16	0.030	1.00	8	44
Churchill	58.8	0.87	0.051	1.26	8	51
Inverness	57.5	1.22	0.029	0.96	9	46
De Bilt	52.1	1.22	0.020	0.65	11	74
Adak	51.9	1.21	0.017	2.82	11	54
Lindau	51.6	1.18	0.022	0.46	11	52
Slough	51.5	1.18	0.021	0.94	11	63
Sottens	46.7	1.17	0.018	1.48	11	67
Ottawa	45.4	1.17	0.023	2.14	11	57
Wakkanai	45.4	1.06	0.030	18.81	11	65
Genova	44.6	1.28	0.022	2.06	11	67
Rome	41.9	1.22	0.024	0.99	11	60
Akita	39.7	1.22	0.020	0.74	11	67
Washington	38.7	1.26	0.024	0.51	11	62
S. Francisco	37.4	1.27	0.029	1.34	11	60
Tokyo	35.7	1.17	0.024	1.56	11	69
Casablanca	33.6	1.22	0.020	1.30	11	72
White Sands	32.3	1.31	0.023	0.36	11	60
Yamagawa	31.2	1.19	0.019	2.81	11	72
Okinawa	26.3	1.17	0.018	1.99	11	72
Puerto Rico	18.5	1.22	0.012	1.30	11	72
Baguio	16.4	1.19	0.020	1.49	11	60
Dakar	14.7	1.23	0.013	1.30	11	84
Panama Canal	9.4	1.31	0.012	2.81	11	72
Ibadan	7.4	1.29	0.013	1.02	11	60

TABLE 3.3 Continued

Station	θ°	p	s(p)	F	ν_1	ν_2
Singapore	1.3	1.34	0.018	1.60	11	60
Leopoldville	-4.4	1.28	0.017	2.50	11	72
Talara	-4.6	1.32	0.023	0.54	11	72
Huancayo	-12.0	1.31	0.015	1.07	11	60
Townsville	-19.3	1.11	0.016	1.92	11	72
Johannesburg	-26.2	1.23	0.020	0.66	11	60
Brisbane	-27.5	1.08	0.025	1.26	11	60
Watheroo	-30.3	1.07	0.016	7.61	11	72
Cape-town	-34.1	1.25	0,013	1.61	11	60
Canberra	-35.3	1.15	0.022	3.79	11	60
Conception	-36.6	1.18	0.017	1.52	11	60
Hobart	-42.9	1.17	0.022	3.63	11	59
Godleyhead	-43.6	1.21	0.015	2.39	11	66
Port Stanley	-51.7	1.20	0.021	0.64	11	55
Campbell Is.	-52.5	1.12	0.019	1.97	11	60
Port Lockroy	-64.8	1.22	0.032	0.38	7	47
Halley Bay	-75.5	1.15	0.044	2.76	5	37

The F-ratio is given by equation (B.1) of the Appendix B and the corresponding degrees of freedom, ν_1 and ν_2, by equations (B.3) and (B.4). The corresponding calculated values are listed in Table 3.3. The important result is noted that for almost all stations the calculated F values do not exceed the tabulated F values at the 5 per cent level or at the 1 per cent level for the corresponding degrees of freedom. Exceptions are the stations of Wakkanai and Watheroo, for which the calculated F values were high. As an example for comparison we report here the tabulated F values which should not be exceeded for $\nu_1 = 11$ and $\nu_2 = 60$ degrees of freedom; they are F = 1.95 at the 5 per cent level and F = 2.56 at the 1 per cent level.

Thus, the statistical analysis has shown that, for the data involved, there is no basis for using different slopes for the different month-sets of data. The pooled exponent will be the best estimate to use. Therefore, for each station the individual monthly exponents p_i have been pooled using equation (B.5). The standard error s(p) of the pooled slope has also been computed from equation (B.7). The results are summarised in Table 3.3. Fig. 3.3 illustrates the latitudinal distribution of the pooled exponent. The variance about the pooled regression lines for each station has also been calculated using equation (B.6) and plotted against geographic latitude in Fig. 3.4.

It may now be asked whether the pooled slopes are significantly different from each other or if a better over-all estimate of the slope will be obtained if the slopes are pooled. The comparison of the pooled exponents of each station can be made in a manner similar to the comparison of the individual monthly exponents. The method is described in detail in Appendix B.2.

From Fig. 3.4 it can be seen that the variance about the regression is independent of latitude and may be assumed to be the same for each station, the small fluctuations in $s^2(E_p)$ being random. Therefore the required condition for applying the theorem of comparison of several regression lines[132] is satisfied and the procedure outlined in Appendix B.2 may be applied. The F-ratio corresponding to all month-samples of data of the 45 stations, using an over-all pooled slope and using "individual-pooled" slopes for each station, was calculated from equation (B.10). The degrees of freedom associated with the F-ratio, for numerator and denominator respectively, are given by equations (B.14) and (B.15).

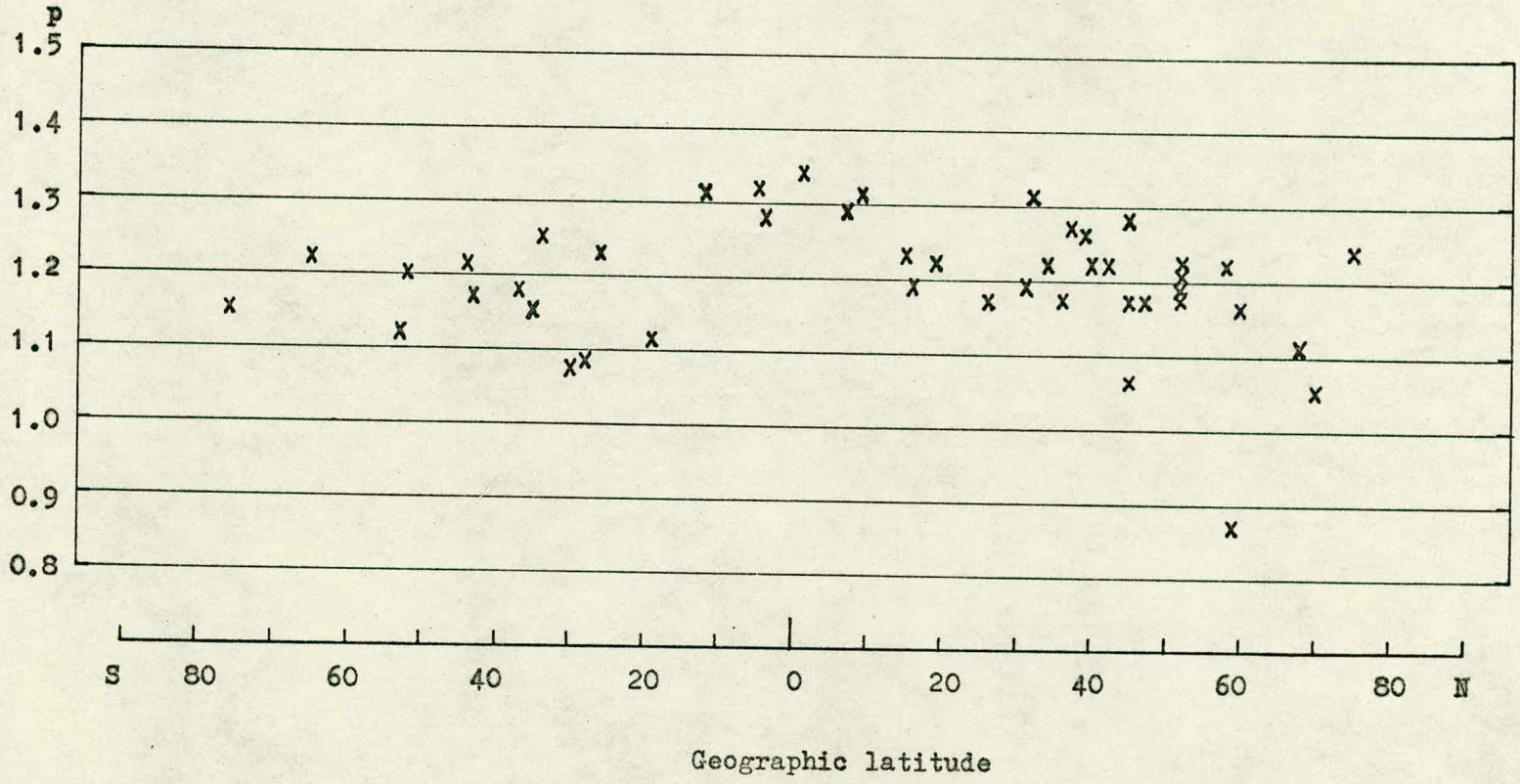

Fig. 3.3 Latitudinal distribution of the diurnal exponent p in equation $(f_oE)^4 = A(\cos\chi)^p$, for 45 stations.

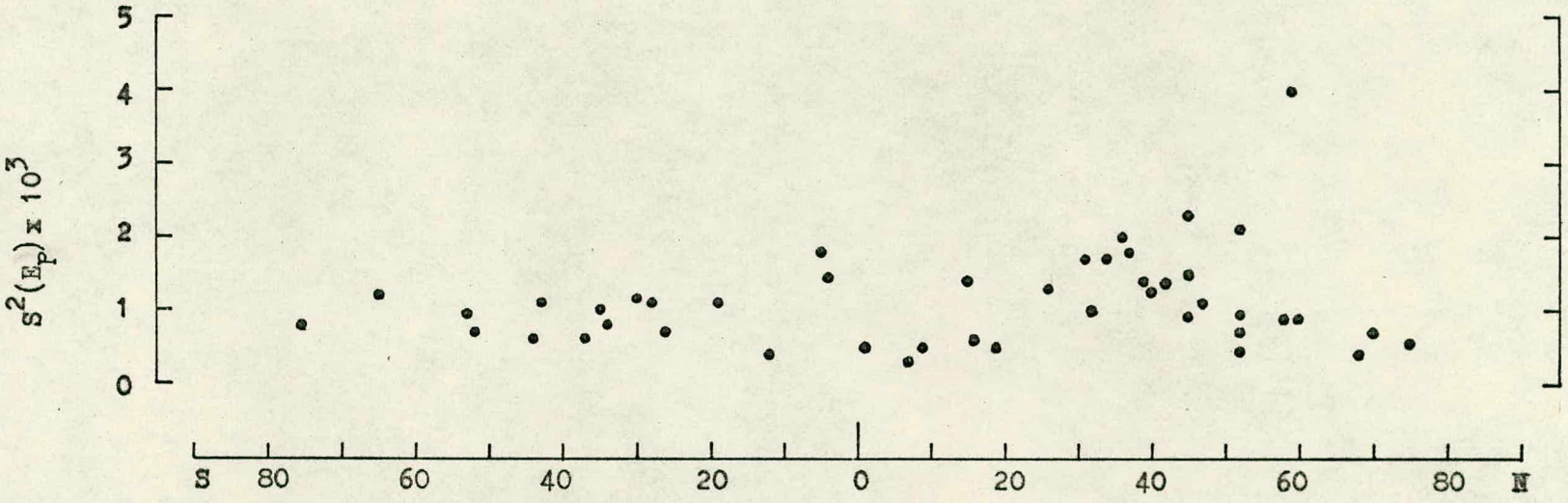

Fig. 3.4 Plot of variance about the pooled regressions (45 stations) with geographic latitude, showing the independence and uniformity of $s^2(E_p)$.

The calculated values thus determined are:

$$F = 1.03 \; ; \; \nu_1 = 508 \; ; \; \nu_2 = 2725$$

The tabulated F value is 1.11 for 508 and 2725 degrees of freedom at the 5 per cent significance level, indicating that there is no significant difference between the slopes of the different stations. Therefore, they may be pooled for a better over-all estimate of the diurnal exponent of $\cos\chi$.

The "over-all pooled" slope has been accordingly evaluated from equation (B.16) and its standard error from equation (B.18).

3.3 RESULTS AND DISCUSSION

The monthly values of the diurnal exponent p_i in equations (3.2) or (3.3) were obtained for each month and station by the least squares method from an examination of the data from 0900 to 1500 hours of eleven-year average values of $(f_oE)^4$ and corresponding $\cos\chi$ values. In Figs. 3.1(a),(b),(c) the individual exponents thus determined are plotted against month of the year for some of the stations used in the analysis. These figures illustrate that the exponent does not show any systematic seasonal variation. This important result has also been demonstrated by means of the F test. The calculated F values together with the corresponding degrees of freedom are listed in Table 3.3, indicating that with the amount of scatter of the individual sets of measurements involved in the analysis, the observed difference between the individual monthly exponents is not significant.

In this context it is interesting to note, as extensively reported in Appendix A.2, that conflicting results have been obtained by various previous workers.

Indeed, Tremellen and Cox[68], and Scott[69] have found that p_i has a minimum value in local winter, whereas Menzel and Wolbach [133][134] have reported that the exponent p_i has maximum values at the equinoxes and minimum values at the solstices; and Appleton and Lyon[10] have found for northern temperate stations that the value of the exponent has minima in local summer and maxima in local winter. An explanation of these conflicting results could be that these workers have examined only a small amount of data or a limited number of stations. This is supported by the results illustrated in Figs. 3.5. Fig. 3.5(a) shows the latitudinal distribution of the mean values of the diurnal exponent for November, December, January, and for May, June and July respectively; while Fig. 3.5(b) illustrates the latitudinal distribution of the mean values of the exponent for March and September. A careful examination of these figures reveals that maxima or minima could be found in all seasons; and therefore the choice of a few stations could lead to erroneous deductions. In other words, the diurnal exponent of $\cos\chi$ does not show any regular variation with season. This important fact can also be noted in the results of Eyfrig[135], though not explicitly reported by him. However it is stated in the work of Appleton published by Muggleton[13]. It is also reported by Rao and Malhotra[61] for the f_0E data at Ahmedabad only, and stated in the work of Swenson[17], where some stations lying inside a very limited latitude zone ($\pm 15^\circ$) were examined. However the above statements were made on a graphical basis only.

Since there was no significant difference between the monthly exponents of each station, they have been pooled for a better estimate of the exponent of $\cos\chi$.

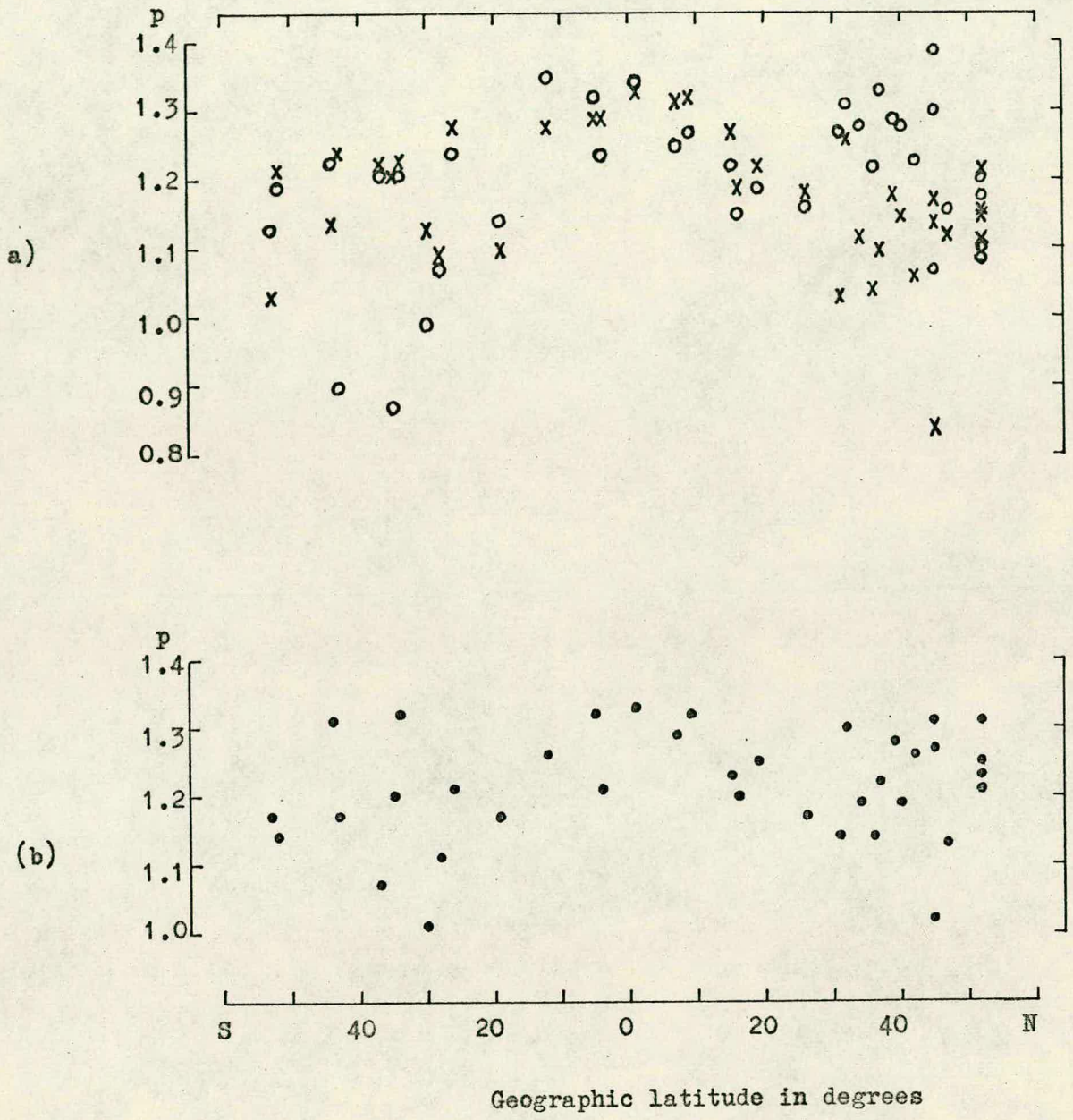

Fig. 3.5 Latitudinal distribution of the diurnal exponent p.
a) (X) mean value of May, June, July and
(o) mean value of November, December, January.

b) mean value of March and September.

The pooled exponents p for each station are shown in Table 3.3 together with their standard errors, s(p), and are illustrated in Fig. 3.3. It can be seen from Fig. 3.3 that p does not alter appreciably with latitude. Moreover it has been demonstrated statistically, using the F test (Section 3.2), that the p values of the 45 stations were not significantly different from one another. This important result contradicts those of Harnischmacher[14], and of Menzel and Wolbach[133][134], who found that the exponent decreases with increasing latitude; but it is in agreement with the statements of Eyfrig[135], Appleton and Lyon[10], Appleton published by Muggleton[13], and Swenson[17], who have all reported that the exponent is substantially independent of latitude. Since Harnischmacher states that his expression for the exponent, given by equation (A.3), is unreliable for $\theta > 60^{\circ}$, the above result is further confirmed, as can be seen from Fig. 3.6(a), which illustrates the distribution with geographic latitude of the pooled exponents at 40 stations lying in latitudes below a geomagnetic latitude of 60°. Moreover, if the data points of Fig. 3.6(a) are fitted to a linear regression line, the obtained correlation and regression coefficients are not significantly different from zero, indicating that there is no linear dependence on latitude. In Fig. 3.6(b) and (c) the p values are plotted against geographic, geomagnetic and magnetic latitude of stations centred approximately on the meridian 5 and 150 degrees East respectively (see Fig. C.1 in Appendix C), showing no dependence on latitude.

The 45 values of p were pooled to obtain a better over-all estimate. The "over-all pooled" value of p and its standard error are given by the expressions:

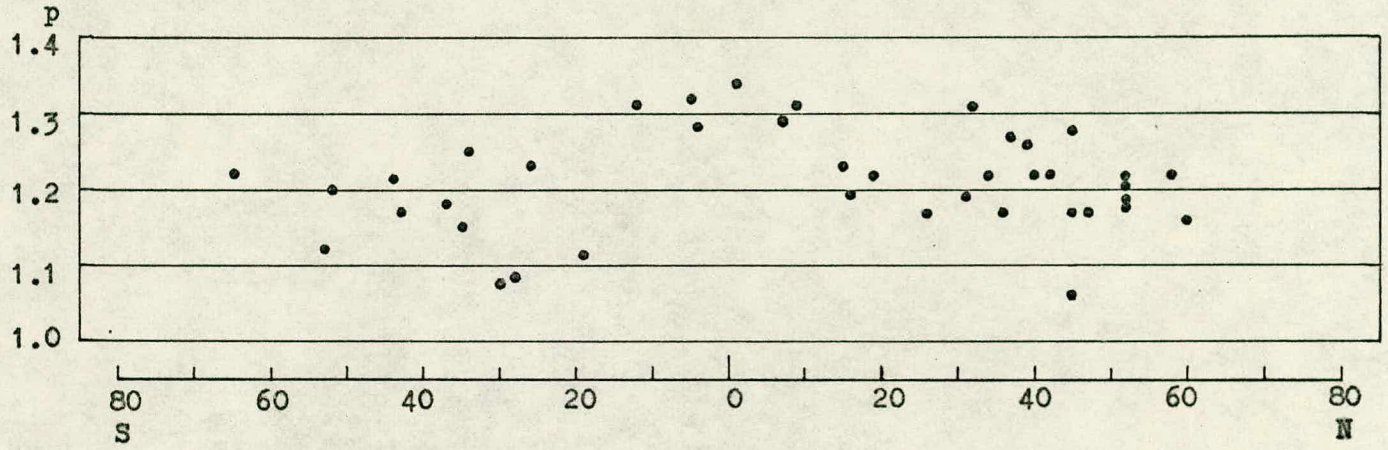

Fig. 3.6(a) Latitudinal distribution of the twelve-month pooled exponent p (40 stations).

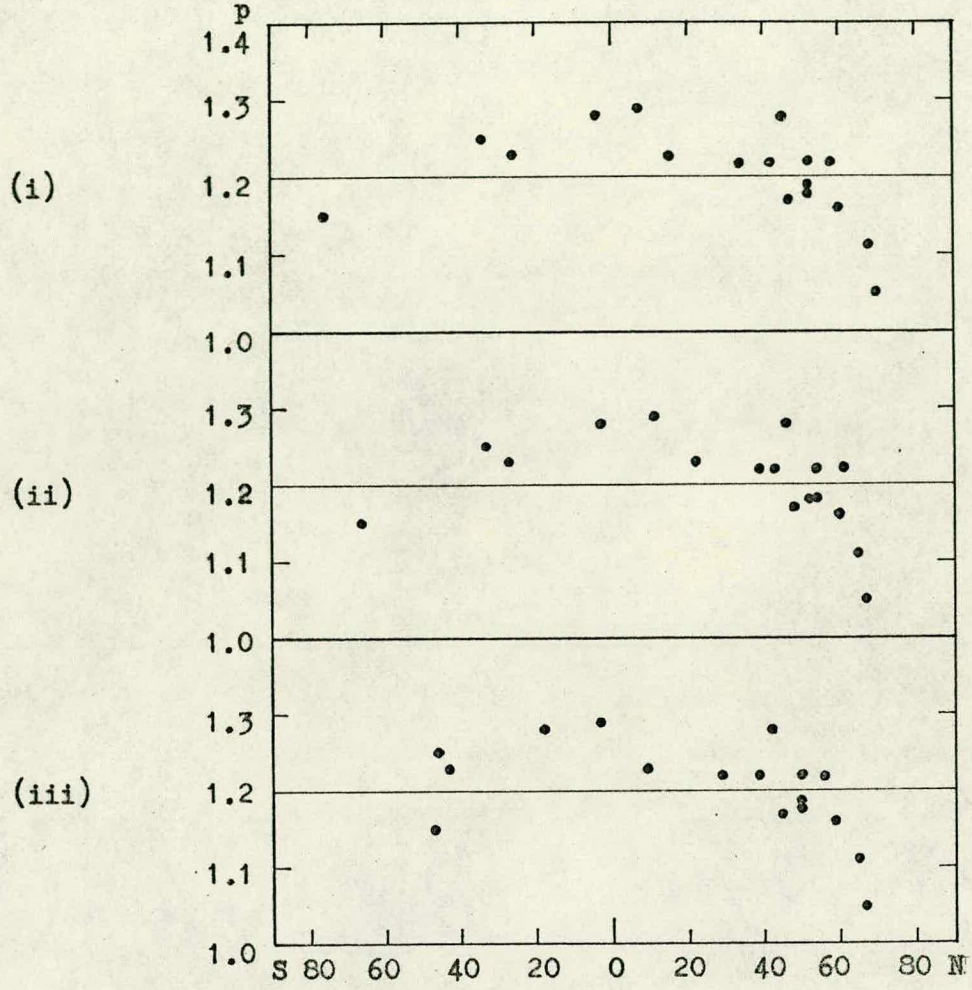

Fig. 3.6 (b) Latitudinal distribution of the diurnal exponent p for stations centred on the 5°E meridian against

(i) geographic latitude

(ii) geomagnetic latitude

(iii) magnetic latitude

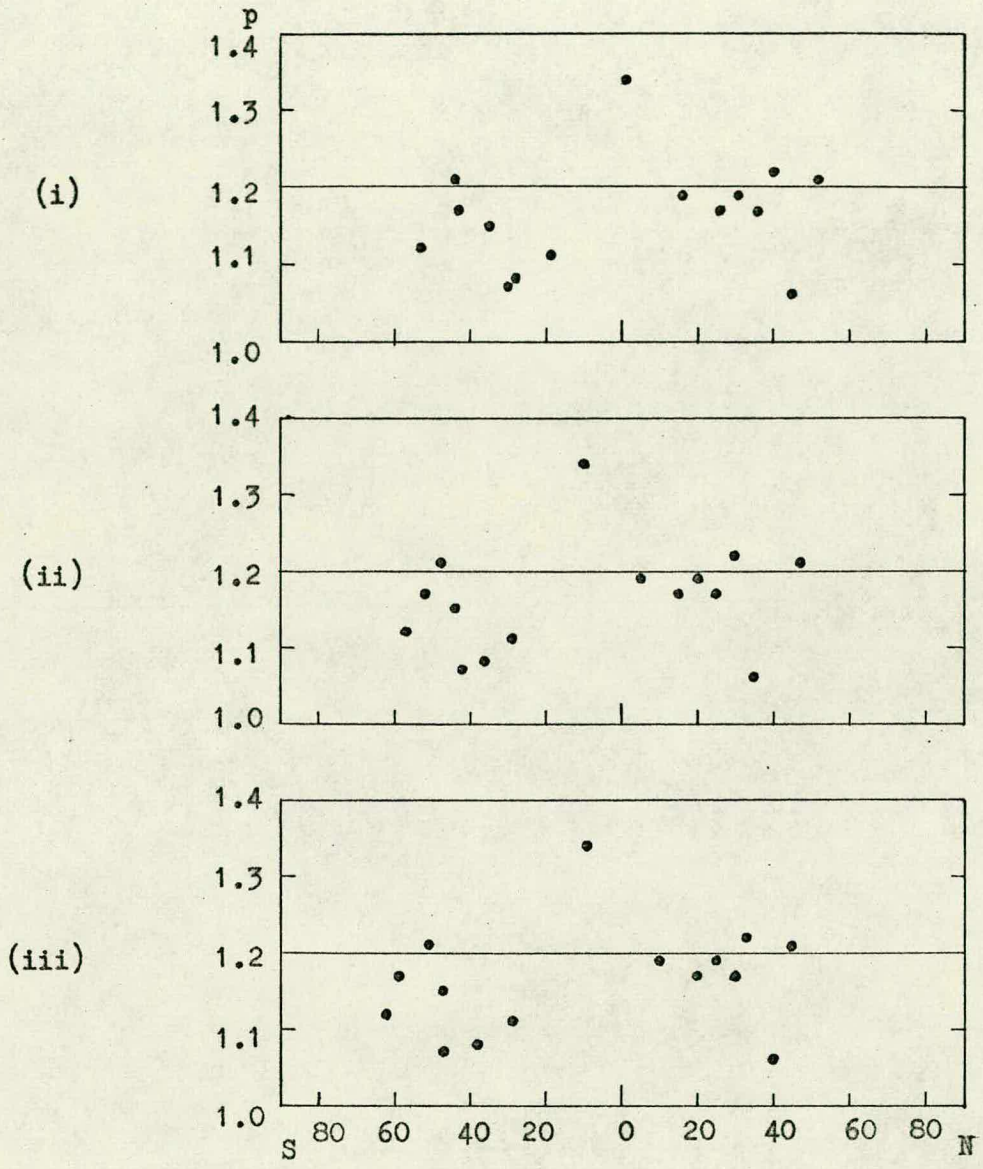

Fig. 3.6(c) Latitudinal distribution of the diurnal exponent p for stations centred on the 150° E meridian against

(i) geographic latitude

(ii) geomagnetic latitude

(iii) magnetic latitude.

$$\bar{p} = \Sigma_j p_j \Sigma_i \Sigma(x - \bar{x})^2 / \Sigma_j \Sigma_i \Sigma(x - \bar{x})^2 \qquad (3.5)$$

and

$$s(\bar{p}) = [s^2(\bar{E}_p) / \Sigma_j \Sigma_i \Sigma(x - \bar{x})^2]^{\frac{1}{2}} \qquad (3.6)$$

with $j = 1,2,3,\ldots\ldots, S$; and $i = 1,2,3,\ldots\ldots, K_j$; and where $\Sigma(x - \bar{x})^2$, is, as usual, the sum of squares of deviation of the independent variable, $\log \cos\chi$, in equation (3.3), for the month i and the station j. $s^2(\bar{E}_p)$ is the variance about the "over-all pooled" regression, K_j is the number of months for the jth station and S is the number of stations. The calculated values are as follows:

$$\bar{p} = 1.203 \; ; \; s(\bar{p}) = 0.003 \qquad (3.7)$$

Although the F test showed that there is no significant difference in the 45 values of p, considering the amount of scatter of the individual month-sets of data involved in the statistical analysis, and although Figs. 3.3 and 3.6 indicate that there is no linear correlation between p and latitude, some distinction may be made between the p values. Indeed, it is evident from these figures that the values of the diurnal exponent p for stations in the auroral zone never reach the over-all mean value of 1.203. This is also the case for nearly all the individual monthly values, p_i, of the auroral stations, as for example is shown in Fig. 3.1(a) for Kiruna. Stations like Tromso or Churchill have still smaller values than Kiruna (Table 3.3). For Churchill, for example, has been found $p = 0.87$, which is somewhat greater than the corresponding value given by Scott[69]. Now, if we consider only stations of less than about 60° of geomagnetic latitude a better homogeneity in the p values is reached as can be seen from Fig. 3.6(a) for example.

We may also note from Fig. 3.6 that the value of p for stations lying within the latitudes of about $\pm 12^{o}$ are persistently around 1.30 rather than around 1.20, which is also observed in the monthly values p_i for these stations as can be seen in Fig. 3.1. Thus, although the difference in the total of the 45 values of p is not significant, it is perhaps more realistic to divide the 40 stations of geomagnetic latitude less than 60 degrees into two groups: (a) the equatorials and (b) the stations of latitude higher than about $\pm 12^{o}$. If equations (3.5) and (3.6) are used to find the "over-all pooled" slopes and their standard errors in the two groups, the calculated values are as follows:

$$\begin{aligned} &\text{(a) equatorials:} \quad \bar{p} = 1.305 \ ; \ s(\bar{p}) = 0.007 \\ &\text{(b) non-equatorials:} \quad \bar{p} = 1.191 \ ; \ s(\bar{p}) = 0.004 \end{aligned} \tag{3.8}$$

For the total of 40 equatorial and non-equatorial stations the corresponding values are:

$$\bar{p} = 1.208 \ ; \ s(\bar{p}) = 0.003 \tag{3.9}$$

The over-all average value of the diurnal exponent of $\cos\chi$ for non-equatorial stations is very close to the previous value, 1.203, given by (3.7), and to the value given by Robinson[6][24], Eyfrig[135], Piggott and Thrane[136] and others, as reported in detail in Appendix A.2. The over-all average value of p in equation (3.2) or (3.3) for equatorial stations is close to the values given by Harnischmacher[14], and Menzel and Wolbach[133][134], for stations near the equator, but it is greater than the value given by Swenson[17] for almost the same stations.

A possible reason why p is greater than 1, the theoretical value, is the existence of a positive scale height gradient, $\mu = dH/dh \fallingdotseq 0.2$ as discussed in detail by Robinson[6][24].

It should be noted that no attempt has been made here to investigate whether p shows any systematic change with solar activity. As mentioned in Appendix A.2, earlier workers have reported a variation with solar activity, their results being sometimes contradictory, whereas more recent workers have found no variation with solar activity.

From the foregoing discussion it is concluded that an average world-wide value of the diurnal exponent, p, is given by (3.7), although the value of $\bar{p}$ given by (3.8)(a) is perhaps more suitable for the equatorial stations.

The next requirement is to establish a model for the seasonal variation of A in equation (3.2). This work is described in Chapter 4.

CHAPTER 4

THE APPLETON E-LAYER SEASONAL ANOMALY

The E-layer seasonal anomaly was first identified by Appleton [10][11] by studying $(f_oE)^2$ under conditions of constant $\cos\chi$ and R. It was thus found that $(f_oE)^2$ is less in local summer than in local winter under the same conditions of $\cos\chi$ and R. Moreover the seasonal anomaly was found to be characteristic of the latitude of the station, but independent of the particular value of constant $\cos\chi$ used[13] and of the level of solar activity[11]. A detailed review of this and other anomalies is given in Appendix A.3.

4.1 INVESTIGATION OF THE WORLD MORPHOLOGY OF THE ANOMALY

The object of the investigation described below has been to determine the latitudinal dependence of the Appleton E-layer seasonal anomaly. For this purpose the seasonal anomaly at 45 stations chosen to provide a world-wide distribution has been determined by means of equation (3.3), which is rewritten here for convenience as follows:

$$\log(f_oE)^4 = \log K + p \log(\cos\chi) \qquad (4.1)$$

As described in Section 3.2, the data points of each month of the year at a given station, that is, the eleven-year average of the hourly values of $(f_oE)^4$ and the corresponding values of $\cos\chi$, were fitted to the best straight line corresponding to equation (4.1). Thus, for each month, i, the value of K_i has been determined by the least squares method for each station. According to Chapman's theory the value of K_i should be constant; instead it was found that K_i exhibits both seasonal and annual variations (see also Appendix A.3).

If the K_i values are corrected for the annual effect[118] and for solar activity, then the variation of the corresponding corrected values, A_i, over the months of the year represents what Appleton called the seasonal anomaly.

This method of determining the seasonal anomaly is essentially the same as was used by Appleton[13]. He found that the variation of A_i throughout the year for any given station was exactly the same as that obtained from constant $\cos\chi$ studies at the same station.

Now, in the statistical study of the diurnal exponent, p, of $\cos\chi$ in equation (4.1), described in Chapter 3, it was found that there was no significant difference between the monthly exponents for a given station and therefore they were pooled for a better estimate of the exponent for each station. These pooled exponents in turn were not significantly different, and therefore they have been pooled for a better over-all estimate of the exponent of $\cos\chi$. The over-all average values of p thus determined for equatorial and non-equatorial stations are given by (3.8). Using these values of p and equations (B.19) and (B.20) of Appendix B, the value K_{ji} for the month i and station j, and its standard error, $s(\log K_{ji})$, have been recalculated.

Next, the K_{ji} values thus determined have been corrected for solar activity and varying Sun-Earth distance. For this purpose equation (2.8) and the value $b_{\bar{\Phi}}$ given by (2.19) have been used. In other words, each K_{ji} value has been divided by $(1 + 0.0094\ \Phi_{ji})$, where Φ_{ji} is the corresponding eleven-year average value of the observed value of 10.7 cm solar radio noise flux referred to a mean minimum value of 66 flux units, the latter corresponding approximately to zero sunspot number.

Moreover, since the Φ_{ji} values are the observed ones, that is, those uncorrected for the variable Sun-Earth distance, no further need for correcting for the annual effect was required[91][117]. Therefore, the variation with the months of the year of the A_{ji} values, namely

$$A_{ji} = K_{ji}/(1 + 0.0094\ \Phi_{ji}) \qquad (4.2)$$

for each given station j, represents the Appleton seasonal anomaly. Figs. 4.1(a) and (b) show the anomaly for Slough and Washington as determined by the constant cosχ method[10] and the method described here respectively. The similarity of the results of the two methods is obvious.

The results of the present investigation are illustrated in Figs. 4.2(a), (b) and (c), for about 40 selected stations lying in three different longitudinal zones centred approximately on the meridian 5°E, 150°E, and 75°W, respectively. The systematic variation with latitude of the anomaly in amplitude and phase can be seen clearly from these plots. For temperate stations there exists in some cases a difference of about 26 to 28 per cent in A (MHz^4) between summer and winter; that is, a difference of the same magnitude as the ones stated by Appleton[10][11] for the same latitudes. On the other hand, for stations near the equator, we find that the seasonal effect is extremely small. A similar result has also been reported by Eyfrig[75] for Lwiro station (2.3S, 28.3E).

4.2 THE LATITUDE-DEPENDENCE OF THE ANOMALY

The results illustrated in Figs. 4.2(a), (b) and (c), show that A is a function of the month of the year and of the latitude of the station.

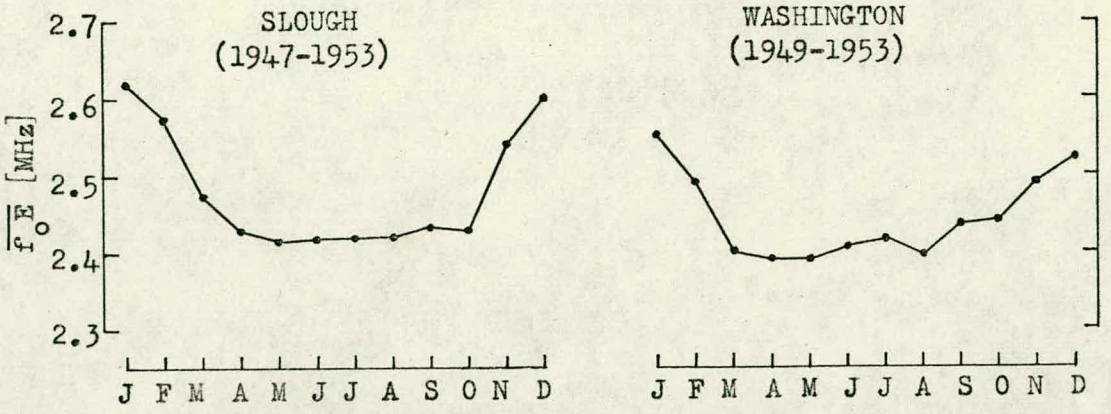

Fig. 4.1(a) The Appleton E-layer seasonal anomaly $\overline{f_oE}$ at constant χ, data corrected for sunspot activity and varying Sun-Earth distance. [After Appleton and Lyon[10]]

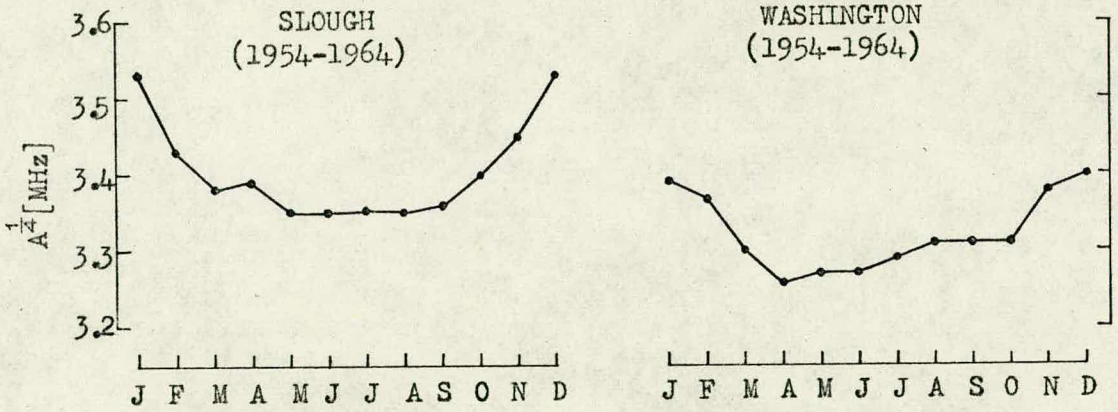

Fig. 4.1(b) The Appleton E-layer seasonal anomaly A in equation $(f_oE)^4 = A(\cos\chi)^P$, data corrected for solar activity and varying Sun-Earth distance.

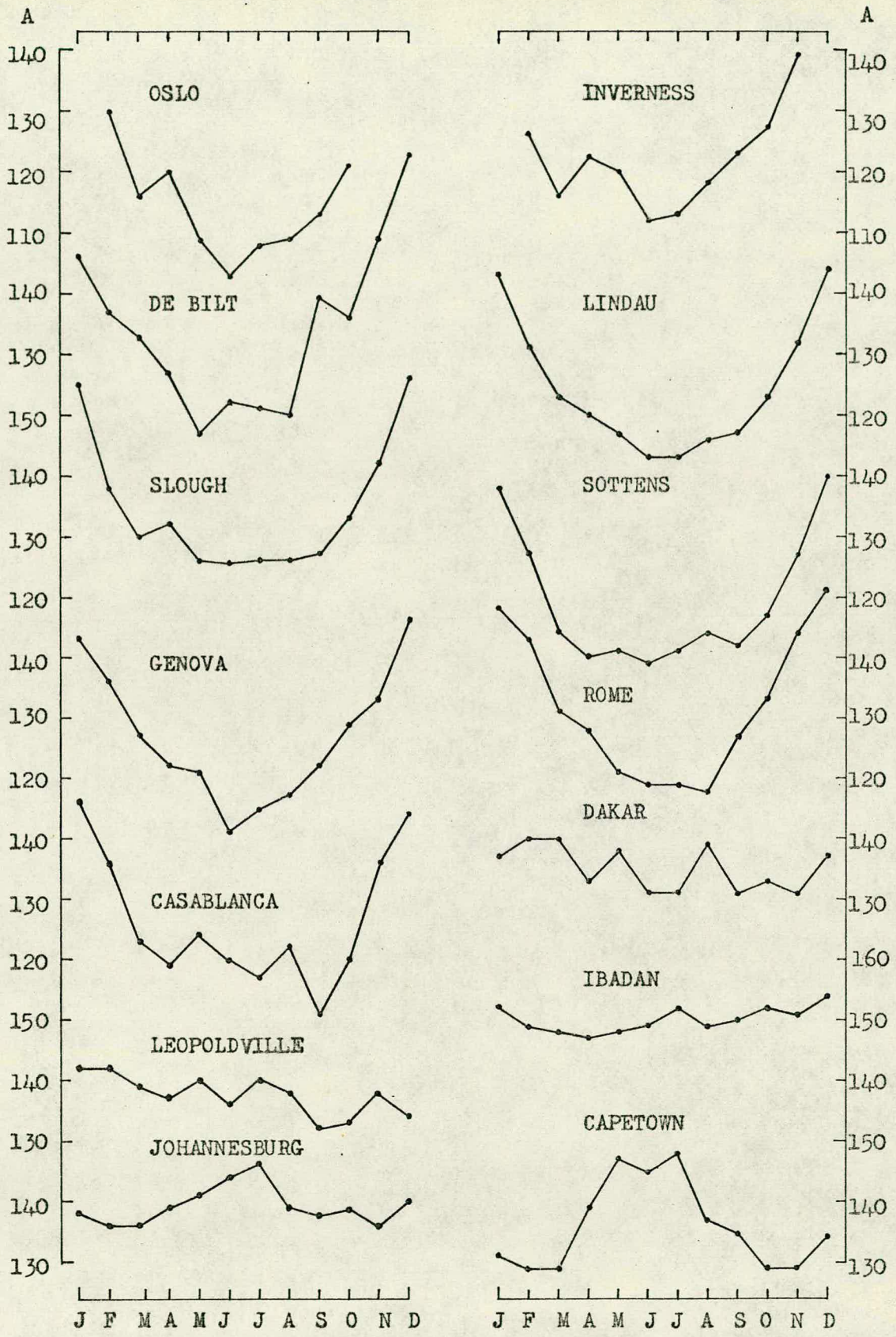

Fig. 4.2(a) The Appleton seasonal anomaly, A in $(MHz)^4$, at stations in a zone centred approximately on $5^{o}E$ (data corrected for solar activity and varying Sun-Earth distance)

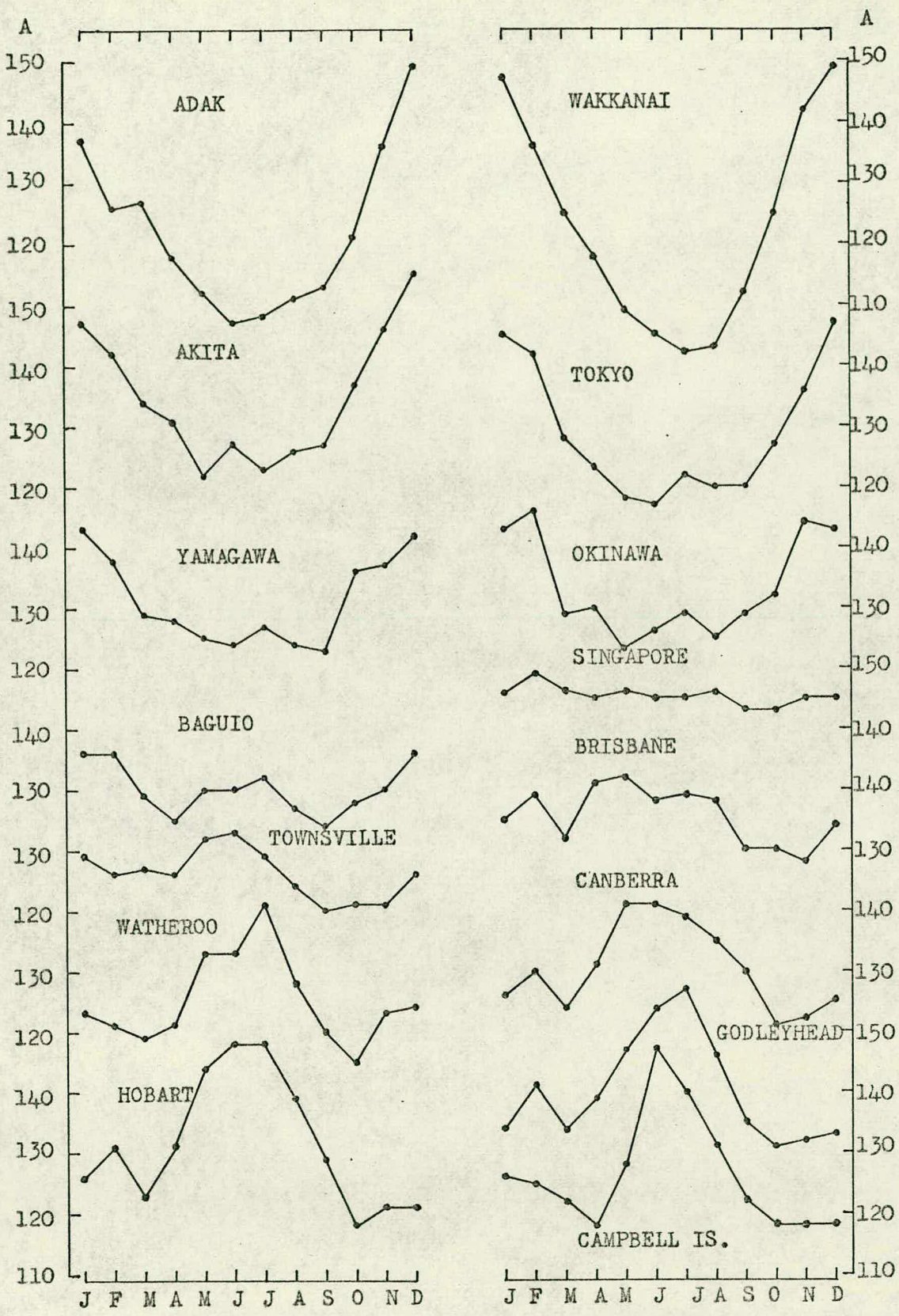

Fig. 4.2(b) The Appleton seasonal anomaly, A in $(MHz)^4$, at stations in a zone centred on the 150°E meridian.

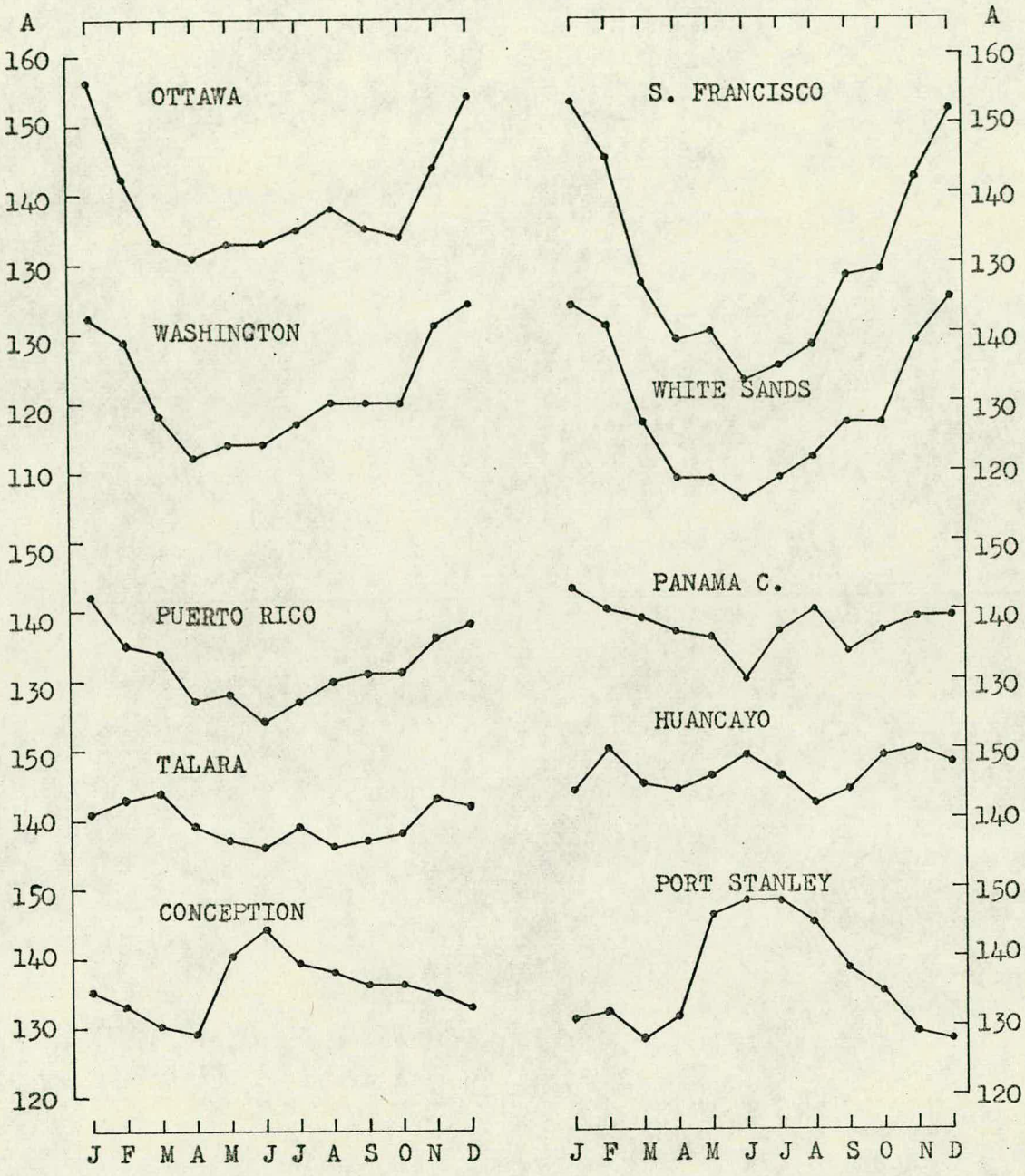

Fig. 4.2(c) The Appleton seasonal anomaly, A in $(MHz)^4$, at stations in the zone centred on about $75^{\circ}W$. (Data corrected for solar activity and varying Sun-Earth distance)

Similarly, the $\cos\chi_{noon}$ value is a characteristic of the month and of the latitude of a given station. Therefore, the A values for a given station could be expressed as a function of the corresponding monthly $\cos\chi_{noon}$ values. In Fig. 4.3 are shown plots of A $\pm$ standard error of A, at a few stations and also, for comparison , the corresponding monthly variations of $\cos\chi_{noon}$. It will be seen that the general seasonal trend of the anomaly follows the corresponding $\cos\chi_{noon}$ curve, except at Townsville where the anomaly has two maxima, in summer and winter respectively. On the contrary at Puerto Rico, a northern station of about the same geographic latitude as Townsville but of different longitude, the anomaly shows (see Fig. 4.2(c)) only one minimum in local summer and one maximum in local winter. This behaviour of the anomaly will be discussed in the next Section, but we may anticipate briefly that the anomaly, apart from being latitude-dependent, is also characteristic of the longitude and hemisphere.

Different mathematical models of the relations $A = A(\cos\chi_{noon})$, and $A = A(\cos\chi_{noon}, \cos\delta)$, where δ is the solar declination, have been examined. The statistical analysis, by means of the usual tests of significance and comparison of correlation coefficients, showed that the following simple linear relationship should be used:

$$\log A = \log B + m \log(\cos\chi_{noon}) \qquad (4.3)$$

The regression analysis has been carried out individually for each station fitting equation (4.3) by the method of least squares to the distribution of the data points; namely the A_i values and the corresponding $\cos\chi_{noon}$ values.

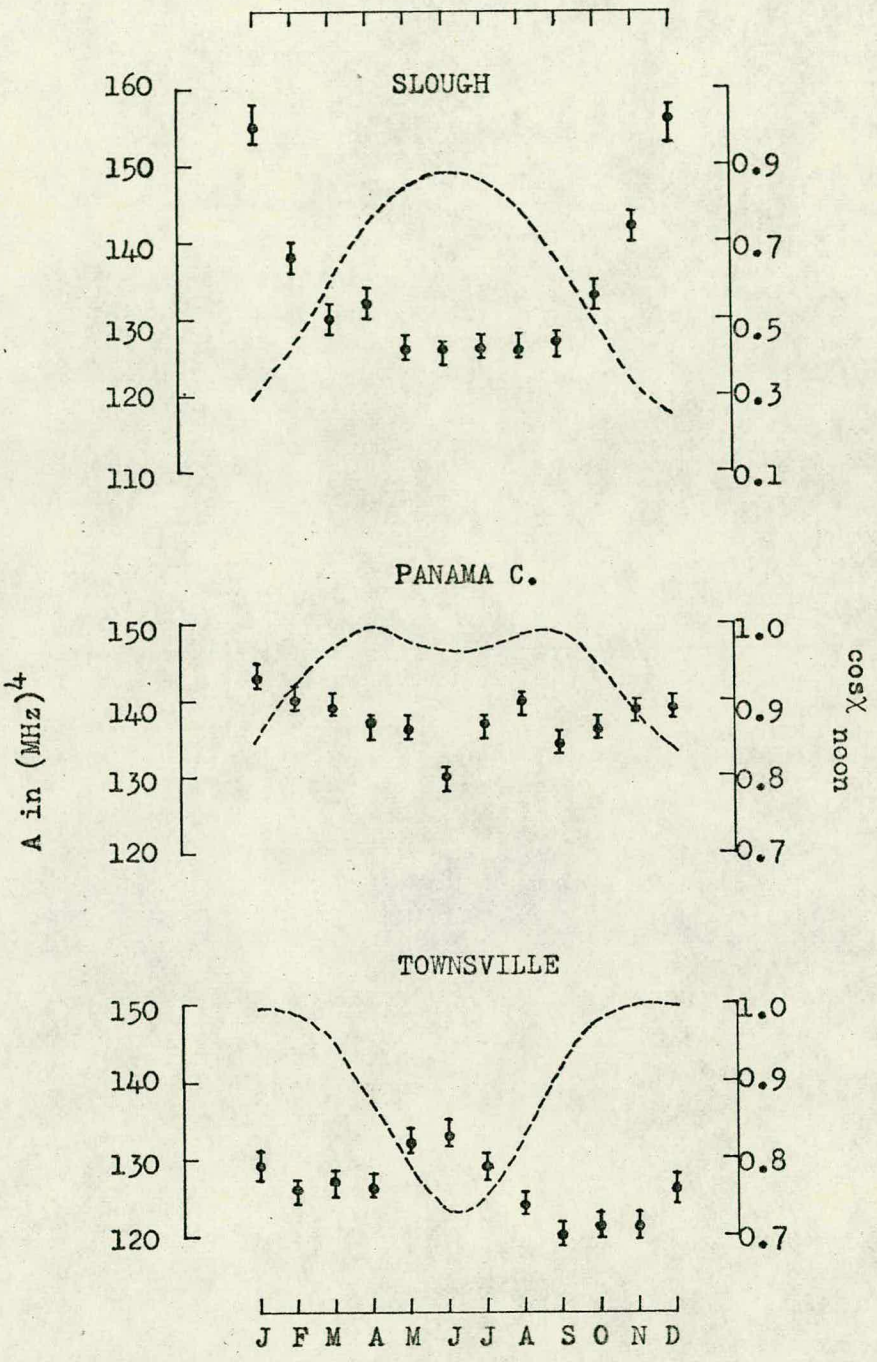

Fig. 4.3(a) Plots of A $\pm$ S.E. and of $\cos\chi_{noon}$ at a few stations, showing that the general seasonal trend of the anomaly could be expressed as a $(\cos\chi_{noon})^m$ curve.

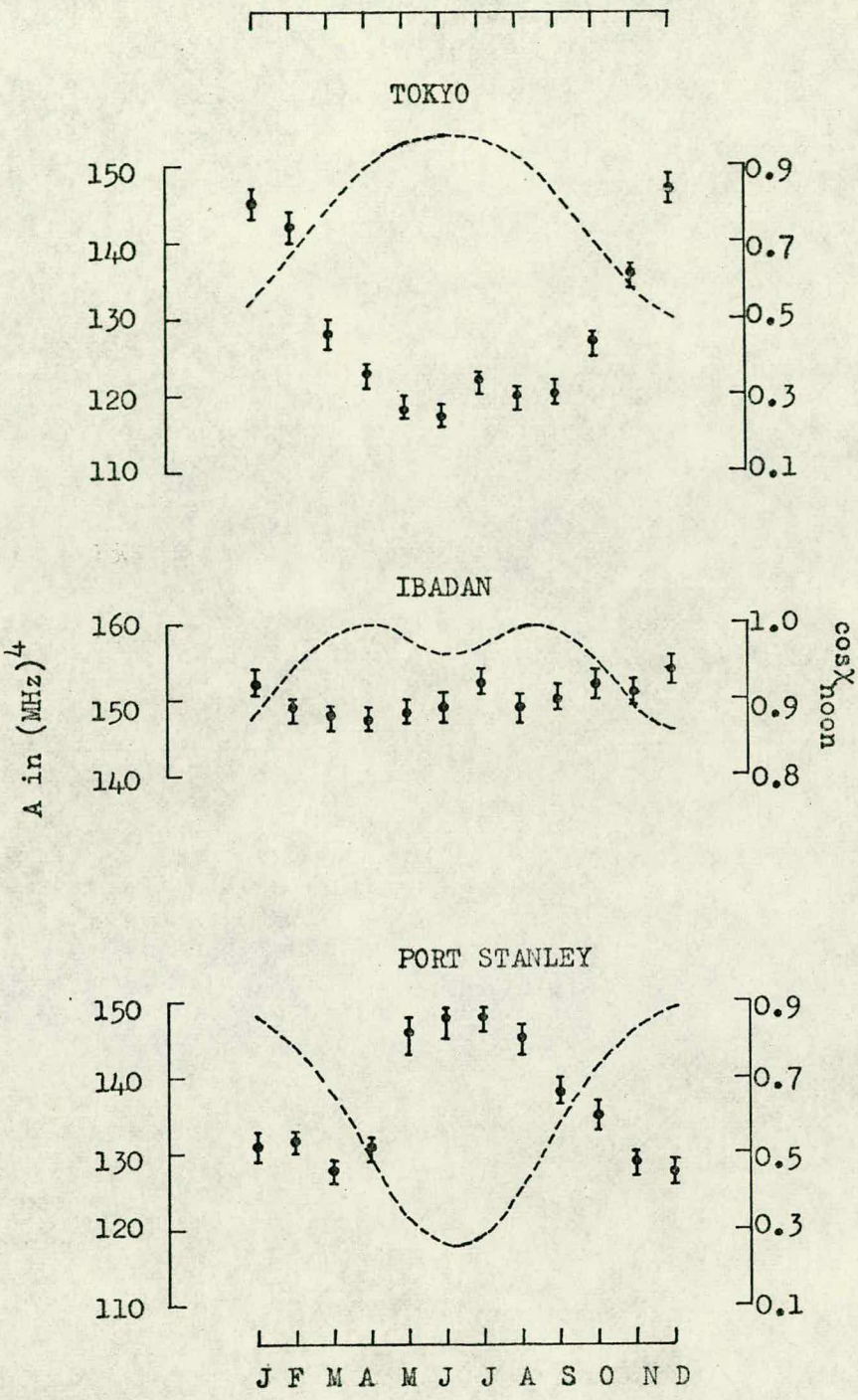

Fig. 4.3(b) Plots of A $\pm$ S.E. and of cos χ_{noon} at a few stations, showing that the general seasonal trend of the anomaly could be expressed as a $(\cos\chi_{noon})^m$ curve.

Thus, for each station the values of m and B were determined. In Table 4.1 are listed the values of m and B thus obtained, and also the corresponding correlation coefficients which show that, except for some stations near the equator, the correlation between A and $\cos\chi_{noon}$ is highly significant. In Fig. 4.4 the values of m and B for stations of each of the three longitudinal zones considered are plotted against geographic latitude. It is seen that the exponent m varies with latitude in a systematic manner, showing a tendency for higher values at about 30 to 40 degrees in geographic latitude in both hemispheres, and a regular decrease towards the equator and the poles. These plots also indicate hemispheric and longitudinal asymmetries in the pattern of m.

In this context it is interesting to note the striking similarity between these curves and the curves obtained by Beynon and Brown[9][50][51] for the seasonal exponent n in the relationship:

$$(f_oE)^n = C\cos\chi \qquad (4.4)$$

for the same three longitudinal zones. Beynon and Brown pointed out that the latitudinal variation of the exponent n was associated with the S_q current system. Moreover, the North-South and longitudinal inequalities observed in the pattern of m have also been found by Hibberd and Henderson[55] in the index n in equation (4.4).

They associated these inequalities in the index n with corresponding observed inequalities in the S_q current system.

TABLE 4.1

Values of m and B in equation $A = B(\cos\chi_{noon})^m$, and corresponding correlation coefficients, r, for stations of the three longitudinal zones centred on 5°E, 150°E and 75°W. B_G and B_M are re-estimated values of B, using the m values given by equations (4.6),(4.9), and (4.8), (4.11), respectively.

Station	θ°	m	B	r	B_G	B_M
Tromso	69.7	-0.08	96.3	0.801	-	-
Kiruna	67.8	-0.19	82.6	0.808	-	-
Oslo	60.0	-0.18	103.0	0.898	105.8	104.1
Inverness	57.5	-0.14	112.0	0.876	110.9	108.7
De Bilt	52.1	-0.21	117.5	0.939	119.0	116.1
Lindau	51.6	-0.19	110.9	0.977	110.5	108.1
Slough	51.5	-0.17	121.5	0.953	120.0	117.5
Sottens	46.7	-0.24	105.9	0.964	106.5	104.5
Genova	44.6	-0.25	113.5	0.962	114.2	112.0
Rome	41.9	-0.29	117.9	0.976	119.7	117.7
Casablanca	33.6	-0.35	115.5	0.867	117.0	117.8
Dakar	14.7	-0.05	134.5	0.152	134.3	134.8
Ibadan	7.4	-0.19	148.6	0.700	146.9	147.1
Leopoldville	- 4.4	-0.01	137.3	0.160	133.8	132.8
Johannesburg	-26.2	-0.11	136.9	0.800	134.7	133.2
Capetown	-34.1	-0.21	128.0	0.911	125.0	126.3
Halley Bay	-75.5	+0.02	116.8	0.104	-	-
Adak	51.9	-0.23	105.9	0.959	108.4	103.7
Wakkanai	45.4	-0.39	101.9	0.968	109.6	106.6
Akita	39.7	-0.28	122.3	0.976	122.8	120.1

TABLE 4.1 continued

Station	θ°	m	B	r	B_G	B_M
Tokyo	35.7	-0.33	117.3	0.945	118.7	118.7
Yamagawa	31.2	-0.27	124.0	0.948	123.4	125.8
Okinawa	26.3	-0.35	125.3	0.921	128.4	130.1
Baguio	16.4	-0.23	127.8	0.706	129.3	130.0
Singapore	1.3	-0.04	145.1	0.172	142.6	142.5
Townsville	-19.3	-0.18	123.7	0.629	124.5	122.5
Brisbane	-27.5	-0.12	132.4	0.600	129.9	128.1
Watheroo	-30.3	-0.24	118.9	0.789	117.9	118.6
Canberra	-35.3	-0.21	122.8	0.917	120.4	121.6
Hobart	-42.9	-0.24	119.0	0.925	118.6	122.8
Godleyhead	-43.6	-0.17	130.2	0.909	126.4	127.5
Campbell Is.	-52.5	-0.12	116.2	0.809	111.7	115.3
Resolute Bay	74.7	-0.18	106.7	0.971	-	-
Churchill	58.8	+0.06	114.4	0.510	-	-
Ottawa	45.4	-0.15	129.9	0.869	125.3	130.6
Washington	38.7	-0.22	113.6	0.927	111.7	114.7
S. Francisco	37.4	-0.42	114.2	0.973	119.2	119.3
White Sands	32.3	-0.38	117.7	0.963	119.8	120.2
Puerto Rico	18.5	-0.32	127.5	0.917	130.4	127.5
Panama C.	9.4	-0.21	135.8	0.516	133.7	132.9
Talara	- 4.6	+0.12	141.3	0.589	140.1	140.3
Huancayo	-12.0	+0.04	146.9	0.524	142.9	143.4
Conception	-36.6	-0.09	132.2	0.687	124.9	130.7
Port Stanley	-51.7	-0.12	126.7	0.890	121.3	118.3
Port Lockroy	-64.8	-0.09	121.0	0.419	119.3	118.5

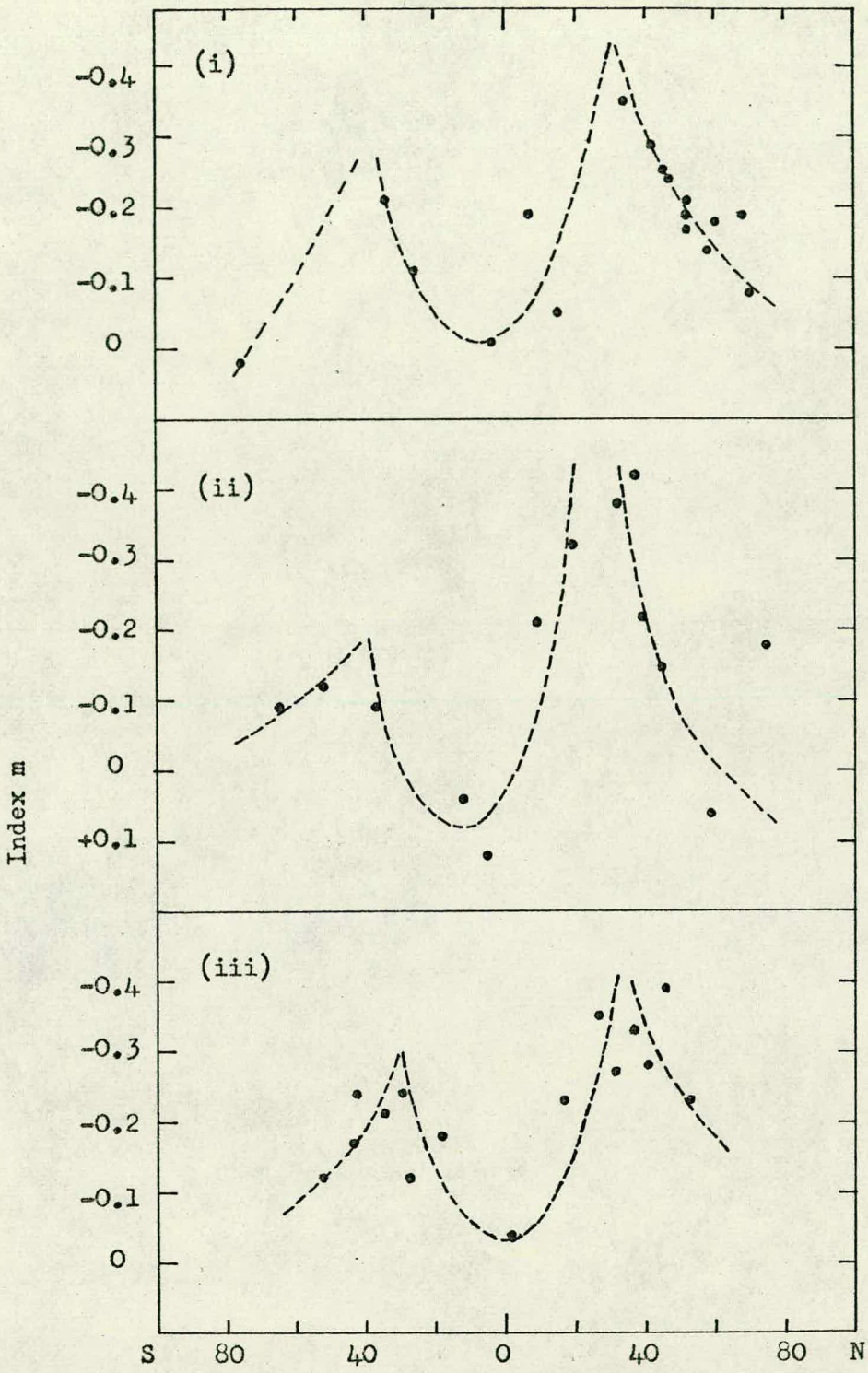

Fig. 4.4(a) Variation with geographic latitude of m in equation $A = B(\cos\chi_{noon})^m$ for stations centred on (i) 5°E; (ii) 75°W; and (iii) 150°E meridians. Of particular note is the striking similarity between the variation of the exponent m and the variation of the exponent n of Beynon and Brown[51] in all zones.
------ Estimated variation.

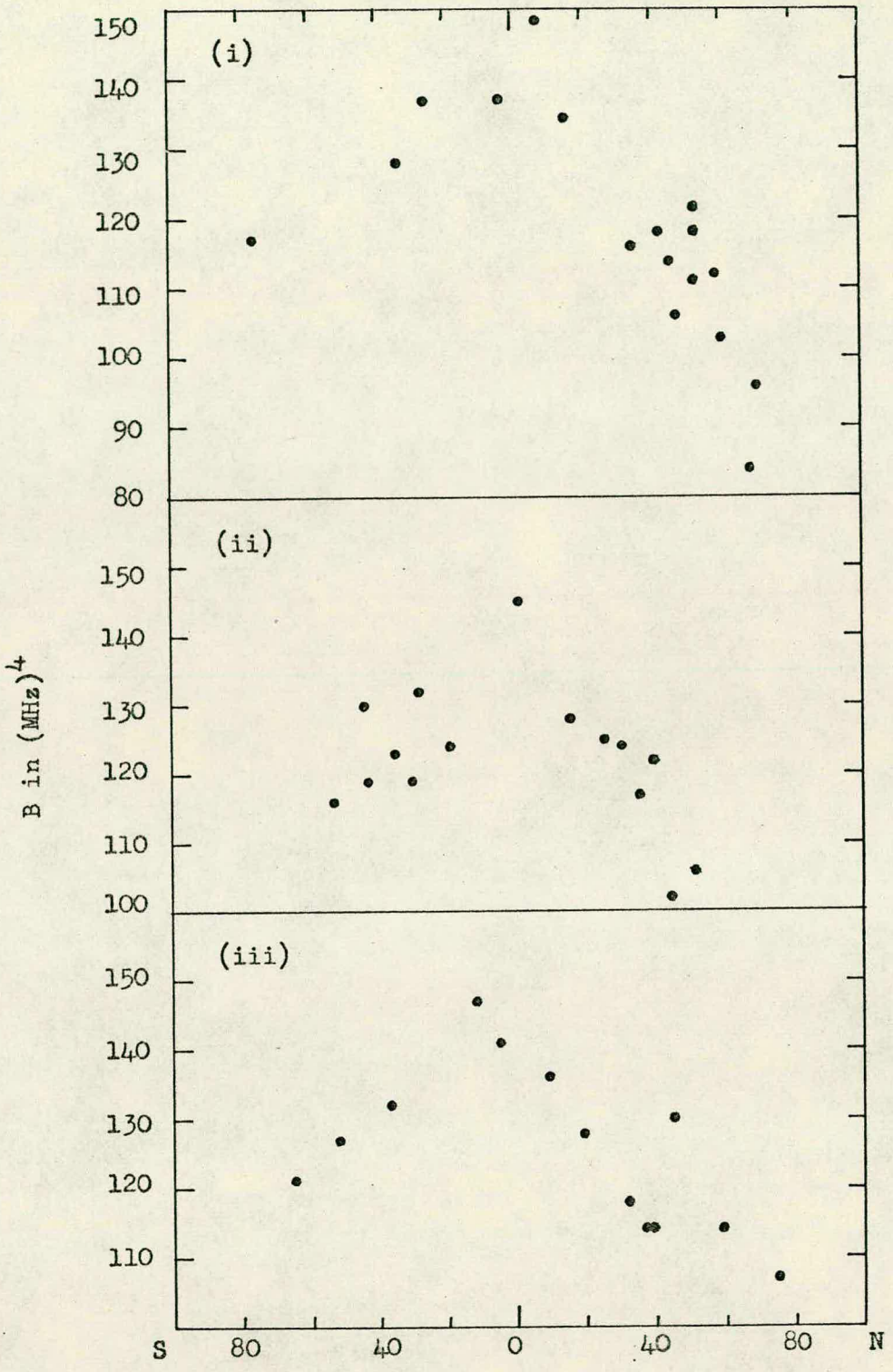

Fig. 4.4(b) Variation with geographic latitude of B in equation $A = B\ (\cos\chi_{noon})^m$ for stations centred on (i) 5°E; (ii) 150°E; and (iii) 75°W meridians.

In Fig. 4.4 is also illustrated the variation with geographic latitude of the parameter B in equation (4.3), for each of the three longitudinal zones. It is noted that the value of B increases towards the equator and that the value in the southern hemisphere seems slightly greater than that corresponding to the same latitude in the northern hemisphere. This equatorial enhancement is essentially the same as was obtained by Appleton[47] and other investigators[8][9][10][48][52], and attributed to the effect of the S_q current system.

In order to obtain analytical expressions for m and B, their values at 40 stations were treated independently of longitudinal zone, since the available stations do not provide complete coverage of each of the three longitudinal zones. These m and B values are plotted against latitude, and independently of longitude, in Fig. 4.5 and Fig. 4.6 respectively. Fig. 4.5 shows plots of the index m against geographic, geomagnetic and magnetic latitude. It will be seen that although there is some scatter in the data points, the distribution of m exhibits two maxima at latitudes between 30 and 40 degrees. If we also do not take into consideration the North-South asymmetry present in the world-wide pattern of the exponent m, an appropriate solution can easily be obtained from the available data. In doing so a small error will, of course, be introduced due to the neglected asymmetries.

Now, the distribution of m suggests that we may consider two linear regressions, or one curvilinear regression, using as independent variable the cosine of geographic or geomagnetic or magnetic latitude. The statistical analysis, however, showed that the linear regression equations were better than the curvilinear models. Therefore the following linear regression was used:

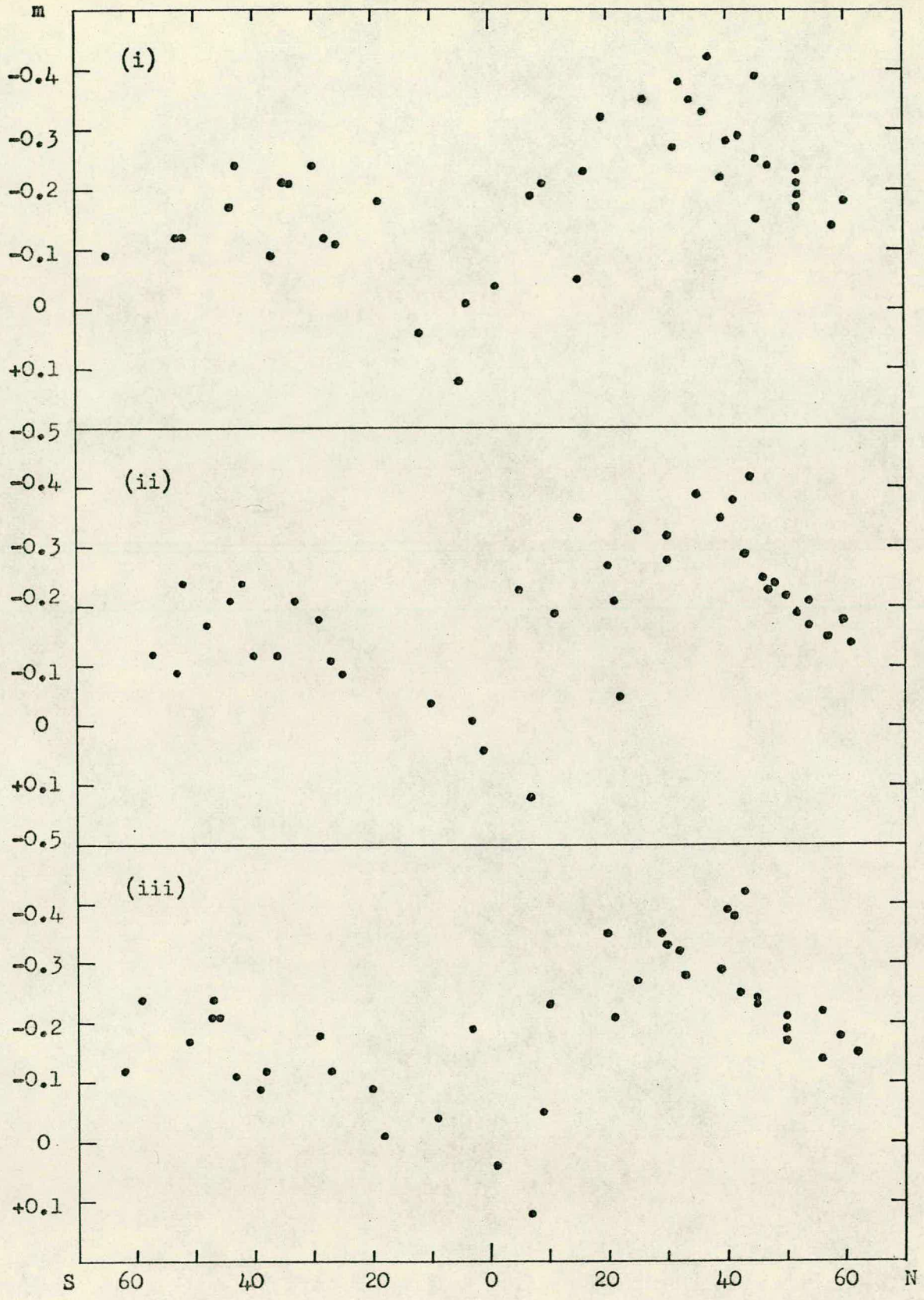

Fig. 4.5 Latitudinal variation of the exponent m in equation $A = B(\cos\chi_{noon})^{m}$ at 40 stations, showing general tendency for higher values of m at about 30 – 40 degrees in latitude. (i) geographic latitude; (ii) geomagnetic latitude; (iii) magnetic latitude.

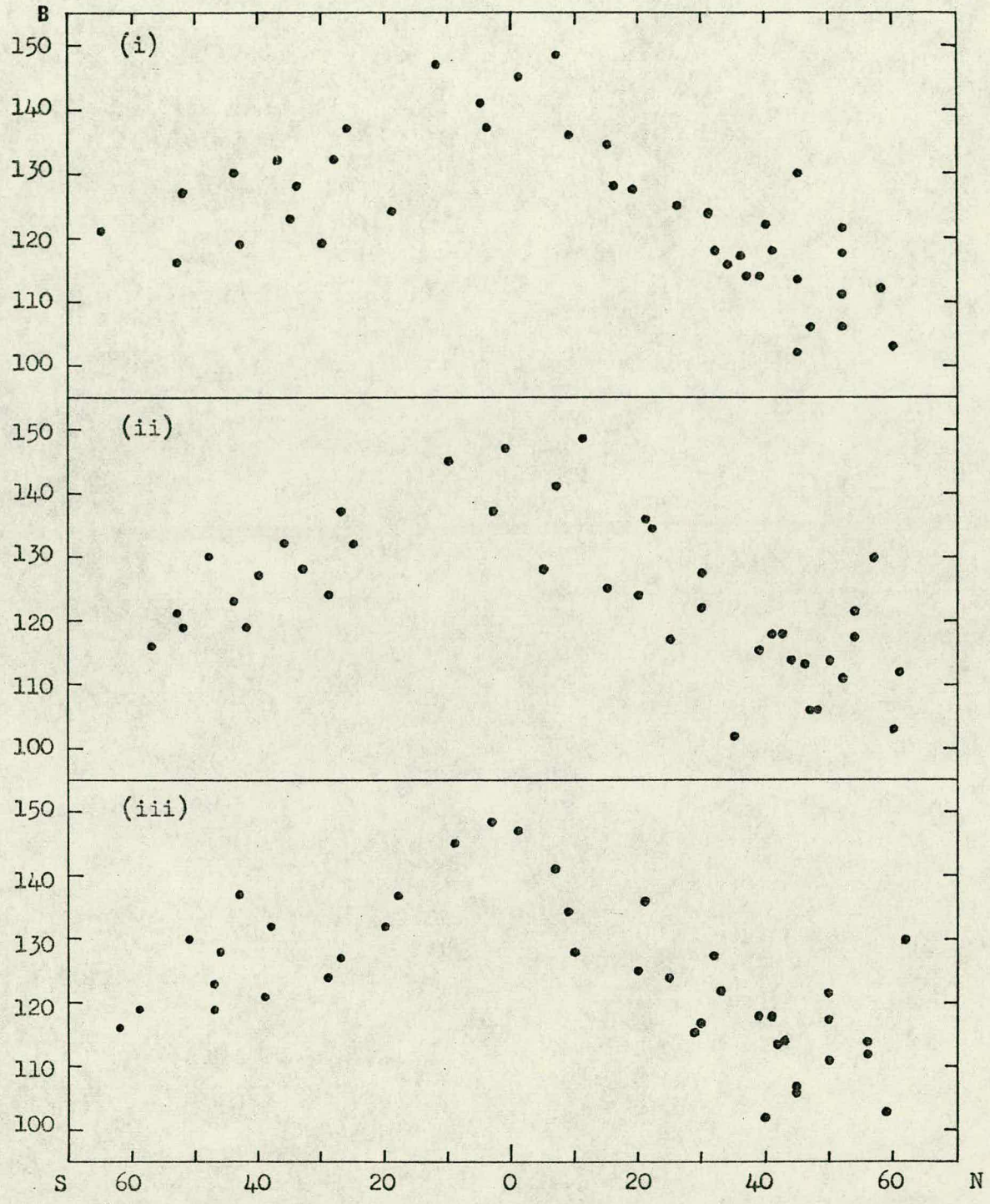

Fig. 4.6 Variation with latitude [(i) geographic; (ii) geomagnetic; (iii) magnetic;] of B in equation (4.3) for 40 stations, showing the equatorial enhancement.

$$m = a + b \cos\theta \tag{4.5}$$

and fitted by the method of least squares to the data between zero and about $\pm$ 32 degrees, and between $\pm$ 32 and about $\pm$ 65 degrees in latitude respectively. The relationships thus determined for about 15 stations between zero and about $\pm$ 32 degrees in geographic, geomagnetic, and magnetic latitude respectively, were found to be as follows:

$$m = -1.93 + 1.92 \cos\theta \tag{4.6}$$

$$m = -1.60 + 1.57 \cos\theta_G \tag{4.7}$$

$$m = -2.13 + 2.13 \cos\theta_M \tag{4.8}$$

The corresponding correlation coefficients obtained were respectively:

$$r = 0.646 \; ; \; r_G = 0.541 \; ; \; r_M = 0.644$$

For the other 25 stations between about $\pm$ 32 and $\pm$ 65 degrees in geographic, geomagnetic and magnetic latitudes, the following linear regressions were obtained:

$$m = 0.11 - 0.49 \cos\theta \tag{4.9}$$

$$m = 0.13 - 0.53 \cos\theta_G \tag{4.10}$$

$$m = 0.11 - 0.53 \cos\theta_M \tag{4.11}$$

The corresponding correlation coefficients were:

$$r = 0.652 \; ; \; r_G = 0.550 \; ; \; r_M = 0.715$$

The correlation coefficients obtained illustrate that the correlation between m and geomagnetic latitude is significant and that the correlation between m and either of the two other latitudes, geographic or magnetic, is highly significant.

The m values as given by equations (4.6) and (4.9) have been used to re-estimate the B values from equation (4.3). These new values B_G are listed in Table 4.1 and plotted in Fig. 4.7 against geographic, geomagnetic and magnetic latitude respectively. Similarly, using the m values as given by equations (4.8) and (4.11), the B values were recalculated by means of equation (4.3). Again, these B_M values are set out in Table 4.1 and illustrated in Fig. 4.8 against the three latitudes.

Next a linear regression of the form:

$$B = k + l \cos\theta \tag{4.12}$$

was fitted by the least squares method to the data between 0 and about $\pm$ 32 degrees, and to those between $\pm$ 32 and about $\pm$ 65 degrees. The independent variable $\cos\theta$ was in turn the cosine of geographic, geomagnetic and magnetic latitude, whereas the dependent variable B took the values B_G or B_M. The regression analysis showed that better results were obtained when B_G was correlated with geographic latitude and B_M with magnetic latitude. The results of the analysis from data of 15 stations between zero and $\pm$ 32 degrees in latitude were:

$$B_G = 23 + 116 \cos\theta \tag{4.13}$$

and

$$B_M = -8 + 148 \cos\theta_M \tag{4.14}$$

with correlation coefficients 0.743 and 0.856 respectively.

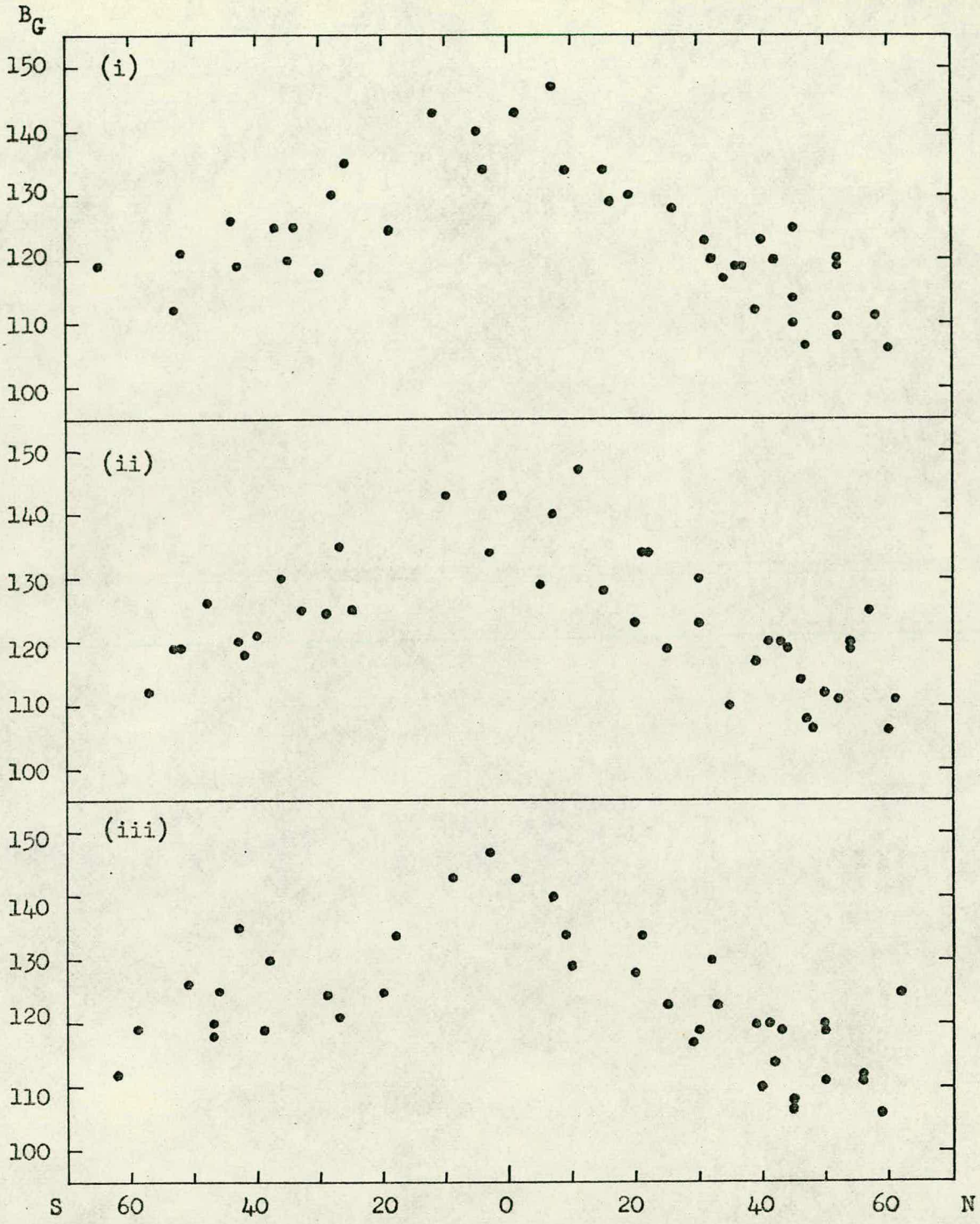

Fig. 4.7 Illustrating the variation with latitude [(i) geographic; (ii) geomagnetic; (iii) magnetic;] of B_G calculated from equation (4.3) using the m values given by equations (4.6) and (4.9).

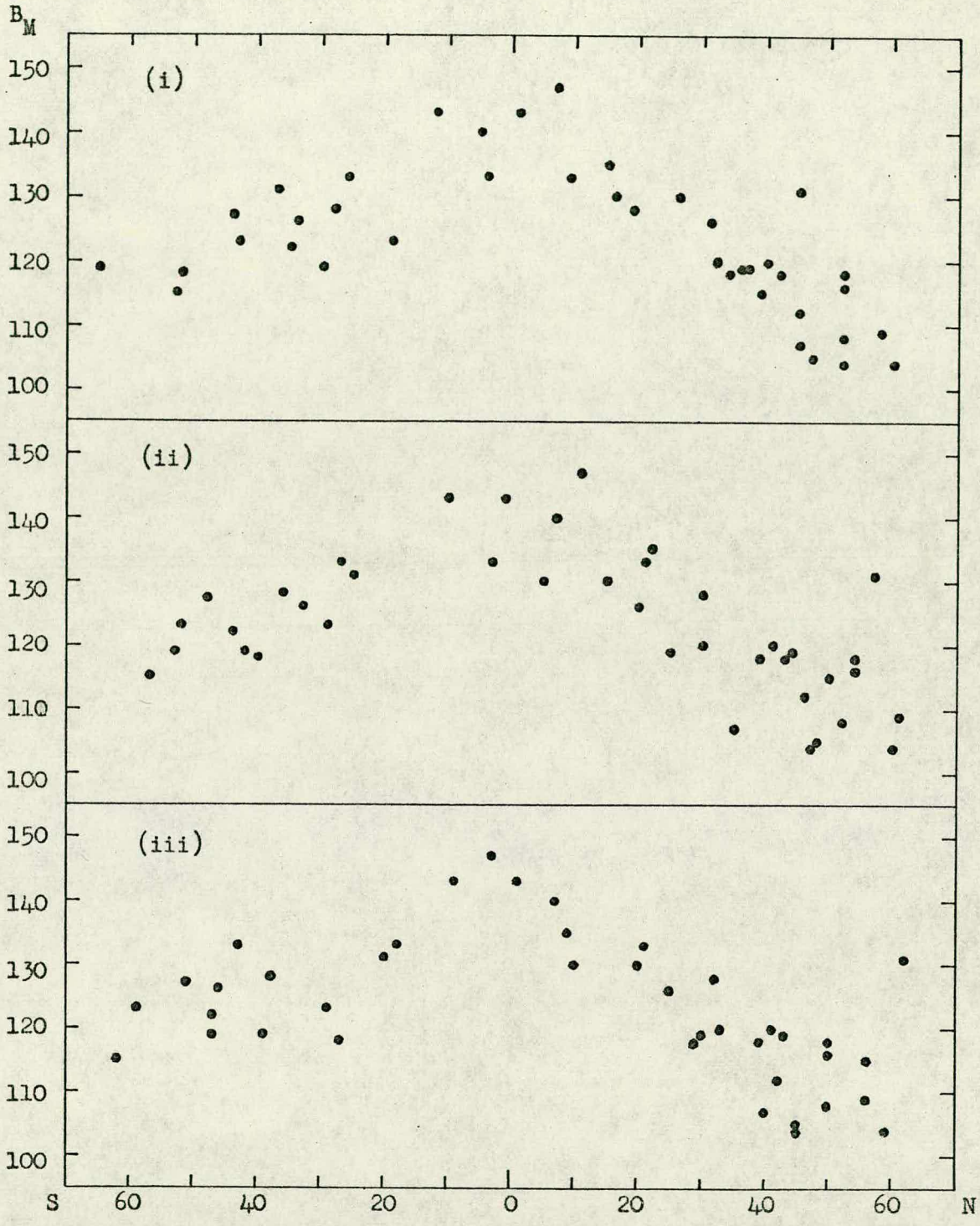

Fig. 4.8 Showing the variation with latitude [(i) geographic; (ii) geomagnetic; (iii) magnetic;] of B_M calculated from equation (4.3) using the m values given by equations (4.8) and (4.11).

For the 25 stations between $\pm 32^{\circ}$ and about $\pm 65^{\circ}$, the following results were found:

$$B_G = 92 + 35 \cos\theta \tag{4.15}$$

with correlation coefficient 0.550, and

$$B_M = 115 \tag{4.16}$$

since the corresponding slope and correlation coefficient (0.052) were not significantly different from zero.

4.3 DISCUSSION OF RESULTS

The world morphology of the Appleton E-layer seasonal anomaly is illustrated by the plots of Figs. 4.2(a), (b) and (c). It is clearly shown that the value of A is less in local summer than in local winter in both hemispheres, the effect being more marked for stations away from the equator. For equatorial stations the seasonal effect seems extremely small. It is also interesting to note that the winter values, i.e. December - January for northern hemisphere, and June - July for southern hemisphere, are almost equal everywhere and equal to the average value of A at the equatorial stations. On the other hand, a careful inspection of these plots reveals that the seasonal anomaly is not only characteristic of the latitude of the station but also of the longitude and the hemisphere. The longitudinal and hemispheric inequalities in the amplitude of A can be seen from Fig. 4.9, which illustrates, for comparison, A-plots of stations of about the same geographic latitude but of different longitudinal zone or hemisphere. These inequalities are also present in the patterns of the seasonal index m and of the factor B in equation (4.3), as will be seen in Fig. 4.4.

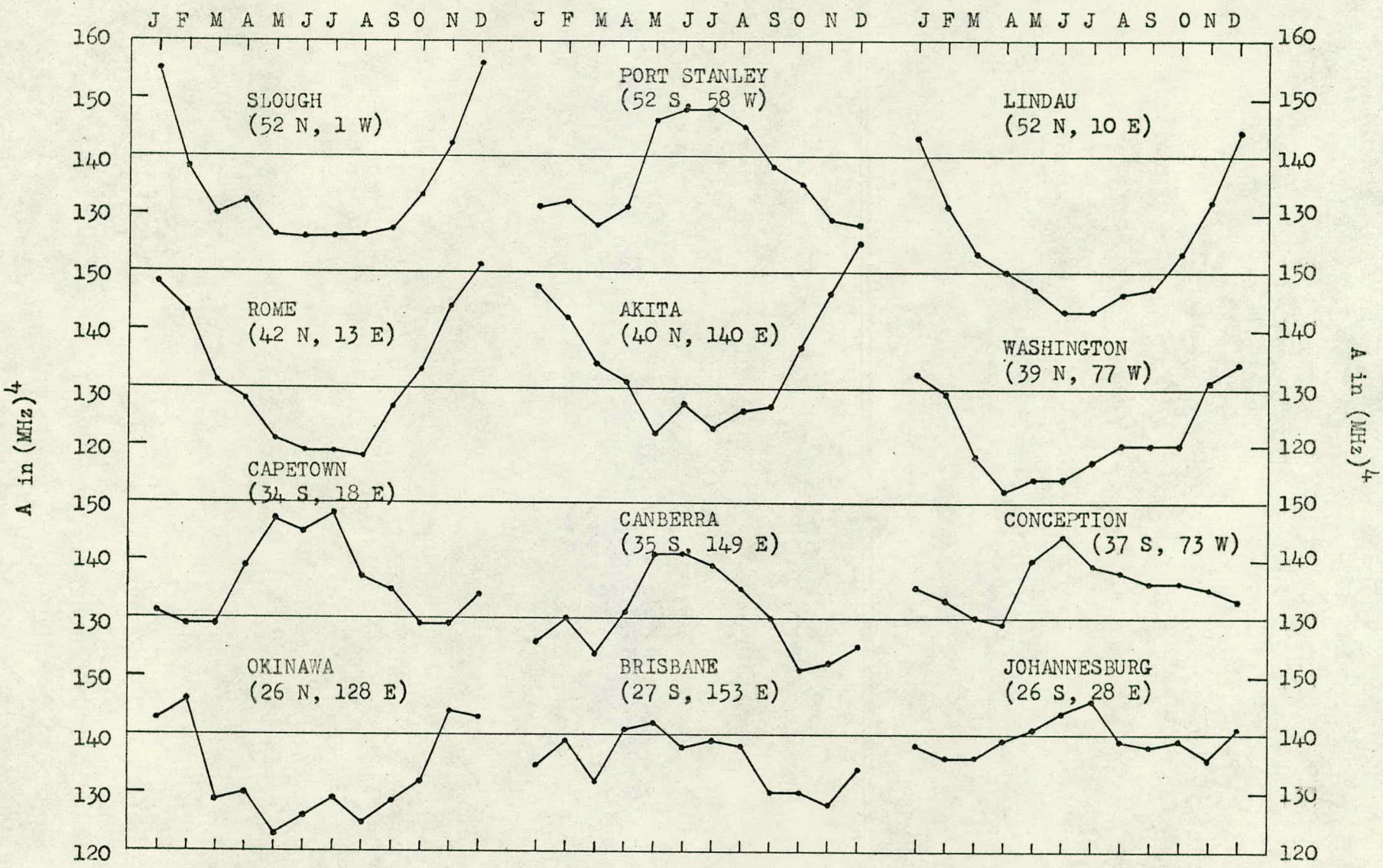

Fig. 4.9 Showing for comparison A-plots at stations of about the same geographic latitude but different longitude and hemisphere.

Moreover, we can see in Fig. 4.4 and also in Fig. 4.5 that the latitudinal distribution of m is not random but very systematic with peak values at about 30 to 40 degrees in latitude. In addition we can see from Fig. 4.6, illustrating the latitudinal distribution of B, that from the latitude of about $\pm$ 30 degrees the values of B are appreciably enhanced towards the equator, whereas towards the poles there is little change. Furthermore, the value of B in the southern hemisphere seems slightly greater than that in the northern hemisphere at the same latitude.

Now, these facts cannot be entirely explained by a seasonal variation in the upper atmospheric parameters such as temperature, temperature gradients or atmospheric composition. In that case one would expect these effects to vary monotonically with latitude only. On the other hand, it is well known that seasonal, hemispheric and longitudinal inequalities in the current intensities and in the positions of the foci of the S_q current system have been observed (see Appendix A.4); and evidence of vertical drift effects on the E-layer as a result of the S_q currents has been given by many investigators (see Appendix A.3). For instance, in connection with the seasonal change in the S_q current intensity, we may see in Fig. 4.2 that there is little change in the value of A from equinoxes to summer months; similar changes in the S_q current intensity for equinoctial and summer months have been found by Matsushita and Maeda[143][144]. They have also found that the current intensity of the S_q current system for equinoctial months and the yearly average, is about 1.2 times larger in the northern than in the southern hemisphere. In connection with this North-South inequality in the S_q current intensity, it is interesting to see in Figs. 4.4, 4.5 and 4.6 similar North-South inequalities in the latitudinal distributions of m and B;

that is, m has higher values in the northern hemisphere, and B is greater in the southern hemisphere than in the northern hemisphere for the same latitude. Also, it has been found[144][145] that the intensity of the equatorial electrojet is greatest in the American zone; and in connection with that we may see in Fig. 4.4 that the zone centred on the meridian 75°W exhibits the lowest equatorial value of m. Therefore, it seems reasonable to suggest that the seasonal anomaly must be attributed mainly to variations in the S_q current system.

We shall now discuss possible explanations for the anomaly. In the first place we consider stations at latitudes higher than those of the S_q foci, namely at latitudes greater than about 30 degrees. It will be seen from equation (1.11) that a vertical drift of velocity v, having a positive gradient $\partial v/\partial h$, causes a reduction of the maximum electron density of the layer. It is evident that the magnitude of vertical drift will change with the seasonal change in the magnitude of the S_q currents. Thus, the vertical drift effect will be greater in local summer than in local winter. Moreover, the seasonal shift of the S_q foci, towards the poles from winter to summer[143][146][147], will increase, at a certain station, the difference in current intensity between summer and winter, resulting thus in a further increase of the vertical drift effect in local summer.

Furthermore, Beynon and Brown[9], and Appleton and Lyon[10] have suggested that seasonal changes in the height gradient of vertical drift velocity might occur. For instance the occurence of a negative $\partial v/\partial h$ in winter would give a reversal in phase in the perturbation compared to summer.

Thus, the resulting effect would be an increase in A in winter and a decrease in summer.

We may also note that stratification in the current density as well as changes in the height of the current-sheets have been detected during rocket flights at different latitudes (Appendix A.4). In fact Cloutier and Haymes[35] have reported that during two flights from Wallops Island, in November 1965 and February 1966, the observed current sheets were confined to the altitude range 106 to 110 Km, that is, in the lower part of the altitude range (105 - 123 Km) of current observed during June 1964 by Davis et al.[31] over Wallops Island. Appleton[26] has also deduced that the S_q currents might be located at different atmospheric levels in summer and winter. Therefore, it may be that the E-layer maximum in a certain season may be in a current layer and in other seasons above or below it. In other words, a seasonal variation in the relative levels of the current maximum and of the E-layer maximum might exist, resulting in a seasonal change in the value of A, increasing it in local winter and decreasing it in local summer.

At equatorial stations, a negative height gradient of vertical drift velocity will raise the value of f_oE, whereas the term involving the drift velocity will reduce it. Since the importance of the term involving the velocity gradient in equation (1.11) seems to be greater than that of the term involving the velocity itself, the net result will be an increase in f_oE at all seasons. However, at equatorial latitudes the drift velocity is much greater than in higher latitudes[41], therefore the velocity term of equation (1.11) may modify the effect of upward drift on f_oE, showing a small seasonal effect over-lapping the former.

This seasonal effect could be the result of both seasonal shift of foci and seasonal change in current intensity. Furthermore, stratification and seasonal changes in the height of the S_q current sheets and in the height gradient of drift velocity may also contribute to the small seasonal anomaly observed. Thus at equatorial latitudes the values of A will be enhanced in all seasons and in addition they will exhibit a seasonal variation depending on the position of the station.

For stations between about $\pm 20^{\circ}$ and $\pm 30^{\circ}$ in latitude, the region where the seasonal shift of the S_q foci occurs, it is reasonable to expect the variability of A to be smaller than that for stations of latitude greater than $\pm 30^{\circ}$. A station e.g. may in local winter be on the poleward side of the focus and in local summer on the side towards the equator; or it may be at the same side of the focus, towards the equator, both in winter and in summer, but in this last case the seasonal change in current intensity will be smaller because of the seasonal shift of the focus. Thus, the result of the seasonal shift of the foci and of the seasonal change in current intensity, together with changes in the height gradient of drift velocity and in the height of the S_q current sheets, will be a rather complex pattern of the A variation with month of the year; the variability of A will be small and the trend may show a minimum in local summer or two minima at the equinoxes. The latter case has been found, for instance, at Townsville and Brisbane, Fig. 4.2(b).

Finally, it is noted that the local winter values of A are virtually equal everywhere and equal to the average value of A at equatorial stations. This suggests that the effect at the equator at any season, and during local winters elsewhere, is the same.

In other words, if the equatorial enhancement is due to an upward drift, then we may expect during local winter, in non-equatorial regions, to have a negative height gradient of vertical drift velocity, thus giving a reversal in phase of the perturbations compared to summer, and consequently causing an increase in A.

In support of the fact that the Appleton anomaly is the result of vertical drifts caused by the S_q currents, we may also note that the distributions of m and B in equation (4.3) are only partially explained by the correlation with the geographic or magnetic latitude. In fact, if the anomaly is the result of the motor influence of the S_q current system, the effect will be determined by the real distribution of the Earth's main magnetic field at the ionospheric levels and by the parameters of the upper atmosphere. Solar radiations and air motions vary with the geographic latitude; electrical conductivity of the ionosphere mainly with the magnetic dip; and the Earth's main magnetic field with the dipole latitude.

We are thus led to conclude that the Appleton seasonal anomaly is mainly the result of effects of the S_q current system. To explain the relatively large variability of A (in MHz^4) between winter and summer (e.g. for northern temperate stations up to about 26 per cent in A), not only seasonal changes of current intensity and shifts of current foci should be taken into consideration, but also possible changes in $\partial v/\partial h$ and in the height of the current layer.

Having obtained in this Chapter a mathematical model for taking into account the seasonal anomaly in f_oE, it now remains to gather together the results of the whole investigation in order to obtain an expression from which f_oE may be calculated. This forms the subject of the next Chapter.

CHAPTER 5

AN ANALYTICAL EXPRESSION OF f_oE FOR PREDICTION PURPOSES

The results of the investigation of the variation of E-layer critical frequency with solar activity, solar zenith angle and season may be combined to obtain an analytical formula for the calculation of f_oE. In fact, combining equations (2.8),(3.2),(4.3),(4.5)and (4.12),and using the values of the coefficients given by (2.19), (3.7), (3.8),(4.6),(4.9),(4.13) and (4.15), we obtain two expressions for f_oE:

1) For stations lying between 32 degrees and about 65 degrees in geographic latitude in both hemispheres,

$$(f_oE)^4 = (92 + 35\cos\theta)(1 + 0.0094\Phi)(\cos\chi_{noon})^m(\cos\chi)^p \qquad (5.1)$$

with $\Phi = \Phi_{obs.} - 66$

$m = 0.11 - 0.49\cos\theta$

$p = 1.20$

and where θ is the geographic latitude, $\Phi_{obs.}$ is the 10.7 cm solar radio noise flux measured at ground level and f_oE is expressed in MHz.

2) For stations lying in the latitude range between $\pm$ 32 degrees and zero degrees,

$$(f_oE)^4 = (23 + 116\cos\theta)(1 + 0.0094\Phi)(\cos\chi_{noon})^m(\cos\chi)^p \qquad (5.2)$$

with $m = -1.93 + 1.92\cos\theta$,

and $p = 1.20$ for stations between $\pm 32^o$ and about $\pm 12^o$,

or $p = 1.31$ for stations between $\pm 12^o$ and zero degrees.

5. ASSESSMENT OF THE ACCURACY OF THE f_oE EXPRESSION

It is important to assess the accuracy of the expressions (5.1) and (5.2) for each of the stations examined,

and also to provide an estimate of world-wide average standard error of f_oE for the data involved.

If E represents the estimated values using formula (5.1) or (5.2), and if Y represents the observed corresponding values, then the standard error of estimate, S_E, is given by[87]:

$$S_E = [\Sigma(Y - E)^2/(N - 6)]^{\frac{1}{2}} \qquad (5.3)$$

N is the number of observations involved, and the six degrees of freedom deducted from N are associated with the six parameters determined in the statistical analysis. Thus, for a given station the eleven-year average monthly values of $(f_oE)^4$ and of f_oE, for each hour (mainly from 0900 hrs to 1500 hrs), in each month, have been estimated using formula (5.1) or (5.2) according to the latitude of the station. These estimated values were substracted from the corresponding eleven-year average of the observed values, and then, by means of equation (5.3), the standard error of estimate of $(f_oE)^4$ and of f_oE for the given station has been evaluated. The results for the 40 stations examined are listed in Table 5.1 and plotted in Fig. 5.1 against geographic latitude. From this figure we see that the standard error is virtually constant throughout the world except at Johannesburg, Brisbane and Watheroo.

In order to minimize the error in equation (5.1) all the data of the 25 stations lying between $\pm 32^o$ and $\pm 65^o$ were combined in a single sample, and, using a least squares solution to the nonlinear model,

$$(f_oE)^4 = (k + l\cos\theta)(1 + \beta\Phi)(\cos\chi_{\text{noon}})^{(a + b\cos\theta)}(\cos\chi)^p \qquad (5.4)$$

the parameters k, l, β, a, b and p were determined by means of stepwise Gauss-Newton iterations.

TABLE. 5.1

Standard errors of estimate of f_oE and $(f_oE)^4$ based on equations (5.1) and (5.2); and also of f_oE based on equation (5.4)

Station	θ Degrees	S.E.(f_oE) in MHz	S.E.$(f_oE)^4$ in MHz^4	(Non-linear Model) S.E.(f_oE)
Oslo	60.0	0.043	6.30	0.069
Inverness	57.5	0.034	4.33	0.040
De Bilt	52.1	0.055	7.65	0.052
Adak	51.9	0.053	7.49	0.069
Lindau	51.6	0.036	4.76	0.047
Slough	51.5	0.054	8.02	0.041
Sottens	46.7	0.080	10.81	0.092
Ottawa	45.4	0.078	13.77	0.067
Wakkanai	45.4	0.093	15.15	0.105
Genova	44.6	0.042	5.65	0.053
Rome	41.9	0.035	5.37	0.035
Akita	39.7	0.041	6.47	0.035
Washington	38.7	0.068	9.78	0.073
S. Francisco	37.4	0.051	8.56	0.049
Tokyo	35.7	0.046	7.60	0.046
Casablanca	33.6	0.059	9.62	0.059
White Sands	32.3	0.040	6.62	0.037
Yamagawa	31.2	0.042	7.29	0.063
Okinawa	26.3	0.049	8.56	0.061
Puerto Rico	18.5	0.052	9.87	0.029

TABLE 5.1

Station	θ Degrees	S.E.(f_oE) in MHz	S.E.(f_oE)^4 in MHz^4	(Non-linear Model) S.E.(f_oE)
Baguio	16.4	0.063	12.78	0.062
Dakar	14.7	0.044	7.64	0.047
Panama C.	9.4	0.044	8.26	0.029
Ibadan	7.4	0.077	16.01	0.078
Singapore	1.3	0.057	12.03	0.055
Leopoldville	-4.4	0.044	8.14	0.038
Talara	-4.6	0.041	7.50	0.042
Huancayo	-12.0	0.054	10.82	0.049
Townsville	-19.3	0.043	7.87	0.067
Johannesburg	-26.2	0.168	30.57	0.076
Brisbane	-27.5	0.107	21.22	0.053
Watheroo	-30.3	0.101	16.76	0.054
Capetown	-34.1	0.044	6.93	0.035
Canberra	-35.3	0.037	6.47	0.040
Conception	-36.6	0.052	9.27	0.053
Hobart	-42.9	0.038	6.31	0.038
Godleyhead	-43.6	0.074	12.47	0.062
Port Stanley	-51.7	0.070	11.30	0.057
Campbell Is.	-52.5	0.055	7.75	0.048
Port Lockroy	-64.8	0.043	6.22	0.050

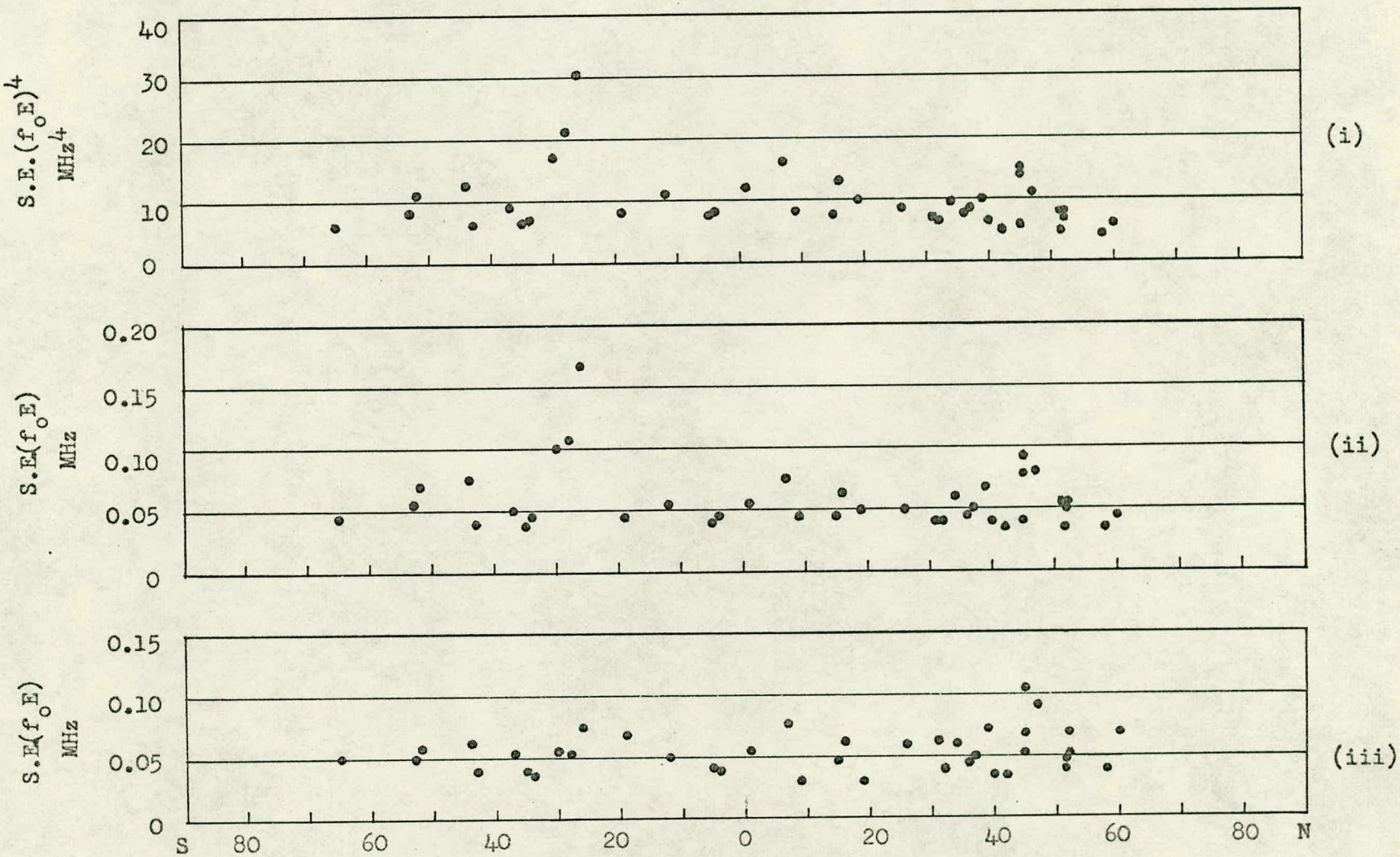

Fig. 5.1 Distribution with geographic latitude of the standard errors of estimate at 40 stations; (i) and (ii) standard errors of $(f_oE)^4$ and f_oE respectively based on equations (5.1) and (5.2); (iii) standard error of f_oE based on equation (5.4).

The values of these parameters were found to be:

$$k = 118 \; ; \; l = 12 \; ; \; \beta = 0.008 \; ;$$

$$a = 0.37 \; ; \; b = -0.82 \; ; \; p = 1.19.$$

Similarly, to minimize the error in equation (5.2) a nonlinear least squares fit of equation (5.4) to all data of the 15 stations between zero and $\pm 32^{\circ}$ was applied by means of stepwise Gauss-Newton iterations on the parameters of equation (5.4). The corresponding values were found to be:

$$k = 92 \; ; \; l = 55 \; ; \; \beta = 0.008$$

$$a = -0.62 \; ; \; b = 0.57 \; ; \; p = 1.19 \text{ or } p = 1.28.$$

The first value of the coefficient p refers to stations between $\pm 32^{\circ}$ and $\pm 13^{\circ}$, and the second value to stations between $\pm 13^{\circ}$ and zero degrees.

Equation (5.4) was then used to estimate f_oE values for a given station in order to calculate the corresponding standard error S_E by means of equation (5.3). The results for the 40 stations are tabulated in Table 5.1 and illustrated in Fig. 5.1(iii). It can be seen that the standard errors at Johannesburg, Brisbane and Watheroo have been considerably reduced. On the other hand it is noted that at northern temperate stations there has been a slight general increase in S_E. Indeed, when the standard error of estimate for the 25 temperate northern and southern stations of latitude higher than 32 degrees was calculated, it was found to be 0.054 MHz when based on equation (5.1) but 0.055 MHz when based on equation (5.4).

Now, for the 15 northern and southern stations lying between 32° and 0°, the standard error of estimate based on (5.2) was 0.070 MHz and that based on (5.4) was 0.053 MHz.

This difference is due mainly to the difference in S_E for Johannesburg, Brisbane and Watheroo.

The standard error of estimate of $(f_oE)^4$ and of f_oE, for all the 40 stations (i.e. 3472 data), based on equations (5.1) and (5.2), were also calculated and found to be:

$$S_E(f_oE)^4 = 10.5 \quad [(MHz)^4];$$

$$S_E(f_oE) = 0.061 \quad [MHz]$$

Similarly, the S_E for the 40 stations based on equation (5.4) were calculated and found to be:

$$S_E(f_oE)^4 = 9.2 \quad [(MHz)^4];$$

$$S_E(f_oE) = 0.054 \quad [MHz]$$

All the above results suggest that the two mathematical models, given respectively by equation (5.4), and by equation (5.1) together with equation (5.2), are virtually equivalent. Considering also that the world-wide average error in f_oE, quoted by URSI[129], is $\pm$ 0.12 MHz, there seems to be no reason to adopt equation (5.4) instead of equations (5.1) and (5.2).

5.2 COMPARISON OF OBSERVED AND ESTIMATED f_oE VALUES

It is interesting to see how the f_oE observed values and those calculated from equations (5.1) and (5.2) are distributed against both time and location. It is also instructive to compare the f_oE values estimated from the proposed expressions (5.1) and (5.2) with the corresponding values calculated from f_oE formulae given by other workers.

Several relationships between f_oE and the parameters on which it depends have been proposed by different investigators. For example Harnischmacher[14] has found that f_oE is related to the geographic latitude, θ, the Zurich sunspot number, R, and the solar zenith angle, χ, by means of equation (A.2), which for convenience is rewritten here:

$$f_oE = K(\cos\chi)^p \qquad (5.5)$$

with $K = 2.25 + 1.5\cos\theta + (0.01 - 0.007\cos\theta)R$,

and $p = 0.21 + 0.12\cos\theta + 0.0002R$.

Davies[15] and also Van Zandt[16] have stated that to a first approximation the critical frequencies of the E-layer are given by

$$(f_oE)^4 = 118.1(1 + 0.008R)\cos\chi \qquad (5.6)$$

claiming that the estimated values of f_oE are usually within 0.2 MHz of the observed values. Swenson[17], for stations lying between geographic latitudes 15^oN and 15^oS, has suggested the following relationship :

$$\log f_oE = 0.540 + 0.00058R + 0.31(\log\cos\chi) \qquad (5.7)$$

Here the errors in f_oE were estimated to be approximately 0.2 MHz at all values of R.

It is proposed now to make use of each of the above relationships for comparisons between estimated and observed monthly-median hourly values of f_oE. For this purpose f_oE measured data which have not been used in deriving the relationships (5.1) and (5.2), were taken from two groups of stations covering a wide range of latitudes and longitudes:

stations previously used in the statistical analysis and stations not used at all. The stations selected for both groups are listed in Table 5.2 together with the period of data used in the comparison.

Using the 1963 to 1969 averages of the Slough data, Fig. 5.2 illustrates for each month of the year comparisons between the measured monthly-median hourly values of f_0E and those calculated from the here proposed formula (5.1), Harnischmacher's formula (5.5) and Davies expression (5.6) respectively. Similarly Fig. 5.3 shows comparisons for Mundaring station ($32^{\circ}S$). It should be noted that in this case either of the expressions (5.1) and (5.2) may be used since both give the same f_0E value for the latitude of 32 degrees. In addition, Figs. 5.4 and 5.5 show similar comparisons for Singapore and Bogota respectively.

From these figures it is clear that there is very close agreement between observed f_0E values and corresponding values calculated from formulae (5.1) and (5.2); and also that this agreement is considerably better than that between observed f_0E values and calculated values using the formulae of Harnischmacher, or Davies and Van Zandt, or Swenson.

Turning now to two stations for which the estimated standard errors in the analysis based on equation (5.2) were unusually high, comparisons have been made between calculated and observed monthly-median hourly values of f_0E for Johannesburg and Brisbane; these are illustrated in Figs. 5.6 and 5.7 respectively for each month of the year. It can be seen from these figures that even at these stations the discrepancy between observed and estimated values is almost everywhere less than $\pm$ 0.1 MHz.

TABLE 5.2

Stations and period of data used in the comparison of calculated and measured monthly-median hourly values of f_oE.

Station	Geog. Lat. in degrees	Geog. Long. in degrees.	Period of Data
*Slough	51.5N	0.6W	1963 - 1969
**Freiburg	48.1N	7.6E	1968
*Rome	41.9N	12.5E	1965 - 1969
**Athens	38.0N	23.6E	1964
*Tokyo	35.7N	139.5E	1963 - 1969
**Bogota	4.5N	74.2W	1963 - 1967
*Singapore	1.3N	103.8E	1963 - 1969
**Rarotonga	21.2S	159.8W	1963 - 1967
*Johannesburg	26.2S	28.0E	1961 - 1963
*Brisbane	27.5S	152.9E	1964 - 1967
**Mundaring	32.0S	116.2E	1963 - 1969

* Stations used in the statistical analysis but with data of different period.

** Stations not used in the analysis.

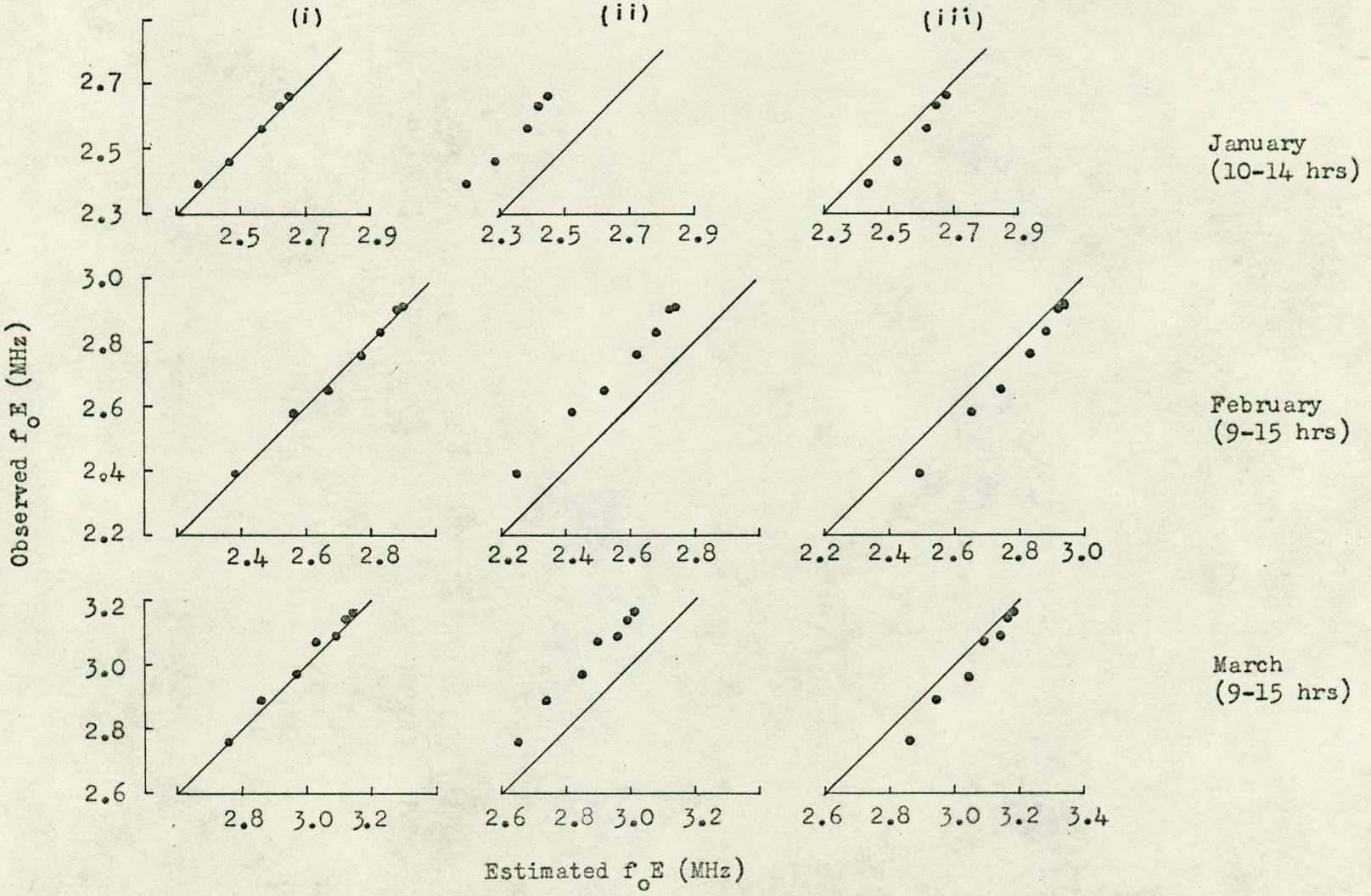

Fig. 5.2(a) Showing comparisons between observed f_oE values at Slough (1963-1969) and those estimated by means of: (i) equation (5.1); (ii) equation (5.5); (iii) equation (5.6). The straight lines represent a one-to-one correspondence.

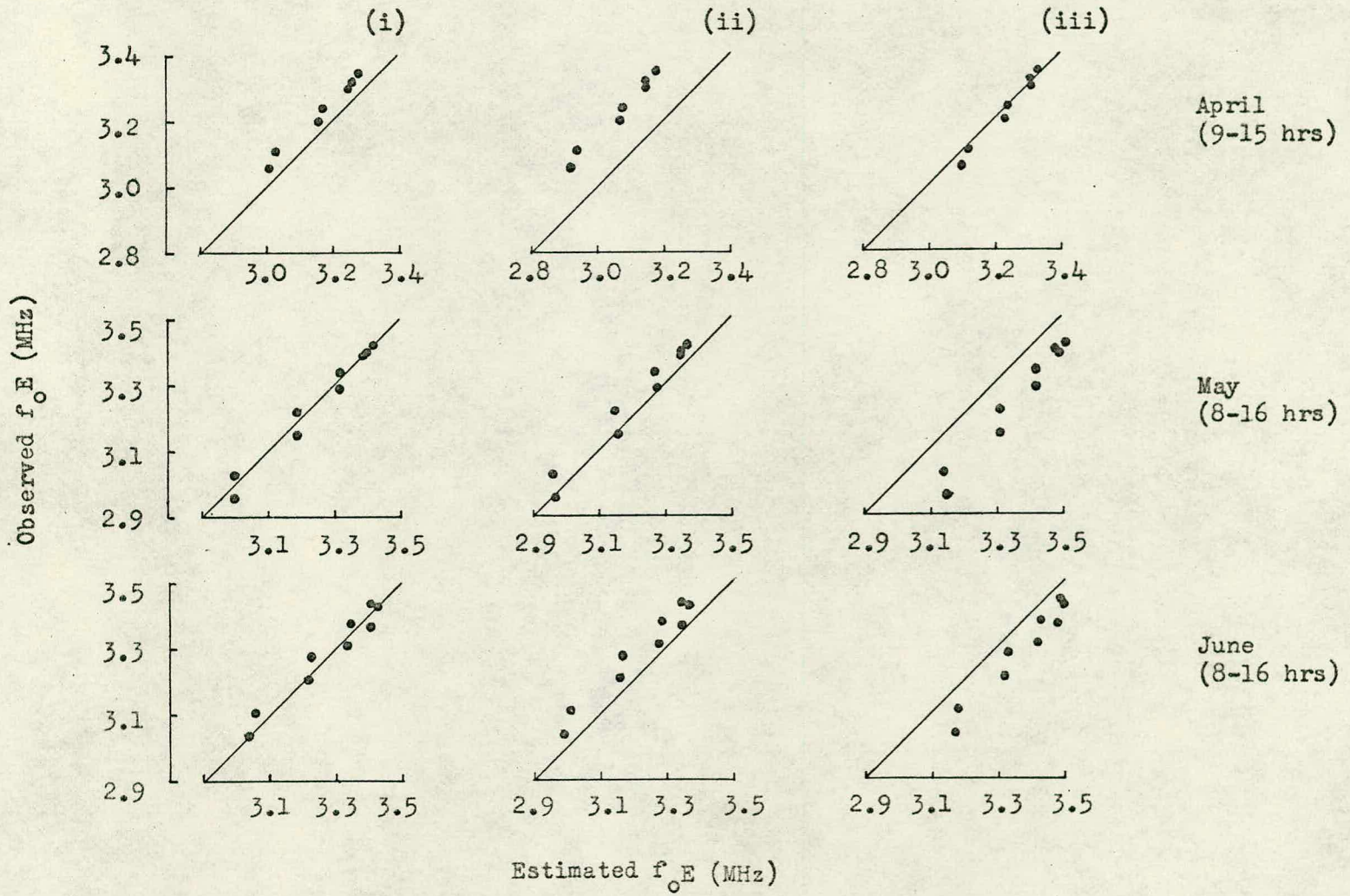

Fig. 5.2(b) Showing comparisons between calculated and observed f_oE values at Slough.

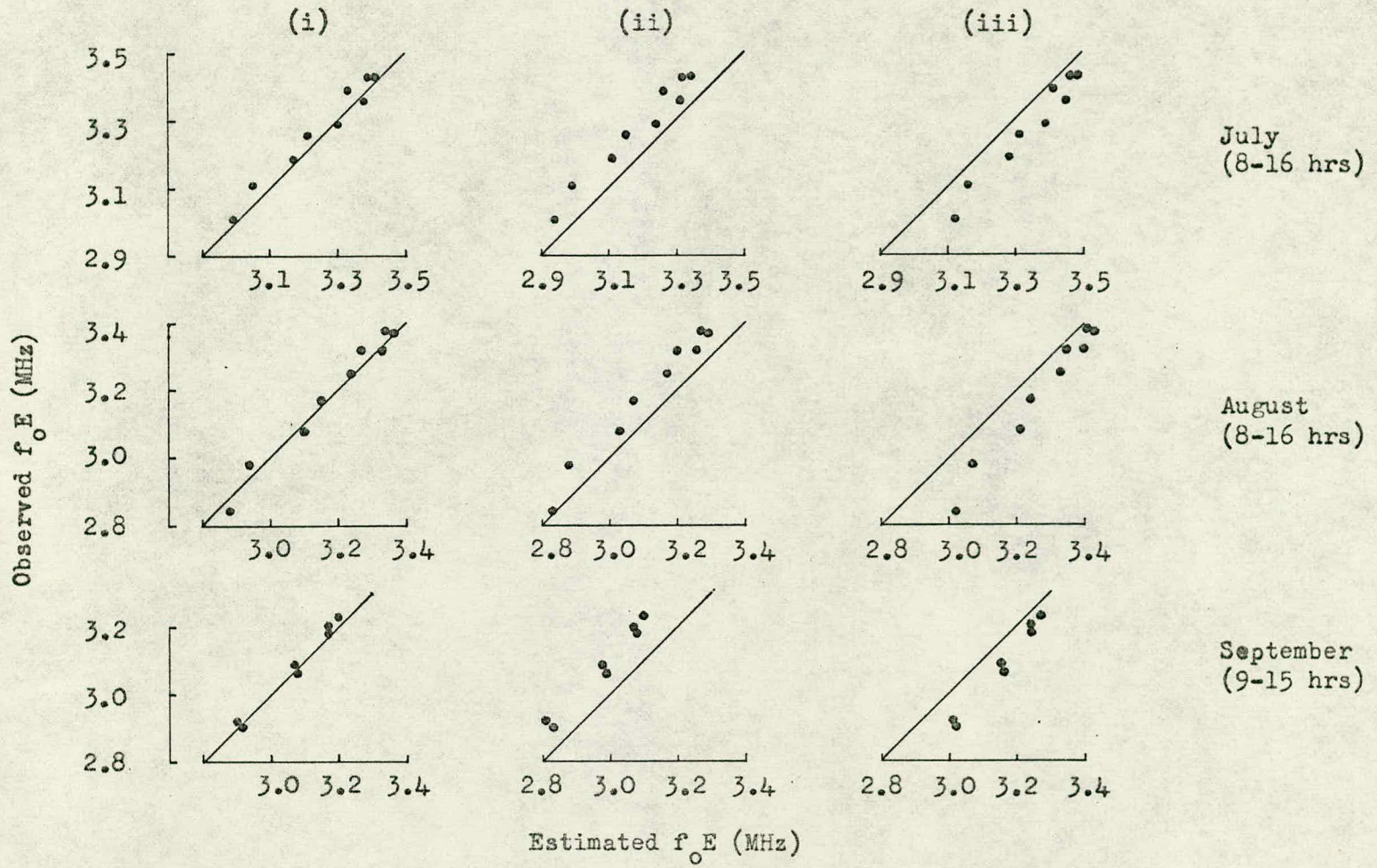

Fig. 5.2(c) Showing comparisons between calculated and observed f_oE values at Slough.

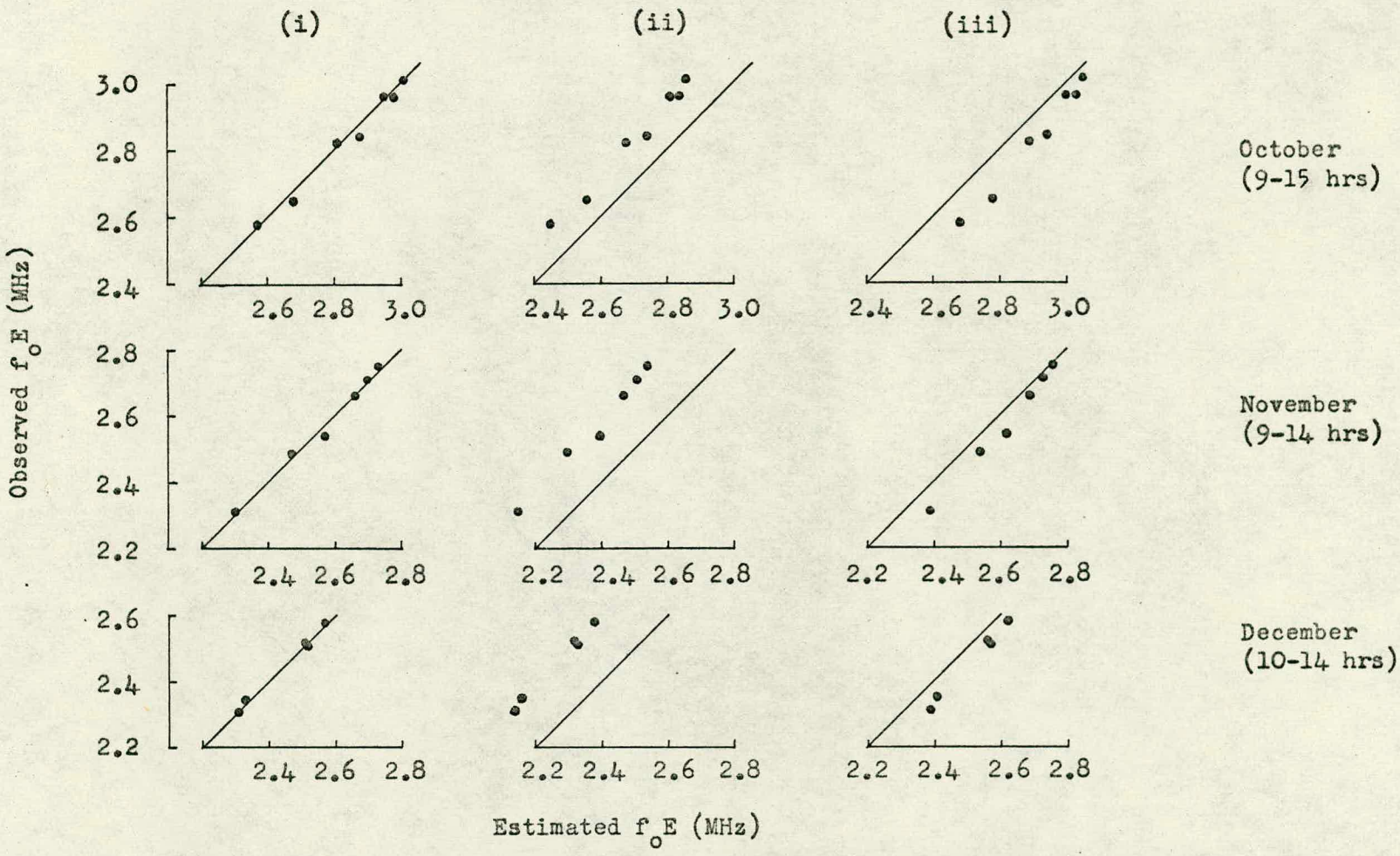

Fig. 5.2(d) Showing comparisons between calculated and observed f_oE values at Slough.

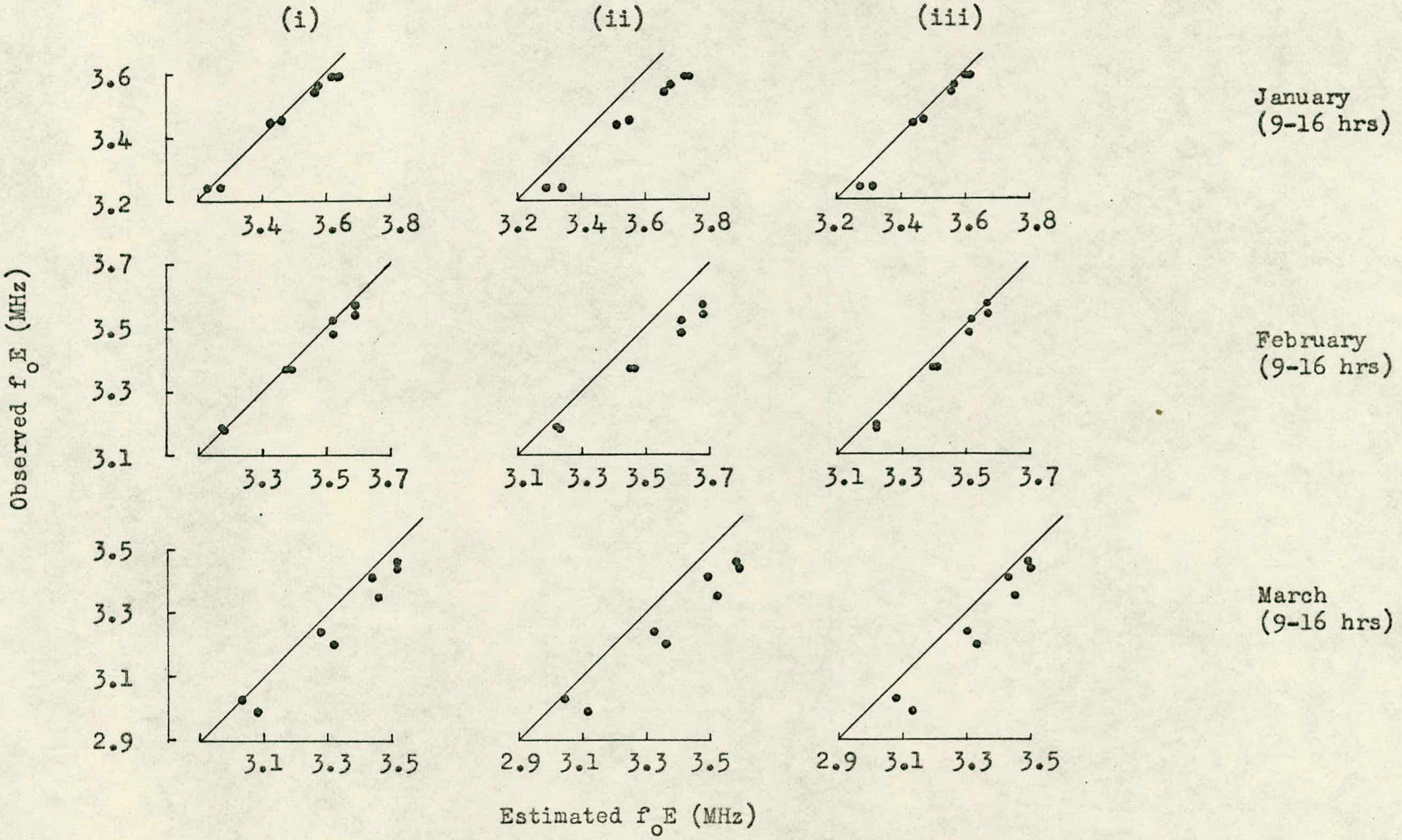

Fig. 5.3(a) Showing comparisons between observed f_oE values at Mundaring (1963-1969) and those estimated from: (i) equation (5.1) or (5.2); (ii) equation (5.5); (iii) equation (5.6).

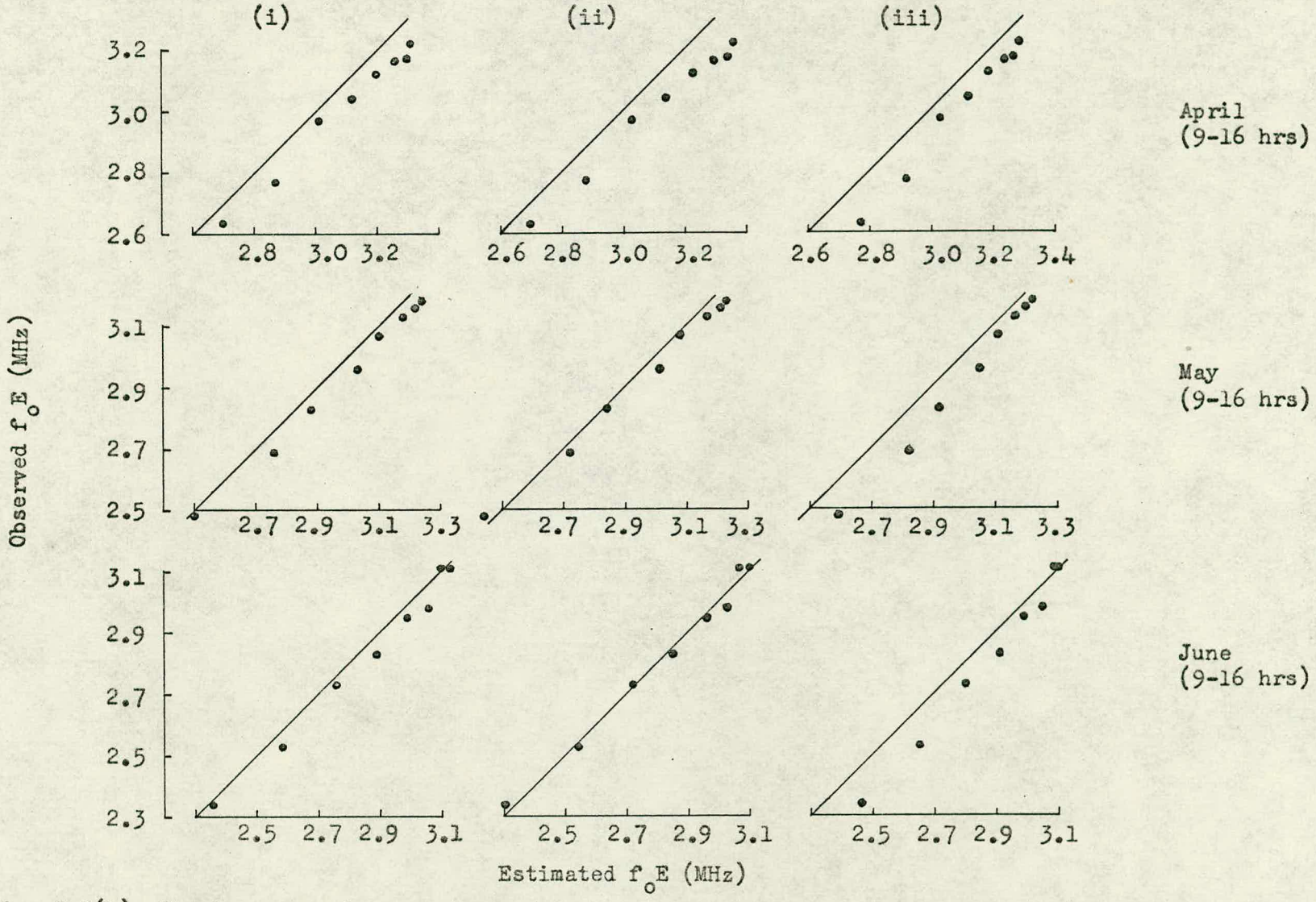

Fig. 5.3(b) Showing comparisons between calculated and observed f_oE values at Mundaring.

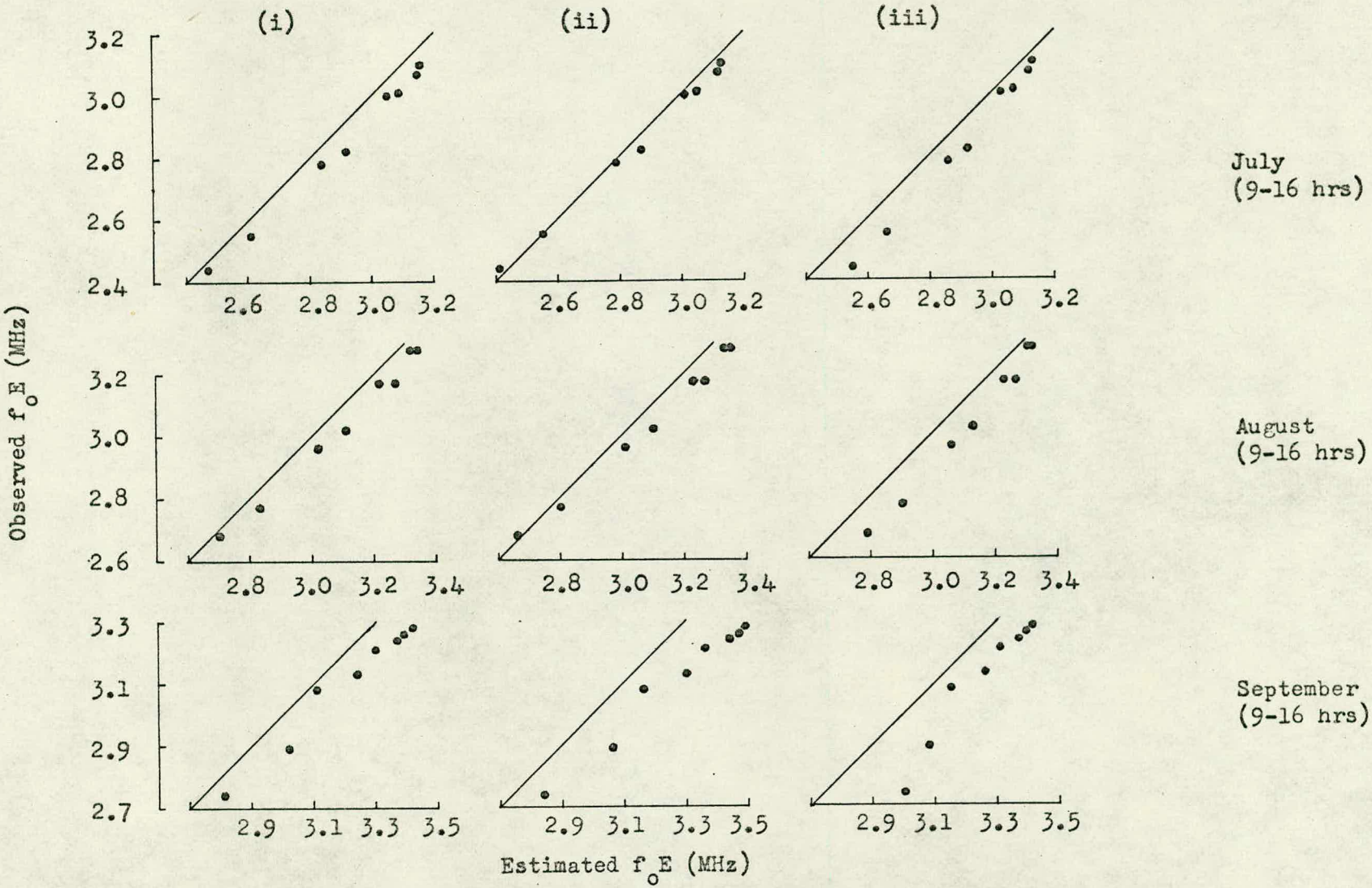

Fig. 5.3(c) Showing comparisons between calculated and observed f_oE values at Mundaring.

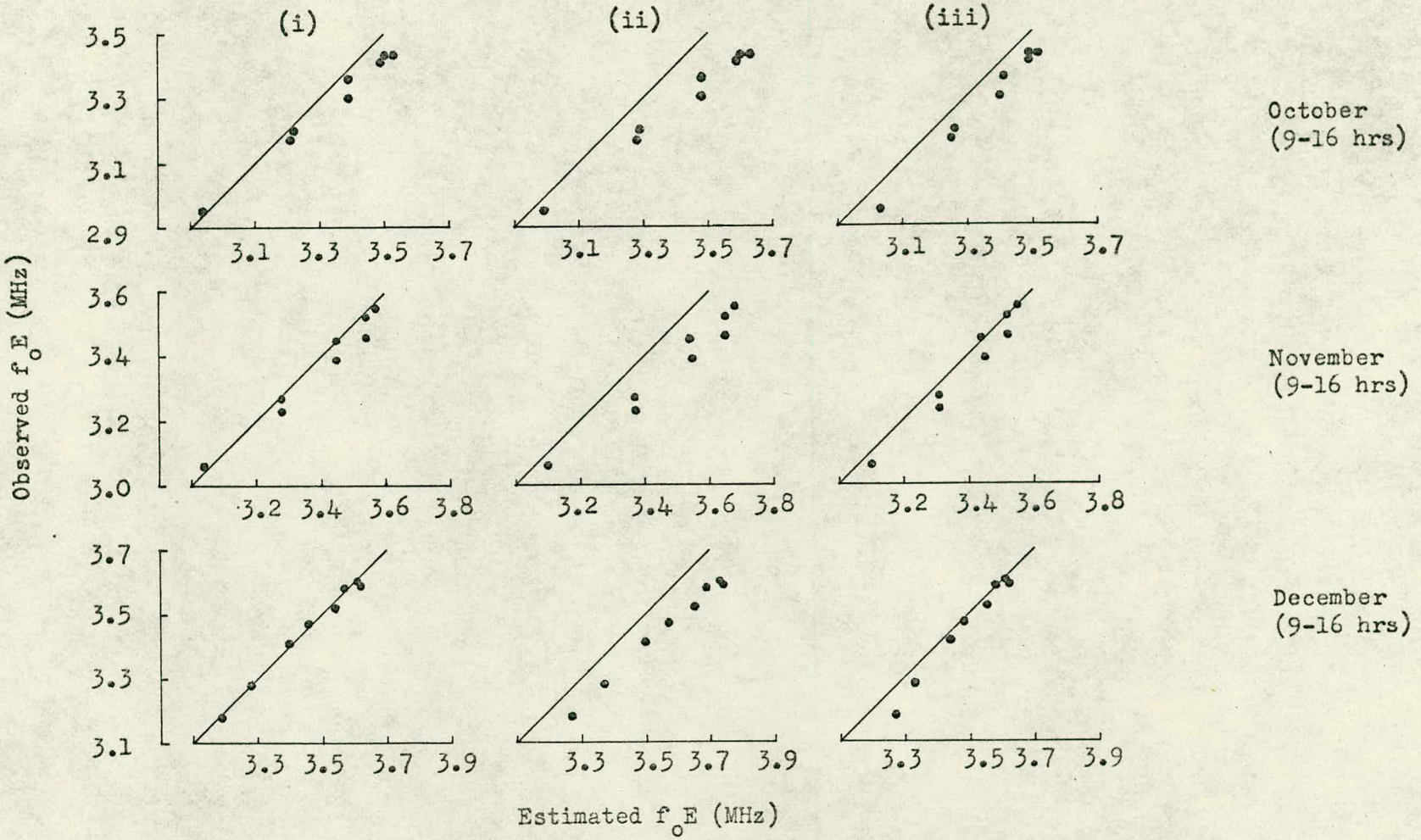

Fig. 5.3(d) Showing comparisons between calculated and observed f_oE values at Mundaring.

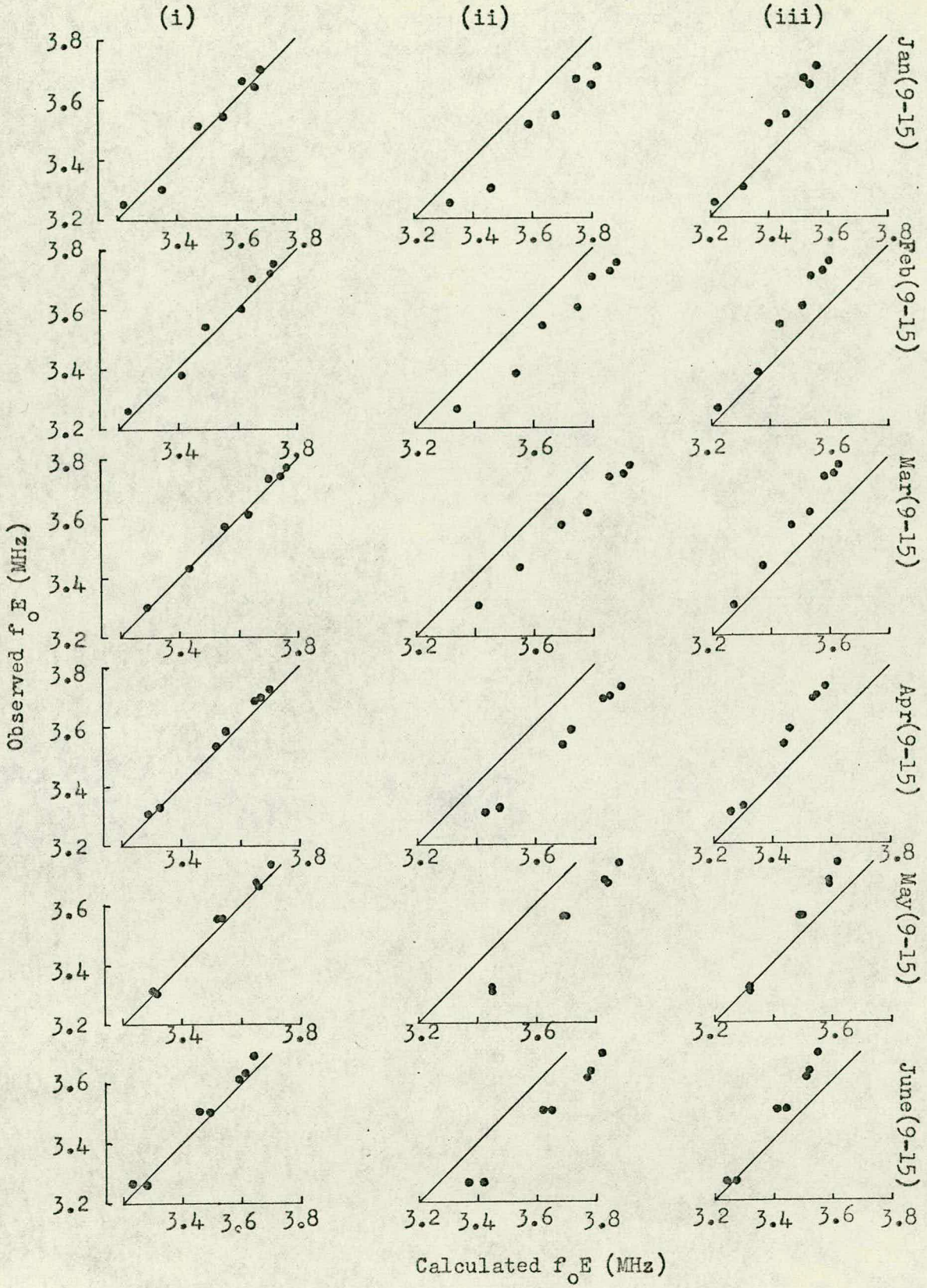

Fig. 5.4(a) Showing comparisons between observed f_oE values at Singapore (1963-69) and those calculated using (i) equation (5.2); (ii) equation (5.5); (iii) equation (5.6).

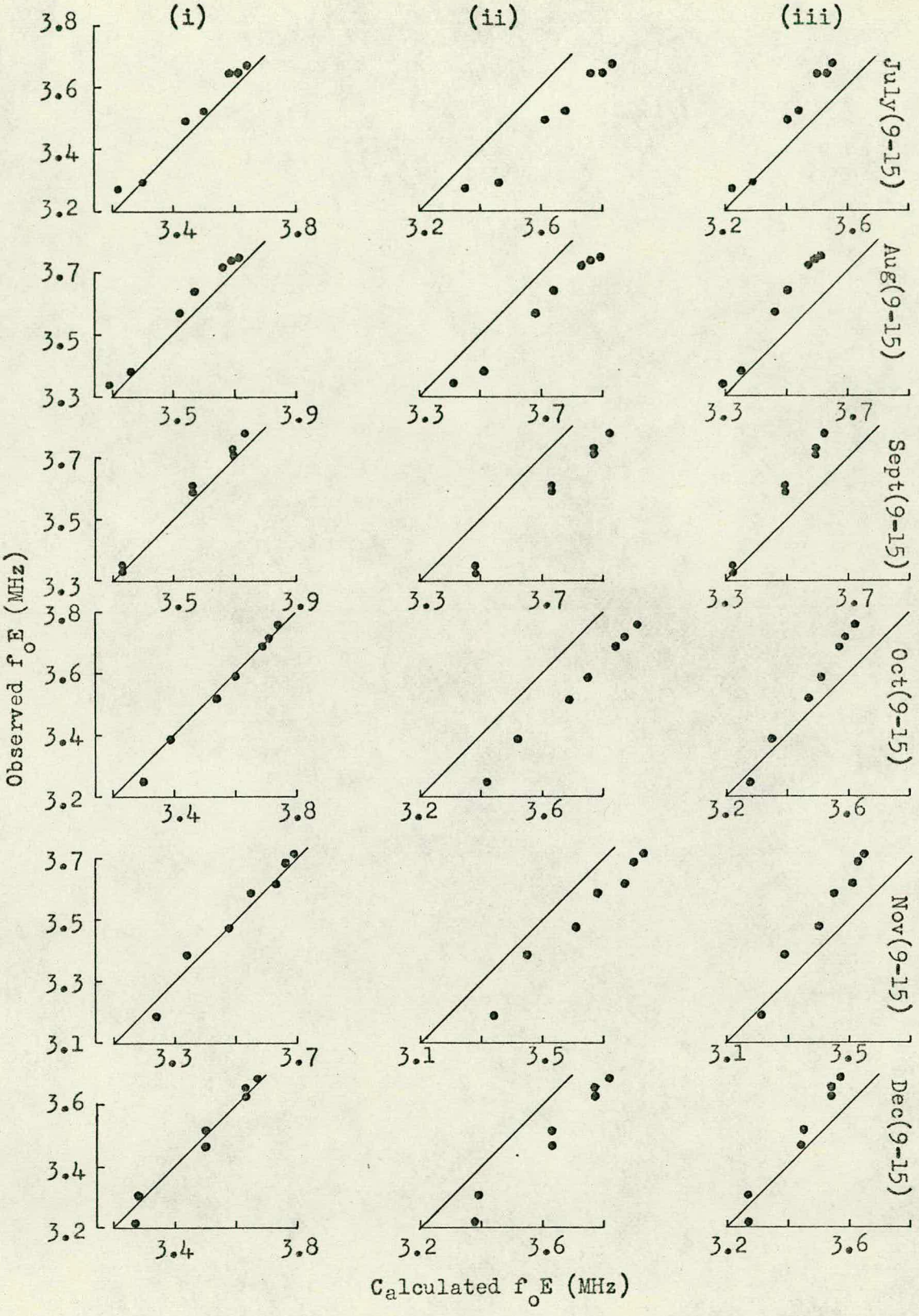

Fig. 5.4(b) Showing comparisons between calculated and observed f_oE values at Singapore.

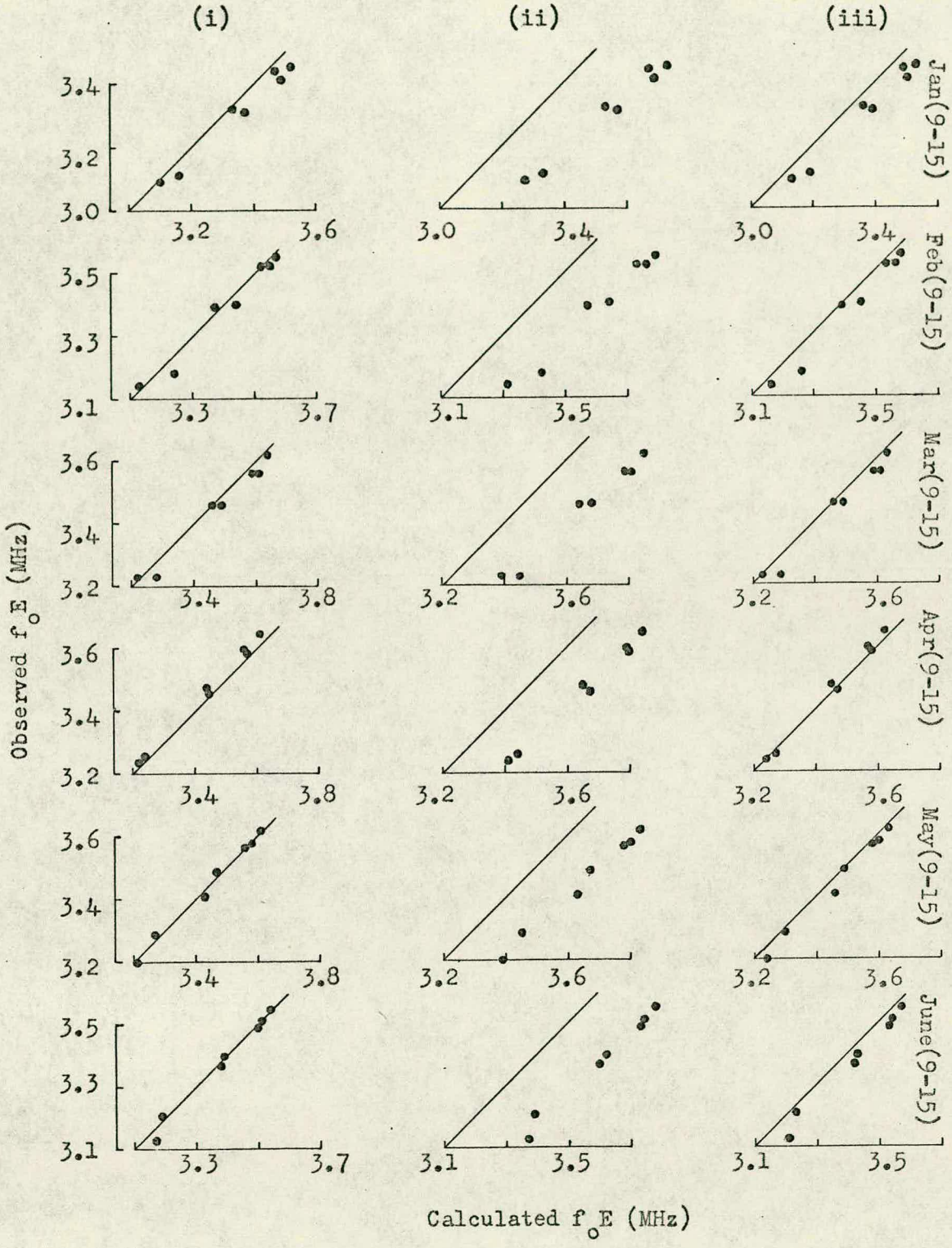

Fig. 5.5(a) Showing comparisons between observed f_oE values at Bogota (1963-1967) and estimated values using (i) equation (5.2); (ii) equation (5.5); (iii) equation (5.7).
The straight lines represent one-to-one correspondence.

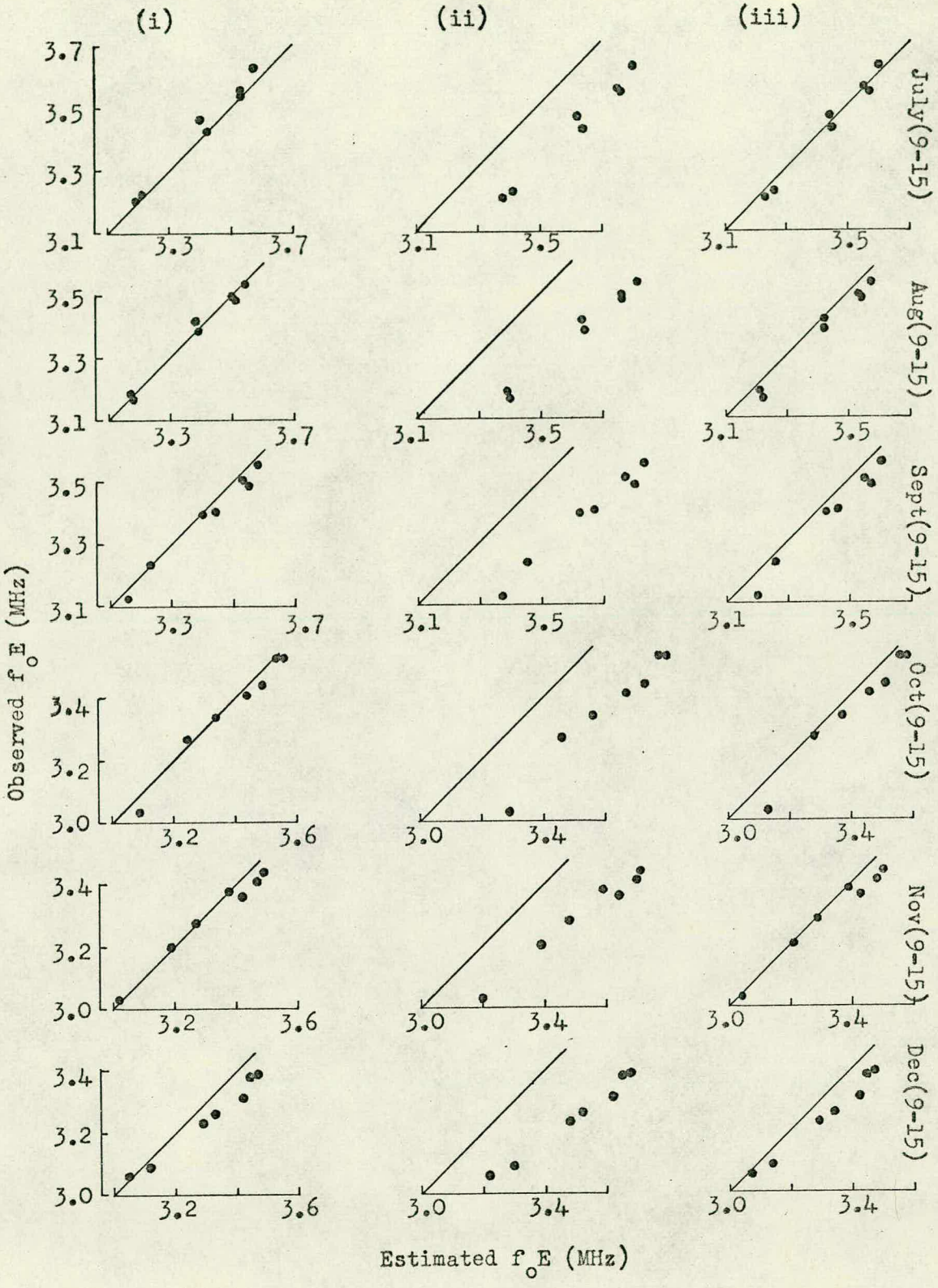

Fig. 5.5(b) Showing comparisons between calculated and observed f_oE values at Bogota.

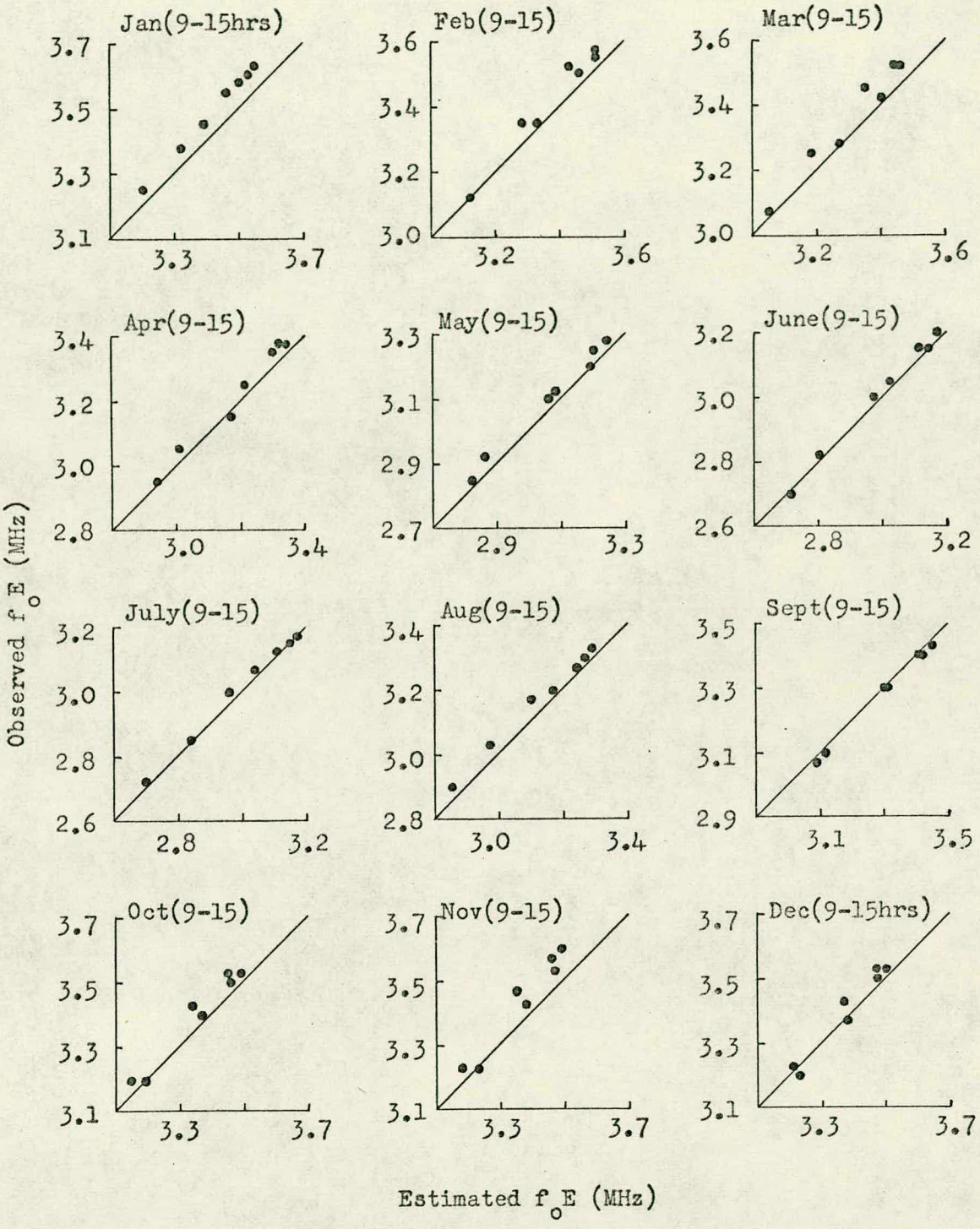

Fig. 5.6 Showing comparisons between observed f_oE values at Johannesburg (1961-1963) and those calculated using equation (5.2).

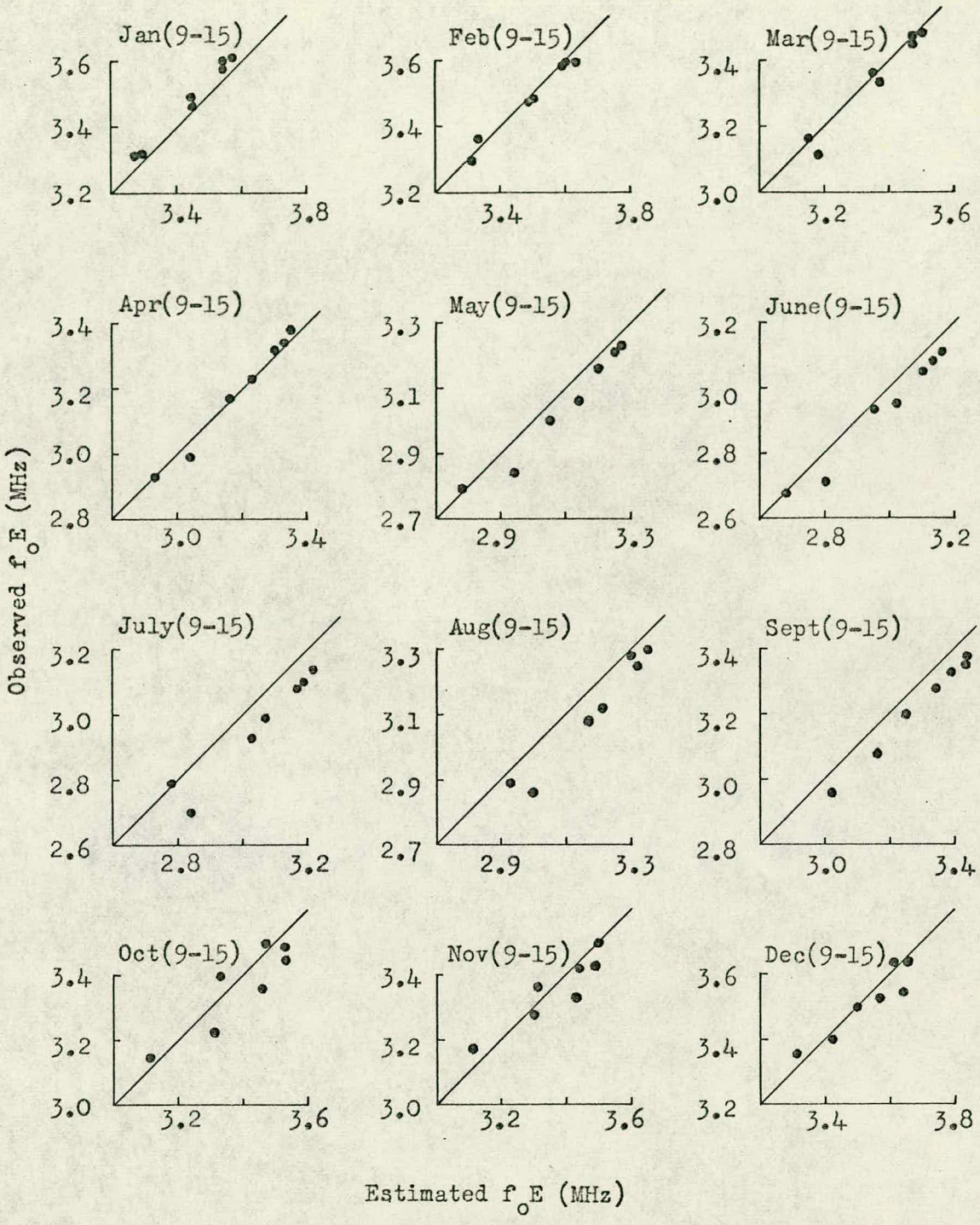

Fig. 5.7 Showing comparisons between observed f_oE values at Brisbane (1964-1967) and those estimated using equation (5.2).

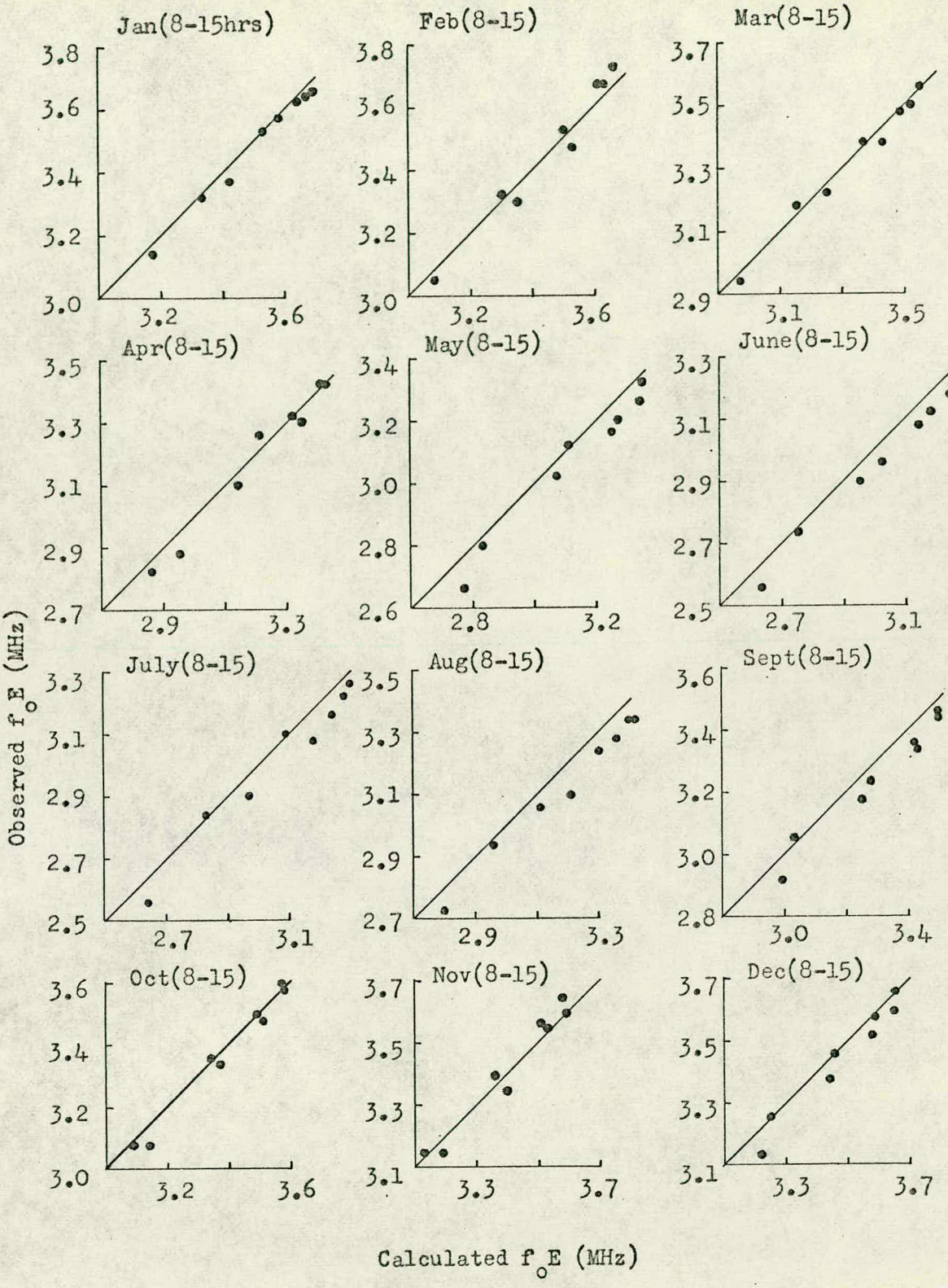

Fig. 5.8 Showing comparisons between observed f_oE values at Rarotonga (1963-1967) and estimated values using equation (5.2).
The straight lines represent one-to-one correspondence.

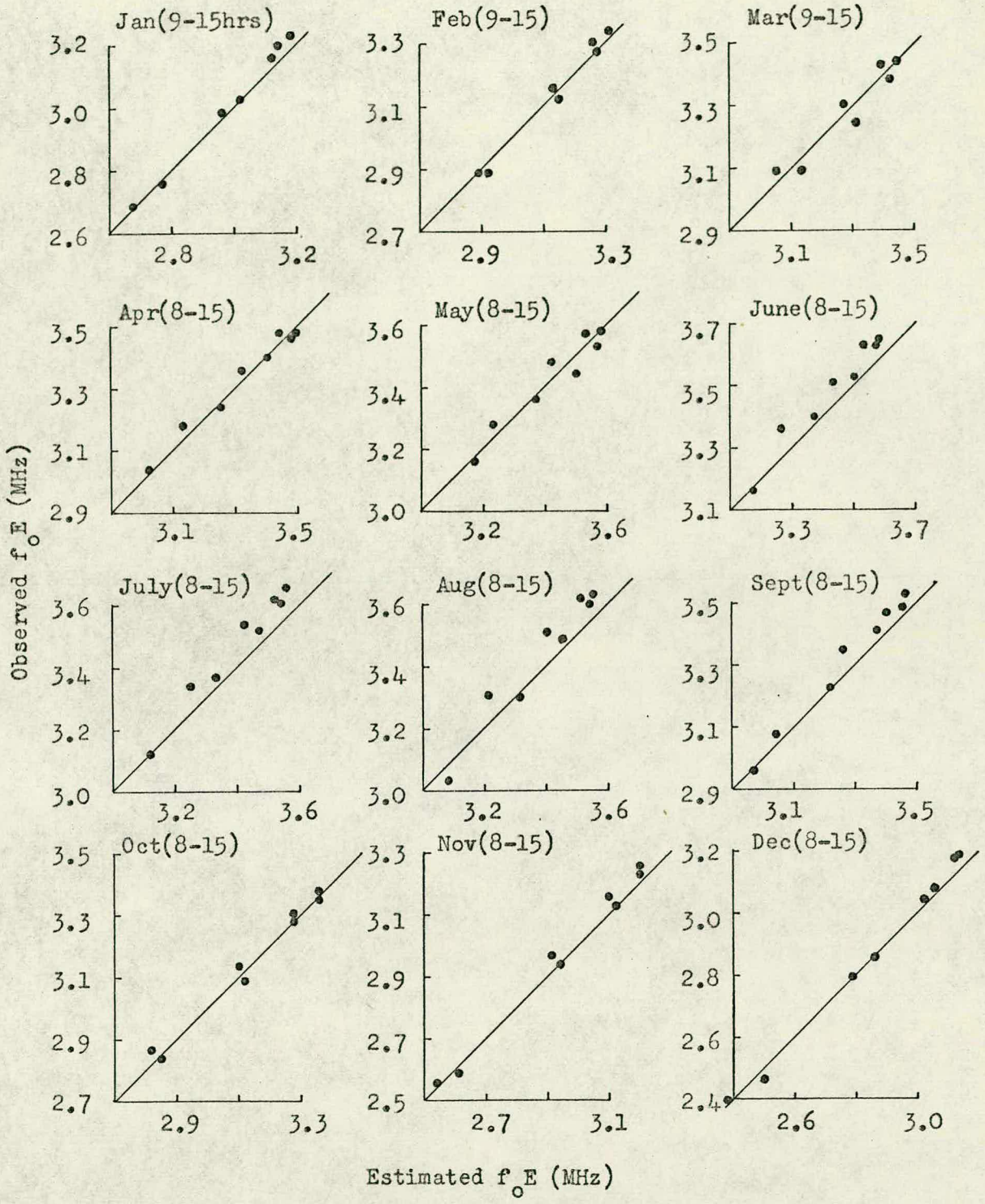

Fig. 5.9 Showing comparisons between observed f_oE values at Tokyo (1963-1969) and those estimated using equation (5.1). The straight lines represent one-to-one correspondence.

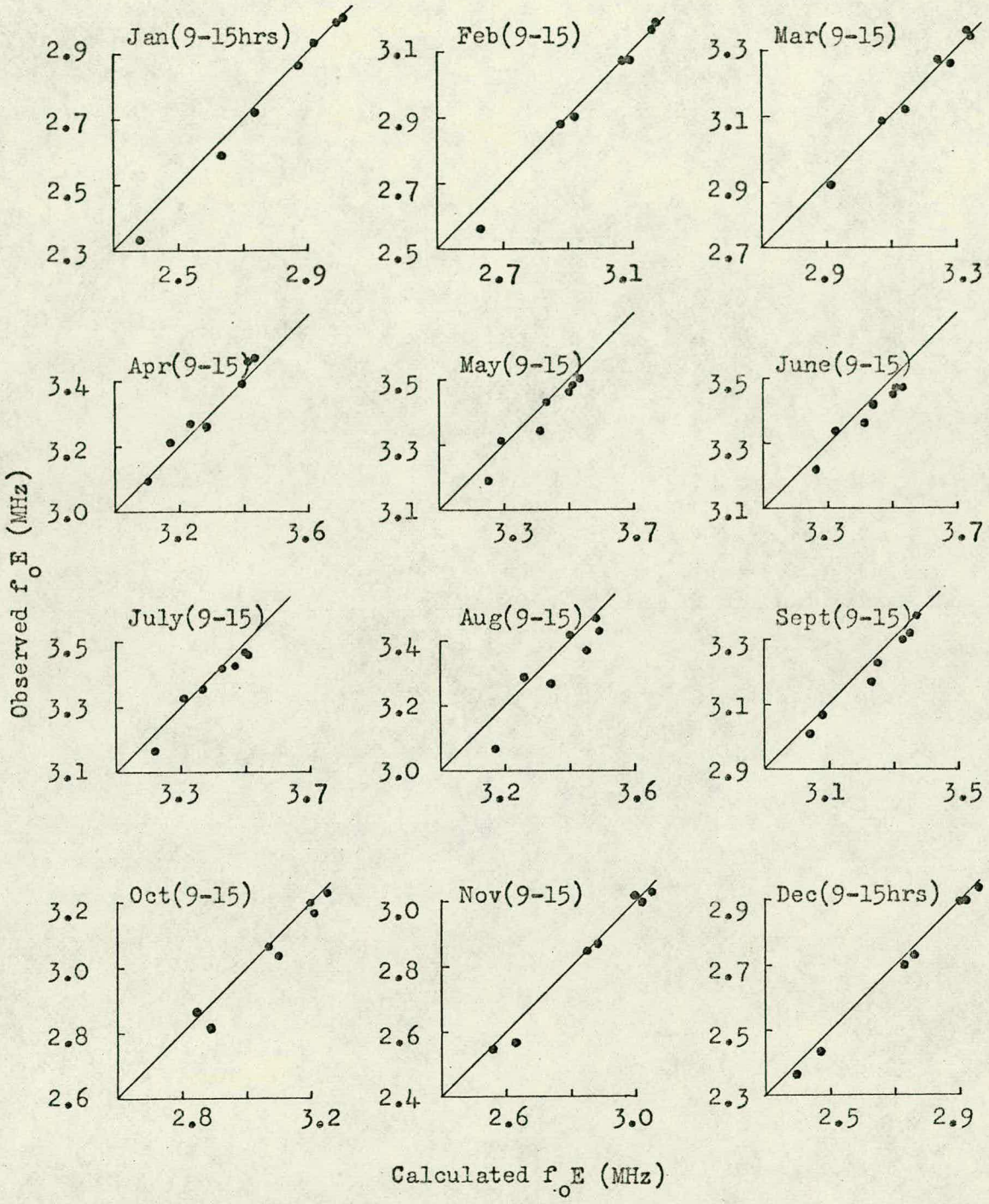

Fig. 5.10 Showing comparisons between observed f_oE values at Rome (1965-1969) and those calculated using equation (5.1).

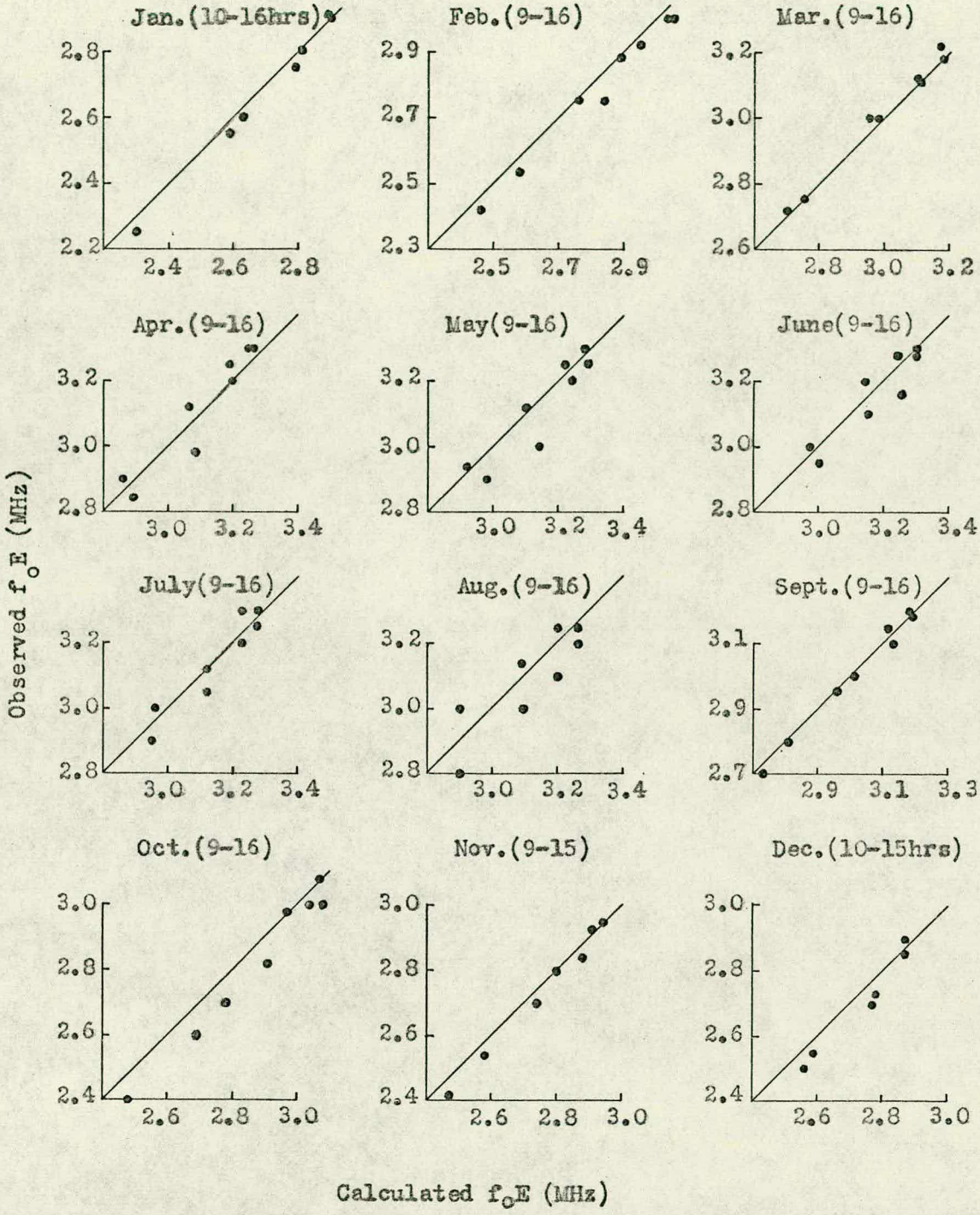

Fig. 5.11 Showing comparisons between observed f_oE values at Athens during 1964 (minimum of solar activity) and those calculated using equation (5.1).

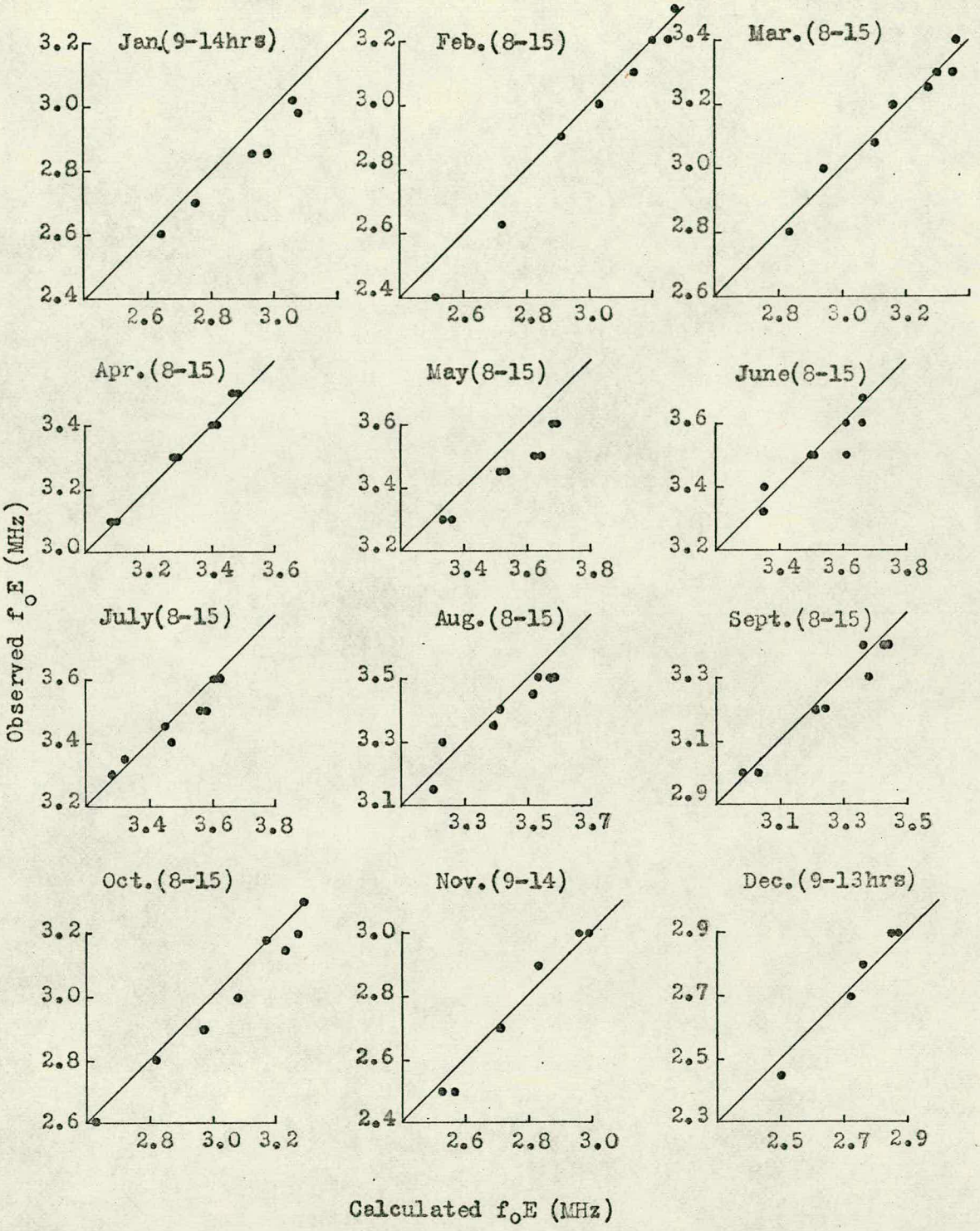

Fig. 5.12 Showing comparisons between observed f_0E values at Freiburg during the year 1968 (maximum of solar activity) and calculated values using equation (5.1).

Figs. 5.8, 5.9 and 5.10 illustrate similar plots of comparisons for the stations of Rarotonga, Tokyo and Rome, so that a wide range of latitudes and longitudes has been considered. It is evident also from these figures that close agreement exists between calculated and observed values.

Now, in all the above comparisons an average level of solar activity was considered. Therefore two further sets of comparisons have been made, one for the year of minimum solar activity 1964, which is illustrated in Fig. 5.11 for Athens, and one for the year of maximum solar activity 1968, which is shown in Fig. 5.12 for Freiburg.

We may therefore conclude that, at different latitudes, different levels of solar activity and different values of χ, close agreement exists between the observed f_oE values and those estimated from the proposed expressions (5.1) and (5.2).

CHAPTER 6

SUMMARY AND CONCLUSIONS

A statistical investigation of the solar and seasonal control of f_oE has been described and the final conclusions of this work are summarised here.

In the study of the solar-activity control of f_oE the more appropriate model of each of the three relationships, f_oE/R, f_oE/Φ and $f_oE/IF2$, was first determined. Appropriate statistical tests showed (Tables 2.2 and 2.5) that the best linear correlations between noon f_oE values and each of the three solar indices are obtained if the following models are used:

$$(f_oE)^4 = a_R(1 + 0.0091\ R) \tag{6.1}$$

$$(f_oE)^4 = a_\Phi(1 + 0.0094\ \Phi) \tag{6.2}$$

$$f_oE = a_I(1 + 0.00144\ IF2) \tag{6.3}$$

where R is the Zurich relative sunspot number, Φ is the solar radio noise flux at 10.7 cm referred to a mean minimum value for the quiet sun of 66 flux units[78], and IF2 is the ionospheric index of solar activity.

The numerical coefficients in these equations are over-all average values of the individual monthly values obtained at each of 47 stations by a least-squares analysis of the corresponding data. It was shown that, at each station, these monthly values of the sensitivity to solar activity changes are independent of season, and, that their twelve-month average is independent of the latitude of the station.

The combined correlation coefficient of each of the three pairs of variates in equations (6.1), (6.2) and (6.3), was determined by means of Fisher's z-transformation from 545 individual linear correlation coefficients and found to be respectively:

$$r_R = 0.971 \quad r_\Phi = 0.973 \quad r_{IF2} = 0.974$$

The usual tests of significance showed that there is no significant difference between the values of these three correlation coefficients. Therefore the choice of the most useful relationship for any particular purpose should be based on other criteria such as operational convenience, availability of current data, and secular variations[90].

Equations (6.2) and (6.3) appear to provide the only f_oE/Φ and $f_oE/IF2$ numerical relationships contained in the ionospheric literature, while equation (6.1) gives the only fourth-power relationship between f_oE and R determined from a large number of data.

In the statistical study of the diurnal variation of f_oE, the value of the exponent p of $\cos\chi$ in equation (3.2) was determined for each month at each station. By means of a statistical F test, applied to these monthly p values for each station, the important fact was demonstrated that the diurnal exponent does not show any systematic variation with season. This confirms similar conclusions of other workers who, however, made their statements on a graphical basis only.

Since the F test showed that there is no significant difference between the monthly p values for a given station, they were pooled for a better estimate of the exponent of $\cos\chi$ for the station.

Moreover, further statistical analysis showed that, for the data involved, of all the 45 stations, there is no basis for using different values of p for the different stations. Hence it was legitimate to use the over-all pooled exponent as the best estimate. This over-all average value was found to be: $p = 1.20$. However, for stations lying within a range of about 12^{o} on either side of the equator a value of $p = 1.31$ was considered to be more appropriate.

In the statistical study of the seasonal dep endence of $f_{o}E$, the values of A in equation (4.2) were determined for each month at each of the 45 stations. The variation of A with month of the year at each station represents the Appleton E-layer seasonal anomaly (13).

It was shown (Fig. 4.2) that the value of A is less in local summer than in local winter in both hemispheres, the effect being more marked at stations away from the equator. For equatorial stations the seasonal anomaly is extremely small. In addition to this strong latitudinal dependence the seasonal anomaly was found to be dependent on longitude and hemisphere (Figs. 4.2 and 4.9). The variability of A was expressed by means of the empirical equation:

$$A = B(\cos\chi_{noon})^{m} \tag{6.4}$$

where

$$m = a + b\cos\theta \tag{6.5}$$

and

$$B = k + l\cos\theta \tag{6.6}$$

where θ is the geographic or magnetic latitude and the coefficients a, b, k, l, are given accordingly in equations (4.6) to (4.11), and (4.13) to (4.16).

The latitudinal distributions of the parameters m and B proved to be systematic. The seasonal index m has peak values at latitudes of about 30 to 40 degrees in both hemispheres, whereas B increases with decreasing latitude. Moreover longitudinal and hemispheric inequalities were found in the patterns of m and B, and it was pointed out that similar inequalities are observed in the pattern and in the current intensity of the S_q current system[143][147]. Finally the conclusion was reached that the Appleton seasonal anomaly is mainly due to seasonal changes of the current intensity and shifts of the S_q current foci; and to seasonal changes in the height of the S_q current sheets.

The mathematical models determined from the statistical analysis of the variation of f_oE with solar activity, solar zenith angle, and season,were combined to obtain an analytical expression from which f_oE may be evaluated.

This expression, appropriate to latitudes between 32^o to about 65^o in each hemisphere, is:

$$(f_oE)^4 = (92 + 35\cos\theta)(1 + 0.0094\Phi)(\cos\chi_{noon})^m(\cos\chi)^p \qquad (6.7)$$

where $\Phi = \Phi_{obs.} - 66$

$m = 0.11 - 0.49\cos\theta$

$p = 1.20$

θ is the geographical latitude and

$\Phi_{obs.}$ is the observed solar radio noise flux at 10.7 cm.

For latitudes less than 32^o in both hemispheres the following expression of f_oE was obtained:

$$(f_oE)^4 = (23 + 116\cos\theta)(1 + 0.0094\Phi)(\cos\chi_{noon})^m(\cos\chi)^p \qquad (6.8)$$

where $m = -1.93 + 1.92\cos\theta$,

$p = 1.20$ for stations between 32^o and about 12^o,

or $p = 1.31$ for stations between 12^o and 0^o.

The standard errors of estimate of f_oE in expressions (6.7) and (6.8) were found to be respectively:

$$S.E.(f_oE) = 0.05 \text{ MHz, and } S.E.(f_oE) = 0.07 \text{ MHz.}$$

The reliability of these formulae was further assessed by comparison of calculated and observed f_oE values at different latitudes, different levels of solar activity and different zenith angles.

Some discrepancy between calculated and observed f_oE values may occur since in the synthesis of the expressions (6.7) and (6.8) no account was taken of the longitudinal and hemispheric inequalities in the seasonal anomaly. It is therefore suggested that further work be planned to take account of these asymmetries. For this purpose two lines of approach could be considered. In the first place the use of a still larger number of stations chosen to obtain a more uniform latitudinal distribution in each of the three longitudinal zones considered in the present work. In the second place the choice of a different independent variable in equations (6.4), (6.5) and (6.6). Indeed, if the seasonal anomaly is the result of the motor influence of the S_q current system, the effect is determined by the real distribution of the Earth's magnetic field at the ionospheric level and by the parameters of the upper atmosphere. Consequently a parameter expressed in terms of geographic, geomagnetic and magnetic latitude[157][160], chosen as the independent variable in the above equations, might give better results.

Finally, to ascertain quantitatively the relation between the Appleton seasonal anomaly and the S_q current system variations, it might be useful to study in detail the behaviour of the two seasonal variations estimated respectively from f_oE and geomagnetic measurements at a number of stations chosen so that each ionospheric observatory is paired with a nearby magnetic observatory.

APPENDIX A

A REVIEW OF THE WORK DONE BY PREVIOUS INVESTIGATORS

Ionospheric studies have shown that the general behaviour of the E layer is very similar to that of an ideal α-Chapman layer, at least to a first approximation. Problems, however, arise when practical electron production and loss processes, variation in atmospheric scale height, diurnal, seasonal and geographical variations, and similar other features are taken into consideration. Additional problems arise from vertical drift effects associated with horizontal currents flowing in the E layer across the horizontal geomagnetic field; these play a small but nevertheless significant role in the morphology of the E layer.

An extensive description of the behaviour of the ionospheric E region was given in 1959 by Robinson[6]. Here we shall review some E-layer phenomena mainly concerning E-layer critical frequencies, as well as the non-Chapmanlike variations identified in f_oE.

A.1 VARIATION OF f_oE WITH SOLAR ACTIVITY

Ionospheric observations over three solar cycles have shown that the ionization of the E layer, and hence the critical frequency, f_oE, is closely related to the level of solar activity. Both X-ray and EUV radiation responsible for the E-layer ionization [93][94][95] vary with the 11-year solar cycle. The maximum-to-minimum variation for the X-ray radiation is sevenfold and for the EUV radiation it is approximately two-fold[94][96]. The corresponding maximum-to-minimum solar cycle variation in the E-layer critical frequency is only about 1.5[72][94].

The level of solar activity is often expressed in terms of a numerical index. There are three different indices at present in international use, namely, the Zurich relative sunspot number, R[84]; the solar radio noise flux at 10.7 cm, Φ[97]; and the ionospheric index of solar activity, IF2[98].

The Zurich sunspot number provides the longest continuous series of values of any solar index available, more than 200 years. Although it is rather arbitrary and artificial it has proved extremely useful as an index of solar activity since it provides a large homogeneous sample of data that forms the best available statistical basis for predicting future solar activity. According to Kiepenheuer[99] the probable error in the daily value is of the order of 15%, and in the monthly mean values it is between 3% and 5%.

The solar radio noise flux at 10.7 cm has been measured regularly by Covington[97][100] in Canada since 1947 and is given in flux units (units of 10^{-22} x Watt/m^2/cycle/sec). These measurements have been very carefully calibrated and the relative errors over long periods of time are only about $\pm$ 2%[78]. This internal consistency is much better for Φ than for R. Another advantage of Φ over R lies in the fact that the former is based upon observations of electromagnetic radiation reaching the Earth, while the latter is based only upon the visual observation of sunspots.

The IF2 ionospheric index of solar activity proposed by Minnis and Bazzard[98] relies on a linear relationship between the monthly mean critical frequency of the F_2 layer, f_oF_2, and the corresponding value of monthly-mean sunspot number.

It is expressed in sunspot number units and represents the part of the solar radiation that produces ionization in the F region. There is evidence of a departure from linearity of the relationship between f_oF_2 and R at high solar activity. This has been called[101] a "saturation effect" in f_oF_2. The saturation phenomenon will be present in IF2. Therefore the IF2 scale will be relatively compressed at high solar activity compared to the scale of R and Φ.

The three solar indices, R, Φ, and IF2, are highly correlated with each other[102], and various relationships between these indices have been given, for instance by Minnis and Bazzard[103], Barclay[104], Gladden[102], Joachim[105], and Muggleton and Kouris[106]. The indices Φ and IF2 can be calculated with relatively short delay. Monthly forecasts of IF2 and Φ are commonly made up to six months ahead. Attempts have been made to forecast R several months ahead but without great success.

The correlation between the E-layer critical frequency and each of the three indices has been studied by several investigators; different methods have been adopted in order to remove the influence of the time of day and of the season, so as toisolate the component which is attributable to changes in solar activity. Appleton and Naismith[107] have used the E-region character figure, $(f_oE)^4 \sec \chi$, which is a measure of the intensity of the solar ionizing radiation[108]. Other workers have used the empirical expression $(f_oE)^n \sec \chi$, instead of the E-region character figure, where the value of n differs from 4. Allen[64][65] has used what he called the "relative critical frequency", which is the ratio of the observed monthly-mean critical frequency to the critical frequency at the same time, season and place, extrapolated to zero sunspot number.

Appleton and Piggott[86] and Appleton[26][62] have employed an expression:

$$(f_oE)^n = a_m(1 + b_mR) \qquad (A.1)$$

where the subscripts of a_m and b_m refer to the separate months of the year. All these methods imply that scale height and recombination coefficient do not change with solar cycle and season.

The Zurich relative sunspot number has been the most employed solar index. A number of relationships between f_oE and R have been given by different investigators and their results are not very consistent. Waldmeier[67] has analysed ionospheric data from Kochel and found the relation:

$$(f_oE)^3 = a(1 + 0.0093R)$$

with a correlation coefficient of 0.873. Tremellen and Cox[68] have given the expression:

$$(f_oE)^{3.2} = a(1 + 0.0073\ R)$$

Allen[65] from a number of stations, and employing a solar cycle of data, has found:

$$(f_oE)^4 = a(1 + 0.0097\ R)$$

Harnischmacher[14], according to Rawer[109], compiled a more exact formula using data from Huancayo (1940-48), Watheroo (1940-48), Freiburg (1940-49) and Slough (1942-48); he has found the following expression:

$$f_oE = K.(\cos\chi)^p \qquad (A.2)$$

with

$$K = 2.25 + 1.5 \cos \theta + [0.01 - 0.007 \cos \theta]R$$

and $$p = 0.21 + 0.12 \cos \theta + 0.0002 R \qquad (A.3)$$

where χ is the solar zenith angle and θ is the geographic latitude. For the latitude $\theta = 60^{o}$, for example, this expression becomes:

$$(f_{o}E)^{3.7} = a(1 + 0.0081 R)$$

Scott[69] has used data from Canadian stations and found that $f_{o}E$ was approximately linearly related to R through the relation:

$$f_{o}E = A(1 + 0.00175 R)$$

which, if $f_{o}E$ is raised to 3.6 (a value found for Ottawa), becomes:

$$(f_{o}E)^{3.6} = a(1 + 0.0063 R)$$

Similarly, Saha[70] for Calcutta, and more recently Noonkester[71] for Washington, and Rao and Malhotra[61] for Ahmedabad have found values between 0.0015 and 0.0016 for the coefficient of R. These values are very similar to Scott's value. None of these investigators have quoted any correlation coefficients.

Logarithmic relationships between $f_{o}E$ and R have been given by some other workers; Shibata and Watanabe[110], and Swenson[17], have suggested the following expressions respectively:

$$\log(f_{o}E)_{max} = 0.498 + 0.00161 R^{0.846}$$

$$\log(f_{o}E)_{max} = 0.540 + 0.00058 R$$

Appleton[26][62] has implied a non-linear relationship between f_oE and R. He fitted the expression:

$$(f_oE)^2 = a_m(1 + b_m R) \qquad (A.4)$$

to the monthly-mean noon data of each month of the Slough station and found the 12-month average value b_m to be b = 0.0039. Later he examined[77] as much as 22 stations all over the world using about two solar cycles of data, and he obtained a better estimation of b = 0.0033. According to Muggleton[63] the value of the coefficient b will depend on the particular epoch selected for investigation because of a periodical secular variation in E - and F - region ionization corresponding to a given value of R[89][104][106][111][112]. For example, he found for Slough that b is equal to 0,00364 for 1938-48, but 0.00355 for 1949-59. After investigating the data of 15 stations corresponding to a wide range of latitudes, he found that b has a world-median value of 0.00334 for the period 1949-59.

Davies[15] and also Van Zandt[16] have given the following expression:

$$(f_oE)^4 = a(1 + 0.008 R)$$

while Schwentek[66] has found two relationships:

$$(f_oE)^4 = a(1 + 0.0097 R) \quad \text{for winter,}$$

$$(f_oE) = A(1 + 0.00145 R) \quad \text{for summer.}$$

It has been reported[62][86] that the value of b varies but little with season. Furthermore b does not appear to be latitude dependent[59][63][77] but it depends on whether years of rising solar activity or years of falling solar activity are considered[88].

The critical frequency, f_oE, for the same sunspot number may be up to 0.1 MHz larger during the rising than during the falling portion of the solar cycle[60].

Beynon and Brown[60] have investigated the correlation between day-to-day variations in f_oE noon values and sunspot number R. It has been found that the relationship is approximately linear only over limited ranges of R, whereas over an extended range of R there is appreciable divergence from linearity. However, it has been noted that a better correlation between f_oE and R appears when monthly values are considered rather than daily ones.

It has also been found[60] that there exists a 27-day periodicity in the critical frequency, f_oE, which is in phase with a similar variation of sunspot number. However, comparison of short- and long-term sensitivities indicates that f_oE is less sensitive to 27-day period sunspot changes than to long-period, 11-year, sunspot changes. According to Beynon and Brown this difference could arise from the different behaviour in the two cases of the background component of the solar radiation.

Comparison between E-region character figure, $(f_oE)^4 \sec \chi$, and solar radio noise flux at 10.7 cm wavelength, was first made by Denisse and Kundu[72]. They used f_oE monthly-mean noon values from Freiburg from 1947 to 1953 and corresponding monthly means of Φ as measured by Covington[78]. It was found that during the course of the solar cycle the variation in E-layer character figure shows a marked resemblance to the variation in the 10.7 cm radio flux. It has been deduced from their correlogram that a close correlation exists between ionizing flux and radio noise flux.

The observed close correlation is not surprising because it has been shown[96] from a comparison of an X-ray photograph with a 10 cm radio-heliograph that the X-radiation responsible for the E-region ionization and the 10 cm solar flux show almost identical source distributions on the solar disc. Minnis[113] has also pointed out this similarity between the distribution of ionizing radiation on the Sun's disc, as derived from ionospheric measurements during an eclipse at sunspot minimum, and the distribution of the 10.7 cm solar flux derived from measurements of solar radio noise on 2800 MHz made during the same eclipse. It has also been reported that the behaviour of the total radiation and background component of the 10.7 cm radio flux was very similar to that of corresponding ionizing radiations in the E layer[114], and that the ratio of total to background component was the same for ionizing radiation and radio noise flux[115]. In addition, the long-term trend of the background component of the ionizing radiation was found to be consistent with the trend of the background component of 10.7 cm radio flux[116]. Furthermore, the 10.7 cm solar radio flux observed values undergo an annual variation[117] resulting from the annual variation of the Earth-Sun distance similar to the annual variation detected by Appleton[118] in f_oE, and of about the same magnitude. Thus, the solar flux Φ appears to be a very useful index of solar activity for the E layer. A lack of perfect correlation between f_oE and Φ can be, to some extent, expected because the E layer ionization is produced by both X-ray and EUV radiation, and the relative importance of each component is not accurately known[96], [119]-[125] and may well change during the course of the solar cycle[19][94].

Kundu and Denisse[73] have made comparisons between E-layer character figure and Φ and R, first using monthly mean values and then 5-day mean values. It was concluded that short-term comparisons hold better correlations with Φ, whereas for long-term comparisons both indices give comparable results. They did not quote the correlation coefficients obtained. Minnis and Bazzard[74] have also studied the relation between E-region character figure and Φ. They investigated the correlation between monthly-mean noon values of the character figure at Slough (from 1947-1956) and the corresponding monthly mean Φ values for individual months. It was found that the correlations were highly significant with an average correlation coefficient of 0.950 for the individual months. Later[126] they extended this analysis to the data from eight stations distributed over the northern and southern hemispheres. Similarly Eyfrig[75], using E-layer data from Lwiro from 1952 to 1960, has found that the average correlation coefficient for the individual months was 0.984. It is to be noted that in the above investigations the authors have corrected the ionospheric data for the annual variation of the Sun-Earth distance while they have used Φ data as measured at ground level. However, this correction does not alter the correlation and regression coefficients because individual months have been considered; but the individual intercepts will be incorrect. Therefore, in order to obtain "correct" relationships both the f_oE and 10.7 cm solar flux data must be corrected, or both uncorrected[91].

Minnis and Bazzard[92][103] have found the following relationship between their E-layer index I_E and Φ:

$$I_E = 1.55\Phi - 0.001\,\Phi^2 + 14$$

where Φ is given in units of $10^{-22} W/m^2/c/s$, and I_E is a new index derived from the E-region character figure corrected for seasonal variations. No other numerical relationships between f_oE and Φ appear to have been given by any of the above authors.

Beynon and Brown[127] have investigated the relation between E-region character figure and ionospheric index IF2, considering f_oE monthly noon data from Lindau for the period 1949-1955, and monthly values of IF2 as published by Minnis[128]. They have found that the two indices were highly correlated (correlation coefficient = 0.97). Smith[76] has reported that a good linear correlation exists between f_oE and IF2, from a very limited investigation using some Slough data. He quoted an average r.m.s. deviation of f_oE of 0.077 MHz, but he did not give any regression coefficients.

A.2 VARIATION OF f_oE WITH COS χ

According to the Chapman theory, the critical frequency, f_oE, of the E-layer, which is proportional to the square root of the maximum electron density, varies quite regularly with the solar zenith distance χ. Under equilibrium conditions, in an isothermal atmosphere, the critical frequency f_oE is related to χ by the equation (1.7), which we rewrite:

$$(f_oE)^4 = A \cos \chi \qquad (A.5)$$

where A is given by (1.8). If scale height, H, and recombination coefficient, α, vary with altitude then equation (A.5) takes the modified form:

$$(f_oE)^4 = A_1 (\cos \chi)^p \qquad (A.6)$$

in which A_1 and p depend on the gradients of H and α. Now, if H varies linearly with height and α remains constant then the exponent p will be given by

$$p = 1 + dH/dh = 1 + \mu \qquad (A.7)$$

However, it must be noted that in equation (A.6) no account is taken of the effect of drifts. If the effect of movements is of any importance then the values of the parameters A_1 and p will be affected.

Many investigators assume, rather, a relation of the form:

$$f_oE = K(\cos\chi)^n \qquad (A.8)$$

and find the value of n at any given station as χ varies during the day (diurnal variation) or during the year (seasonal variation), or at a given time as χ varies with latitude (latitude variation). In general the results are derived from routine published data, accepted at their face value.

Diurnal variations: When diurnal variations are considered, the value of the exponent n has been found to be different from the theoretical value of 0.25. Waldmeier[67], using data from Kochel station, has shown that n was near to $\frac{1}{3}$. Tremellen and Cox[68] have found, for a large number of stations, that an average value of n is 0.31, with variations from 0.28 to 0.34, and with the larger values in local summer and at high sunspot numbers. Harnischmacher[14] from monthly f_oE data of four stations for the period 1940 to 1948 has found that n had approximately a mean value of 0.31; and that both n and K in equation (A.8) tend to decrease with increasing latitude under constant conditions of sunspot activity. Furthermore he found that n also depends on the sunspot number. Scott[69] has found, for a large number of stations, that n is usually about 0.33 at moderate

latitudes and about 0.25 to the north of the auroral zone, but drops sharply to between 0.10 and 0.20 at the northern auroral zone. In addition, in a closer investigation of f_oE data from Canadian stations, he found that the exponent n varies with solar activity and season, showing minima in winter and maxima either at the equinoxes or in the summer. He found that the subsolar critical frequency, K, in equation (A.8), was roughly independent of latitude in contrast to previous and later work as we shall report when considering latitudinal variations of χ. Menzel and Wolbach[133][134] have used data from a wide range of stations in both northern and southern hemispheres, for the years 1944 - 1953. They found that both parameters n and K in equation (A.8) exhibited a latitudinal dependence. Their n values ranged from about 0.260 at 65°N to 0.315 at the equator, and showed maxima at the equinoxes and minima at the solstices. In a later work[137], in which no distinction has been made between diurnal and seasonal data in respect of the choice of f_oE, Menzel et al.have obtained similar results, the two quantities n and K exhibiting higher values near the equator than at higher latitudes. Haubert[138] found at Casablanca a mean value for n = 0.32. Eyfrig[135], using the data from 1952 to 1959 of 20 stations, found the exponent n to be between 0.31 ± 0.02, and K diminishing with increasing latitude. In addition, from a careful examination of the results of four stations (Lindau, Freiburg, Nha-Trang, and Lwiro), he pointed out that the exponent n does not show any systematic variation with solar activity and latitude. Appleton and Lyon[10] have also found that n does not change markedly with latitude; but they observed a variation with solar activity, with the value of n remaining close to 0.30 at sunspot maximum and close to 0.32 at sunspot minimum. This variation

is opposite to the one suggested by some previous workers[14][68]. On the other hand Shimazaki[139] has noted that the index p in equation (A.6) does not undergo any systematic variation with Φ, the 10.7 cm solar radio flux. In other words he found that the exponent of $\cos\chi$ is independent of solar activity.

Appleton and Lyon[10] have also reported that some seasonal variation was found at northern temperate stations but they found no corresponding variation at southern temperate stations. For example for Washington (1949-1953) they found that the value of n varied from about 0.31 in summer to about 0.35 in winter. This result is opposite to the results of other workers[68][69] who found maxima in summer and minima in winter as already mentioned.

Piggott and Thrane[136], using monthly median measured f_oE values for the spring equinox of 1956 from Kjeller (Oslo), have reported that the value of the index n was 0.3. Rao and Malhotra[61], using Ahmedabad monthly mean f_oE values of the years 1953 to 1963, have found that a probable value of n was 0.34 and that n did not show any seasonal variation. Furthermore, an inspection of their results reveals that there is no significant variation with solar activity either. Similar results have been obtained by Swenson[17], using monthly median f_oE values from a number of stations lying between latitudes 15^oN and 15^oS. He has found that the exponent n had an average value of 0.31 and was independent of season, latitude and solar activity. He reported also that the value of K in equation (A.8) similarly did not show a significant variation with latitude or season, but there was a significant variation of K with solar activity. Nevertheless, we may note that in the latitude range of 0^o to $\pm 15^o$ the latitude variation of K, if any, is expected to be small.

The f_oE data used in the above investigations were monthly median values published by ionospheric observatories all over the world. According to Bellchambers and Piggott[140], and Belrose[141], when accurate measurements for individual days are used, the values obtained for the exponent n are in general agreement with the results deduced from monthly median routine data. For data acquired and reduced with sufficient accuracy, for individual days, at Halley Bay and at Vancouver, they have found n = 0.33 and n = 0.31 respectively.

The departure of the exponent n from its theoretical value of 0.25 can be explained by postulating the existence of a height gradient of the scale height, H, and/or of the recombination coefficient, α. However, observations of the critical frequency alone do not yield any additional information to distinguish experimentally between a variation of α and a variation of H with height. Robinson[6][24], assuming α constant and H varying linearly with height, determined from the layer shapes that the gradient of the scale height, μ, was 0.20. Now from equations (A.6), (A.7) and (A.8) we obtain:

$$n = 0.25\ (1 + \mu) \qquad (A.9)$$

which, for a scale height gradient of 0.20, gives n = 0.30 which is reasonably consistent with the values of n obtained by the different workers mentioned above. On the other hand, equation (A.9) requires modification if the temperature gradient, which must be present to account for the magnitude of the scale-height gradient, causes the recombination coefficient, α, to vary with altitude. Robinson[6][24], and also Grace[142], have found that α might decrease with altitude and that the rate of decrease appears to be greater than could be produced by possible changes of temperature with height. However, recombination effects have been found to be so

small that drifts or other disturbances in the E region could greatly modify the apparent value of α [24].

Latitude variations. For the study of the latitude variation of f_oE with cos χ a number of methods, largely but not completely equivalent to each other, are available. One of these is to select a fixed value of χ and find how f_oE varies with latitude. This method has been used by Tremellen and Cox [68] and it has been found that f_oE increases towards the equator. As already mentioned above, Harnischmacher [14], Menzel and Wolbach [133][134], and also Eyfrig [135], by comparing the diurnal variation at different stations, have found that the quantity K in equation (A.8), that is, the critical frequency at $\chi = 0$, decreases with increasing latitude.

Another way of studying the latitude variation is to fix season and time of day and consider variations of χ by using data from different stations at different latitudes. For example, Appleton [47] has shown that there is a tendency for the value of f_oE to be greater at low latitudes than at high latitudes. In other words there is an equatorial enhancement; the percentage increase in f_oE from latitude 50°N to the equator is about the same in all seasons, and of magnitude about 5 per cent. Shimazaki [7][8][52][53][54] has also found that there is more ionization towards the equator, f_oE values being larger at low latitudes and smaller at high latitudes than the theoretical values. He has also reported that the values of the exponent of cos χ undergo a seasonal variation having maxima at the equinoxes and minima at the solstices [52][54], and that the scale-height gradient varies with time of day ; being positive throughout all hours and maximum at 1300 hours; the mean value for the period 0900 to 1500 hrs is about 0.2 [7][53]. Beynon and Brown [9],

comparing temperate and equatorial stations, have found that for a given χ the equatorial values of f_oE are larger by about 0.2 MHz than those for temperate latitudes. Appleton and Lyon[10] have found that the exponent of cos χ is of the same order of magnitude as for the diurnal variation, and they have also demonstrated the equatorial enhancement.

Seasonal variations. The seasonal variation of f_oE with cos χ can be studied by considering at a fixed hour and at a given station the corresponding values of f_oE and cos χ for all months of the year. Since solar activity and Earth-Sun distance vary from month to month, corrections must be made for changing solar activity and Earth-Sun distance. When seasonal variations are considered, most workers prefer to deal with equation (A.8) in the following form:

$$(f_oE)^m = C \cdot \cos\chi \qquad (A.10)$$

Allen[65] has used the noon observations and the averages of the values obtained at 0900 hrs and 1500 hrs, corrected for varying solar activity and Earth-Sun distance, from 14 stations, and fitted the data to equation (A.10). The average value he found for the index m is 3.72 ± 0.09, very close to the theoretical value m = 4. However, careful examination of Allen's m values, determined for each of the 14 stations, shows that there is a latitude dependence, with the lower values of the seasonal exponent m occuring near the equator. Allen has also noted that there is a tendency for the noon observations to give somewhat greater values of m than those for 0900 hrs and 1500 hrs. In this connection Beynon and Brown[9][50] have shown that the seasonal exponent undergoes a diurnal variation. They have determined, from routine ionospheric monthly median f_oE values, the seasonal

exponent m for each hour between 0900 hrs and 1500 hrs for a number of stations. It was thus shown that m varies asymmetrically over the day, forenoon values being considerably larger than corresponding afternoon values, with a maximum about an hour before noon. Moreover, it has been found that the diurnal variation of the seasonal exponent, m, was more marked for stations near the Sq current system foci. Eyfrig[135] has confirmed the diurnal variation of m by considering data from Freiburg for 1952 - 1954. He has found that the Freiburg values of the seasonal exponent m were slightly smaller than the corresponding values for Slough quoted by Beynon and Brown, but the diurnal trend was the same. On the other hand, by considering data from Lwiro station (2.3°S, 28.3°E), he found that the exponent m was markedly smaller than in the above stations, and that no regular diurnal variation could be detected for this station. Thus, he has concluded that the seasonal exponent has a diurnal variation only for stations well away from the equator. Appleton and Lyon[10] have also confirmed the finding of Beynon and Brown by determining the diurnal variation of the seasonal exponent in a number of stations lying in latitudes from about 50°N to about 20°N.

Beynon and Brown[9][50] have also determined another important property of the seasonal exponent m. Using monthly-mean noon data for the years 1952 - 1954 for a number of stations situated in a longitude zone centred on the 150°E meridian, they have found that the value of the seasonal index m varied with latitude in a systematic manner, with marked singularities near the mean latitudes of the foci of the Sq current system. The value of m is about 3 in low latitudes, it attains sharp maximum values of about 5 at Tokyo and Watheroo, and then decreases again at higher latitudes. The maxima at latitudes

$\pm$ 35° were, however, not discernable when the values of m were derived from the seasonal variation in f_oE at 1500 hrs at all stations. Similar results were obtained for stations in two other longitude zones centred on 15°E and 70°W meridian respectively[51]. Beynon and Brown have concluded that the latitudinal variation of the seasonal exponent m was due to vertical drift effects of the Sq current system and the seasonal variation of its current intensity. Moreover, when the influence of the Sq currents is negligible, for instance at 1500 hrs, they found that m decreases gradually towards the equator. This may indicate that the characteristics of the E layer, at temperate latitudes, are different from those at equatorial latitudes. A similar study of the seasonal variation of f_oE with cos χ, at a given hour and place, has also been made by Hibberd and Henderson[55]. They have used monthly mean values of f_oE from a large number of stations for the period 1957 - 1958 and corrected the data for varying Earth-Sun distance; but no correction has been made for any changes in solar activity from one month to the next. Hibberd and Henderson confirmed the findings of Beynon and Brown about the latitudinal variation of the seasonal exponent, showing peaks at latitudes between 30 and 40 degrees in each hemisphere in each of the three zones. The value of m they obtained in equatorial latitudes was only 1.5, this is lower than the value obtained by Beynon and Brown for these latitudes. They too have attributed the variations of the seasonal exponent, m, to Sq current effects.

The motor influence of the Sq currents on the E layer will be discussed in detail in the next section.

A.3 ANOMALIES IN THE E LAYER

Studies of f_oE data have shown small but measurable departures from the theoretical behaviour of a simple Chapman layer[10]. For example, Appleton[47] has shown that the critical frequency f_oE is not uniquely dependent on $\cos\chi$; there is a tendency for the f_oE values to be high in low latitudes. Indeed, he has found that at the equinoxes, although f_oE reaches its maximum value at the subsolar point, the contours of constant f_oE are not circles, as would be expected if f_oE depends uniquely on $\cos\chi$. They are, instead, of elliptical shape, the major axis lying along the equator; this implies that at a given $\cos\chi$ the critical frequency f_oE decreases with latitude. Again, at the solstices, he has found that f_oE does not attain its maximum value at the subsolar point, but at a latitude shifted from $\chi = 0$ towards the equator by about 10 degrees. These results have been interpreted by Appleton, Lyon and Turnbull[48] as an indication of the influence of the Sq currents which flow from west-to-east in low latitudes and tend to raise the value of f_oE at these latitudes, independently of the season[149]. On the other hand, in higher latitudes the Sq currents flow from east-to-west, the downward drift velocity decreases with increasing height, and the value of f_oE is reduced. Appleton et al.[48] have also detected, at temperate latitudes, a marked depression in the maximum ionization density N_m(or f_oE) at about 1000 - 1100 hours local time which has been attributed to the downward drift effects of the Sq current system. In low latitudes drift effects are reversed causing an enhancement of N_m in the forenoon. Beynon and Brown[9] have found that, for temperate latitudes, this depression varies with the seasonal change in the intensity of the Sq currents, that is, the decrease in N_m is

most marked when the current is a maximum (local summer). The magnitude of the drift effect on f_oE at Slough is about 4 per cent in mid-summer, 1 per cent at the equinox months, and virtually zero effect in mid-winter. At equatorial latitudes, where a forenoon elevation of f_oE would be expected, they have reported that there is little evidence of layer distortion in the diurnal variation of f_oE. For Huancayo (12^oS), for example, it has been found that an elevation of f_oE over the hours 1100 to 1300 occurred in local winter but no significant departure from the theoretical variation was found in local summer; in general the departures from the theoretical behaviour for all the other months were very small and as likely to be in the negative direction as in the positive.

Another evidence of the motor influence of the Sq current system on E-layer characteristics has been given by Appleton, Lyon and Pritchard[49]. They have determined the delay of the N_m maximum relative to noon, for June (mean of values for 1949 and 1953), for eleven stations covering a wide range of latitudes, and found that the latitudinal variation of the noon delay followed a definite pattern. They have suggested that the pattern is related to the Sq current system which can influence the ionization by introducing vertical drift effects when it flows across the earth's magnetic field. At temperate latitudes their results show that N_m reaches its maximum several minutes after noon (positive delay), while in equatorial regions the maximum is reached a few minutes before noon (negative delay). Thus, the perturbation has opposite phases in low and temperate latitudes, changing phase near $\pm 20^o$ of latitude, that is, near the position of Sq current foci, and is most marked in local summer at temperate latitudes[10]. Swenson[17] confirmed the above

results for certain equatorial stations, namely he found that the time of occurrence of maximum f_oE was earlier than apparent local noon by some 3 to 4 minutes.

The influence of the Sq current system on the E-layer characteristics has also been identified by Beynon and Brown[9][50] from an examination of the latitude variation of the noon seasonal exponent m of more than forty widely scattered stations. They have found that the index m of equation (A.10), as a consequence of the dynamo-perturbation of f_oE, undergoes a systematic variation with latitude and, although m is smaller at equatorial than at temperate latitude stations, it attains sharp maxima at stations which are near the mean latitudes of the Sq current foci. Now the value of the exponent m is a measure of the seasonal variation in f_oE, and it is very sensitive to any seasonal or annual influence which affects f_oE. According to Beynon and Brown the high values of m obtained for stations between about 30 and 40 degrees suggest some influence on f_oE of the Sq currents. They stated that in order to explain these values, a differential effect on f_oE from season to season is required. This effect could arise from: a) a seasonal shift in the latitudes of the foci of the Sq currents; b) a seasonal change in the intensity of the Sq currents; c) a seasonal change in the vertical gradient of vertical drift velocity in equation (1.11). Beynon and Brown[9] have examined magnetic data from Japanese observatories placed near the Sq foci and have noted that this does not support suggestion (a), i.e. a seasonal shift of Sq foci, in the sense required. On the contrary, in support of suggestion (b), they have found a seasonal variation of the vertical drift effect, which is greater in local summer than in local winter, resulting

from a seasonal change in the intensity of the Sq currents. They have also suggested that the seasonal variation of the drift effect may possibly be explained in terms of the seasonal variation in the relative levels of the current sheet and of the E-layer peak. In this context it is interesting to note that Appleton[26] has shown that the geomagnetic component Y varies, seasonally, by a greater amount than does the electron density of the E-layer. Thus he has concluded that the difference in the seasonal variations of $(f_oE)^2$ and Y must be attributed to the fact that the Sq current system is located at a different atmospheric level within the E-layer in summer and winter, or has a different configuration in the two seasons.

Hibberd and Henderson[55] have made a similar study on the seasonal exponent m of equation (A.10) and have confirmed the findings of Beynon and Brown. They have also deduced that the marked singularities in the values of m cannot arise from a seasonal shift of Sq currents foci, and that the actual mechanism by which the maxima in m are produced is not yet clear. They have shown that there are N-S and longitudinal asymmetries in the worldwide pattern of the seasonal exponent m which resemble corresponding asymmetries in the worldwide pattern of the Sq current system; and have concluded that the variations in the exponent m are the result of vertical drift effects due to Sq currents.

Evidence of vertical drift effects on the E layer as a result of the Sq current system has also been given by Shimazaki[7][8][52][53][54]. He has used data from stations of a wide range of latitudes and, for a given hour and season, has considered latitudinal variations of f_oE and χ in equation (A.6), which is rewritten here for convenience:

$$(f_oE)^4 = A_1 (\cos \chi)^p \qquad (A.11)$$

The results of Shimazaki can be summarised as follows: the greatest value of A_1 always appears at lower latitudes, and the value in the southern hemisphere is slightly greater than that corresponding to the same latitude in the northern hemisphere. The observed f_oE values tend to be greater at lower latitudes and smaller at higher latitudes as compared with the theoretical values of the above equation (A.11), particularly during morning hours. He attributed these results to an upward drift which will raise the value of f_oE in low latitudes, and to a downward drift which will reduce f_oE in higher latitudes. He has also examined the difference between f_oE calculated by equation (A.11) and f_oE observed:

$$\Delta = [(f_oE)^4_{calc.} - (f_oE)^4_{obs.}] \qquad (A.12)$$

and has found that this difference has a systematic latitudinal pattern. Δ is negative at low latitudes and positive at temperate latitudes, passing through zero at about 30 degrees of latitude. This tendency seems to be most marked in the morning hours in March and September, and it may support the view that the above perturbations in the E layer are a result of the Sq currents effect. In June and December there is a change in the latitude pattern of the difference Δ, becoming particularly marked in the summer hemisphere but rather insignificant in the winter hemisphere. He attributed these results to the seasonal change of the intensity of the Sq current system. The value of Δ sometimes reaches about 10 to 15 per cent of either term on the right-hand side of equation (A.12). These departures from simple E layer theory cannot be explained by a seasonal change of temperature. In support of this he quoted the fact that several

rocket observations throughout various seasons showed that the temperature at about 100 Km does not undergo any systematic seasonal change.

Further interesting departures in the E layer from the simple Chapman behaviour can be illustrated in other ways. Appleton[11][118] has pointed out, by using data from a number of stations and over a period of one solar cycle (1949 - 1959), that the maximum electron density is not uniquely determined by cos χ, at a given place, under conditions of constant sunspot number R, but there exists both a seasonal and an annual variation in the value of $(f_oE)^2$ at constant χ.

The annual variation is to be attributed in part to the effect of the varying Earth-Sun distance. In fact, the Earth moves in an elliptical orbit around the Sun and the result of this eccentricity is that the intensity of the solar electromagnetic radiation, as received on the Earth, is 6.5 per cent less in early July than in early January. Therefore, the rate of electron production in the E layer will exhibit an annual variation of the same magnitude. Appleton[118] found an annual variation in $(f_oE)^2$ of 7.5 per cent which is greater than the expected value. He concluded that there must be a small additional annual variation due to some unknown cause. Earlier workers[14][68] have also reported that there was a small annual variation in f_oE, for a given value of χ, the values being increased in November, December and January, and reduced in May, June and July, all over the world; the effect was of about the order of magnitude to be expected from the annual variation of the Sun-Earth distance. Menzel and Wolbach[133][134] also noted this effect but attributed it to sporadic E ionization and other E-layer anomalies prevalent during winter months. Shimazaki[54][139][150] has also

reported a small additional annual variation due to some unknown causes. Muggleton[151] applying a new technique to the data from 20 stations, found an annual variation of 3.7 per cent in $(f_oE)^2$ and has shown that monthly values of $(f_oE)^2$ may be stripped of the effect of the annual variation of the Sun-Earth distance by multiplying by $(d)^{1.2}$; d being the corresponding monthly ratio of the Earth-Sun distance, at mid-month, to the average value for the year. As the value found for the variation (3.7 per cent) is, in fact, within the expected range (3.2 per cent to 6.5 per cent), the observed variation is described by the variation in Sun-Earth distance alone.

Appleton[11] has demonstrated the seasonal anomaly by examining, under conditions of constant cos χ and sunspot number R, eleven-year average values of $(f_oE)^2$ at individual stations. He has shown that the maximum electron density in the E layer is less in local summer than in local winter under conditions of constant χ, R and Sun-Earth distance. At Slough[10], for instance, he found a difference of about 8 per cent in f_oE between summer and winter. Appleton has also illustrated the seasonal anomaly by taking noon values of $(f_oE)^2$ at different places over the Earth's surface, at the solstices, and showing that the value of noon $(f_oE)^2$ is less in the summer hemisphere than in the winter hemisphere for the same value of χ. In addition, it was found that both the seasonal and annual variations were independent of the level of solar activity[11], and also that the seasonal anomaly was independent of the value of constant-cos χ used, but it was characteristic of the latitude of the station[13].

In the early work of Tremellen and Cox[68] it has also been reported that there was an additional seasonal effect in f_oE, causing a small reduction of f_oE values in local summer. Robinson[6],

from considerations of the difference between the diurnal and seasonal exponents of cos χ, has deduced that the maximum electron density, for the same χ, is less (by about 6 per cent) in local summer than in local winter. Shimazaki[52][54], and also Eyfrig[75], have reported that f_oE showed smaller values in the summer hemisphere than in the winter hemisphere for the same value of χ, and attributed this to the seasonal change of the Sq currents vertical drift effect on the E layer. Eyfrig has also determined at sunspot minimum (1952 - 1954) the values of K in equation (A.8) by extrapolating to $\chi = 0$. The obtained K values were corrected for the variable Earth-Sun distance, and therefore they illustrated the Appleton seasonal anomaly at $\chi = 0$[13]. From this investigation he has found that at equatorial latitudes, if any residual seasonal effect was present, it was small (0.1 MHz at Lwiro, 2.3°S) as compared with the seasonal variations attained at northern temperate latitudes (0.3 MHz at Freiburg, 48.1°N). Rao and Malhotra[61] have also noted at Ahmedabad (23°N) a small seasonal variation in the subsolar critical frequency, which was less in summer than in other seasons for the same value of χ and R. The difference in f_oE between summer and winter was found to be of magnitude of about 3 per cent. However, it seems that no corrections for varying Earth-Sun distance were made by them. Swenson[17] has reported that the subsolar critical frequency did not show a significant variation with time of year, at a number of stations placed between 15 N and 15 S degrees of geographic latitude. Recently Muggleton[13] by considering $(f_oE)^2$ values under conditions of constant χ, solar activity and Sun-Earth distance, at an equatorial station, has illustrated the existence of the Appleton seasonal anomaly at equatorial latitudes.

The seasonal anomaly, according to Appleton, could be interpreted as indicating that at the E-layer level the atmospheric response to solar ionizing radiation varies seasonally. Eyfrig[75] suggested that an explanation has to be found in the seasonal variation of the geomagnetic perturbation arising from the motor effect of the Sq current system. On the other hand, Bishoff[152] has suggested that the seasonal anomaly could be explained by the weak seasonal dependence of the recombination coefficient α. Minnis[153] has interpreted the seasonal anomaly at $\chi = 0$ as the result of the different values of the seasonal and diurnal exponents of $\cos \chi$. Shimazaki[150] has argued that the Appleton seasonal anomaly may be attributed in part to the vertical drift effect of the Sq current system and the seasonal change of its current intensity, and in part to a seasonal variation in the upper atmospheric parameters such as temperature, temperature gradient, and composition. Landmark[12] has asserted that the Appleton seasonal anomaly appears to be due to some other cause rather than to the motor influence of the Sq current system on the E-layer.

Clearly the seasonal variation of f_oE at constant χ, constant Sun-Earth distance and constant solar activity is a well-attested phenomenon, albeit a second-order effect. There is some controversy concerning the cause of the variation. According to some investigators the seasonal anomaly should be attributed to the influence of the Sq current system. In the next section this current system is reviewed in some detail.

A.4 ON THE Sq CURRENT SYSTEM

Various workers have developed and formulated mathematically the theory of the Sq current system[44][46][144][154][155][156][157]. Appleton and Piggott[25][26] have pointed out that the Sq currents must flow in the ionospheric E region, and rocket-borne magnetometers have located the Sq current sheets between 90 and 140 Km[27] - [37].

The horizontal distribution of the Sq currents can be deduced from spherical harmonic analysis of the Sq variation field on the ground. World maps of the Sq current system have been given by Chapman and Bartels[154] for a year of sunspot minimum (1902), and by Matsushita and Maeda[143] for years of sunspot maximum (IGY). Two current loops, one in each hemisphere, fixed in relation to the Sun, but, relative to an observer on the Earth, continuously moving westward and varying in intensity with a predominently 24-hour period, are found. In the sunlit hemisphere the currents flow counterclockwise in the northern hemisphere, and those in the southern hemisphere flow clockwise, contributing to a west to east current flow where they combine near the equator. In the dark hemisphere, however, the direction of the current flow is just the reverse of that in the sunlit hemisphere.

The positions of the centres, or foci, of the Sq current loops vary considerably with longitude, hemisphere, season, and even from day to day. According to Chapman and Bartels' current system, the foci are situated at the equinoxes at a geographic latitude of 40° and at a longitude of 11 hrs local time, while there is a seasonal shift of about 10° in the latitude of each focus towards the equator in local summer. Hasegawa[158] has also

reported a similar seasonal shift towards the equator in local summer from an investigation on the positions of the foci on the basis of the Second Polar Year data (1932 - 1933, sunspot minimum). On the contrary, a seasonal shift of the Sq foci in the opposite direction was observed during the IGY. Molina and Battelli[146] from the data of three observatories in Italy have found that the focus drifts to lower latitudes from summer to winter. In fact, they found that the mean position of the focus in the European zone during 1958 - 1959 was at latitudes less than 38 degrees in winter, whereas in summer and equinoxes it was at latitudes higher than 38 degrees. Matsushita and Maeda[143], and Matsushita[144][145], in a more general study, for three longitudinal zones, European, Asian, and American, using IGY data from a large number of stations, have also found that the latitudinal position of the Sq current focus is lower in local winter than in local summer in the southern hemisphere for all zones, and in the northern hemisphere for the American zone, but not for the European and Asian zones. Their results are summarized in Table A.1, together with the results of Hasegawa for the yearly average positions of the foci during the Second IPY, for the same three zones. From Table A.1 it can be seen that there is a substantial difference between the two results during the two different periods of years. Fatkullin and Fel'dshteyn[147] have also used IGY data and found, in agreement with the previously mentioned results from data of the same period, that the positions of the foci of the Sq current system shift towards the poles from local winter to local summer in both hemispheres, sometimes up to 10 degrees in latitude. It should be noted here that on individual days considerable changes in the latitude of the foci of up to 15 degrees may occur[29][158].

Moreover, it has been found[143][147] that the average seasonal positions of the foci of the Sq current system in the northern and southern hemisphere, are not symmetric with respect to the geographic equator or to the magnetic equator even during the equinoxes. Another hemispheric asymmetry is that the focus in the southern hemisphere lags 1 - 2 hours behind that in the northern hemisphere, depending on season[159].

We may therefore conclude that the latitudinal positions of the Sq foci depend on season, longitude and hemisphere, but it is not easy to formulate a model of the manner in which the seasonal shift of the foci varies in magnitude and direction with longitudinal zone and hemisphere.

Seasonal, hemispheric and longitudinal inequalities in the pattern of the Sq current system have also been observed. According to Chapman and Bartels[154] the current intensity in the summer hemisphere is about 2.5 times greater than that in the winter hemisphere, and about 1.5 times higher than that at the equinoxes. These ratios have been obtained for the sunspot minimum year 1902. Matsushita and Maeda[143][144][145] from IGY data, have found that the current intensity in the summer hemisphere was about 1.5 times that in the winter hemisphere. Moreover, the current intensity for equinoctial months was always larger than that for mean solstitial or yearly averages, and in many cases even larger than that for summer months. This is different from what Chapman and Bartels have found. Furthermore, Matsushita and Maeda have also found that for equinoctial months and the yearly average the current intensity is larger (about 1.2 times) in the northern than in the southern hemisphere. It has been suggested that this difference

might be caused by the large sea area in the southern hemisphere. Their results, concerning current intensities during the IGY, for each zone and season, are set out in Table A.1.

It has also been observed[154][159] that the average intensity of the Sq current system varies with solar activity. Furthermore, considerable changes in current intensity from one day to the next, sometimes by a factor of 2, have been reported. These are caused by ionospheric tidal wind variations rather than by changes in the electron concentration and conductivity[156].

Concerning the equatorial electrojet, it has been found that the intensity has seasonal and longitudinal effects. The intensity is highest during the equinox[147], and largest in the American zone and smallest in the European zone[143][144]. It has been pointed out that the equatorial electrojet is a part of the Sq current system[145][147][148].

It follows from the above that the pattern of the Sq currents shows a considerable dependence on season, hemisphere, and longitudinal zone. Longitudinal and hemispheric asymmetries seem to be caused by differences of ionospheric wind pattern with respect to the Earth's magnetic field.

Whereas the horizontal distributions of the Sq currents can be estimated from routine ground magnetograms, the vertical distribution of the current density can be determined only by rocket-borne magnetometers. Many attempts have been made to detect and locate the Sq ionospheric current sheet or sheets by rockets. The first direct measurement of ionospheric currents was made at equatorial latitudes by Singer, Maple and Bowen[27], and at midlatitudes by

Burrows and Hall[29]. Several other investigators have subsequently reported a number of observations made by rocket flights at various latitudes[28],[30]-[37]. Their observations were in general agreement with the global current patterns calculated from the Sq ground data. The altitude profiles of the current pattern showed in most cases the existence of a diffuse current sheet extending between 90 and 140 Km. The position of the current maximum was found to be between about 110 and 120 Km altitude in midlatitudes and between about 100 and 110 Km near the equator. Moreover, the lower edge of the current layer descended to about 90 Km near the equator and to about 105 Km at midlatitudes. While these are the general features reported by the various investigators, there have also been found some remarkable differences. Cahill[28], Maynard and Cahill[32], Maynard[34], Cloutier and Haymes[35], Sastry[36] and Shuman[37], have reported the existence of a stratification of current sheets. A thin maximum usually found near 100 Km is believed to be connected with sporadic E ionization[28][35]. On the other hand, Burrows and Hall[29], and Davis et al.[31][33], have reported that the currents are concentrated almost entirely in a single layer.

Furthermore, it has been detected[35][36] that a variation occurs in the height of the current sheets when these were measured at the same place but in different years and seasons. This has been attributed to changes of solar activity[36], but it may also be due to seasonal influences. However, the presence of multiple current sheets, and the solar activity and seasonal control of the height of them, require further investigation before their effect can be quantitatively assessed.

TABLE A.1

Location of S_q foci and total intensity of external S_q current. (After Matsushita and Maeda[143]).

Season	Hemisphere	EUROPEAN ZONE S_q focus Magn. Lat.	EUROPEAN ZONE S_q focus Geog. Lat.	EUROPEAN ZONE S_q current ($\times 10^{+3}$ Amp)	ASIAN ZONE S_q focus Magn. Lat.	ASIAN ZONE S_q focus Geog. Lat.	ASIAN ZONE S_q current ($\times 10^{+3}$ Amp)	AMERICAN ZONE S_q focus Magn. Lat.	AMERICAN ZONE S_q focus Geog. Lat.	AMERICAN ZONE S_q current ($\times 10^{+3}$ Amp)
D months	N	35°	39°	129	24°	31°	152	32°	22°	112
	S	-45°	-36°	-177	-37°	-26°	-183	-30°	-45°	-205
E months	N	35°	39°	225	22°	28°	219	37°	27°	237
	S	-40°	-23°	-211	-35°	-26°	-175	-23°	-34°	-175
J months	N	35°	39°	264	22°	28°	184	38°	29°	199
	S	-37°	-22°	-147	-33°	-26°	-125	-22°	-34°	-116
Yearly Average	N	35°	39°	206	24°	31°	182	37°	28°	181
	S	-40°	-23°	-168	-35°	-26°	-154	-25°	-36°	-165
Hasegawa's Yearly Average	N	-	37°	-	-	31°	-	-	31°	-
	S	-	-36°	-	-	-32°	-	-	-40°	-

APPENDIX B

B.1 COMPARISON AND POOLING OF THE MONTHLY DIURNAL EXPONENTS OF $\cos\chi$ FOR EACH STATION

The twelve monthly p_i values of the diurnal exponent of $\cos\chi$ in equation (3.2) were obtained for each month at each station by the least squares method; that is, the eleven-year average hourly values of $(f_oE)^4$, mainly from 0900 hours to 1500 hours, for each month, and the corresponding values of $\cos\chi$, were fitted to the best straight line corresponding to equation (3.3).

We may now want to know whether the individual slopes, p_i, thus determined are significantly different from each other, and if not, to combine them in order to obtain a better estimate of the value of the exponent. We shall only outline the procedure for testing whether there is any significant difference between the p_i values for each station, and give the various equations for evaluating the regression statistics. Theoretical justification and detailed discussion of the method can be found in appropriate statistical texts[79][132].

The statistical method is to determine the sum of squares of deviations from the best straight line through the individual month-sets of data with a pooled estimate of the slope, and from the best straight line through the individual sets with individual slopes. The mean squared deviation (i.e. sum of squares of deviations divided by the appropriate degrees of freedom) using a single straight line and the mean squared deviation using a straight line for each data set, provide a variance ratio which can be tested by the F test.

If this F-ratio is not significantly larger than might be expected by chance for the number of degrees of freedom available, then for the data involved there is no basis for using different slopes for the different sets of data; the pooled slope will be the best estimate to use. In applying the F test of significance the fundamental condition for the validity of the F test must be satisfied; namely that the variance about the regression is independent and uniform. The F-ratio for the comparison of several regression coefficients is given by

$$F = \frac{[\Sigma(y - E_p)^2 - \Sigma_i \Sigma(y - E)^2]/[K - 1]}{[\Sigma_i \Sigma(y - E)^2]/[N - 2K]} \qquad (B.1)$$

with i = 1,2,3,.....,K; where K is the number of samples, that is, the number of months, and N is the total number of data-points , namely

$$N = \sum_{i=1}^{K} n_i \qquad (B.2)$$

where n_i is the number of data points of the month-sample i. In the above expression (B.1) the term $\Sigma(y - E_p)^2$ is the sum of squares of deviation from individual regression lines drawn through each set of data, but all drawn with the same slope, i.e. the pooled slope. $\Sigma_i \Sigma(y - E)^2$ is the sum of the sums of squares of deviation from the best straight line through each sample of data taken separately. This quantity, of course, is the minimum deviation that can be obtained by linear regressions.

If the calculated F value does not exceed the tabulated F value at the 5 per cent significance level or at the 1 per cent level for the given degrees of freedom:

and

$$\nu_1 = K - 1 \tag{B.3}$$

$$\nu_2 = N - 2K \tag{B.4}$$

then it is permissible for the regression lines to be drawn parallel through each set of data, with the "pooled slope" given as follows:

$$p_{pooled} = \Sigma_i[p_i(\Sigma(x - \bar{x})^2)_i]/\Sigma_i(\Sigma(x - \bar{x})^2)_i \tag{B.5}$$

where p_i is the individual slope of month i and $\Sigma(x - \bar{x})^2$ is the sum of squares of deviations of the independent variable of the month i.

The variance about the "pooled regression" is given by

$$s^2(E_p) = \Sigma(y - E_p)^2/(N - K - 1) \tag{B.6}$$

and the variance of the "pooled slope" is given by

$$s^2(p) = s^2(E_p)/\Sigma_i(\Sigma(x - \bar{x})^2)_i \tag{B.7}$$

The individual intercepts are given by the simple equation :

$$A_i = \bar{y}_i - \bar{x}_i \cdot p_{pooled} \tag{B.8}$$

and their variance by the expression:

$$s^2(A_i) = s^2(E_p)[1/n_i + \bar{x}_i^2/\Sigma_i(\Sigma(x - \bar{x})^2)_i] \tag{B.9}$$

B.2 COMPARISON AND POOLING OF THE"INDIVIDUAL POOLED" SLOPES p_j

The "individual pooled" exponents of $\cos\chi$ for each station, as evaluated by the method described in Section B.1, can now be compared with one another. It is obvious that the procedure described in Section B.1 could also be applied directly to the best regression lines of all months and stations considered together, but the comparison of the "individual pooled" slopes of each station seemed to be more informative.

Thus, we shall illustrate here the procedure for testing whether the pooled exponents of $\cos\chi$ for each station are significantly different from one another.

The comparison between the sum of squares of deviation from the parallel separate lines drawn through the data points of each month with the same slope, i.e. the "over-all pooled" slope, and the sum of the sums of squares of deviation from the "individual pooled" regression lines through each set of data separately provides the variance ratio which is tested by the F test of significance. Here again the condition of independence and uniformity of the variance of estimate from the pooled regression line of each station must be satisfied.

The variance ratio, F, is actually given by

$$F = \frac{\Delta}{\nu_1} \Big/ \frac{\Sigma}{\nu_2} \tag{B.10}$$

where

$$\Delta = [\Sigma(y - \bar{E}_p)^2] - [\Sigma_j \Sigma(y - E_p)^2] \tag{B.11}$$

is the difference between the deviations using the "over-all pooled" slope and using "individual pooled" slopes, and ν_1 its degrees of freedom; and where

$$\Sigma = \Sigma_j \Sigma(y - E_p)^2 \tag{B.12}$$

is the sum of the sums of squares of deviations from the "individual pooled" regression lines drawn through the data of each month separately, and ν_2 its degrees of freedom. j takes the values 1, 2, 3, ..., S; where S is the number of stations.

The total number of sets of data is $\Sigma_j K_j$, where K_j is the number of month-sets, of equal slope, at station j. Writing N_j for the total number of data at the station j, the degrees of freedom associated with the variance about the "over-all pooled" regression are given by

$$\Sigma_j N_j - \Sigma_j K_j - 1 \tag{B.13}$$

i.e. the total number of data $\Sigma_j N_j$, minus the number of intercepts $\Sigma_j K_j$, minus one, as all these regression lines have the same slope. Therefore simple calculations lead to the following expressions for the degrees of freedom ν_1 and ν_2:

$$\nu_1 = \Sigma_j K_j - 1 \tag{B.14}$$

$$\nu_2 = \Sigma_j (N_j - 2K_j) \tag{B.15}$$

If the F value calculated from equation (B.10) does not exceed the tabulated value at the 5 per cent level or at the 1 per cent significance level with ν_1 and ν_2 degrees of freedom, then the difference Δ is not significant; and the regression lines may be drawn with the same "over-all pooled" slope given by the following expression:

$$\bar{p} = \Sigma_j p_j \Sigma_i \Sigma(x - \bar{x})^2 / \Sigma_j \Sigma_i \Sigma(x - \bar{x})^2 \tag{B.16}$$

with $i = 1,2,3,\ldots\ldots,K_j$ and $j = 1,2,3,\ldots\ldots,S$; and where p_j is the pooled slope of station j and $\Sigma(x - \bar{x})^2$ is the sum of squares of deviations of the independent variable ($\log \cos\chi$) of the month i of station j.

The variance of estimate is the ratio of the sum of squares of deviationsfrom separate lines through each set of data drawn with the same slope, "the over-all pooled" slope, to the corresponding degrees of freedom given by (B.13); that is,

$$s^2(\bar{E}_p) = [\Sigma(y - \bar{E}_p)^2] / [\Sigma_j N_j - \Sigma_j K_j - 1] \tag{B.17}$$

The variance of the "over-all pooled" slope is:

$$s^2(\bar{p}) = s^2(\bar{E}_p) / \Sigma_j \Sigma_i \Sigma(x - \bar{x})^2 \tag{B.18}$$

The individual intercept for the month i of station j, is given by

$$A_{ji} = \bar{y}_{ji} - \bar{p}\,\bar{x}_{ji} \qquad (B.19)$$

and its variance by

$$s^2(A_{ji}) = s^2(\bar{E}_p)\,[1/n_{ji} + \bar{x}_{ji}^2/\Sigma_j\Sigma_i\,\Sigma\,(x - \bar{x})^2] \qquad (B.20)$$

where $\bar{y}_{ji}$ and $\bar{x}_{ji}$ are the means of the dependent and independent variable respectively, for the month i of station j, and n_{ji} the corresponding size of the sample.

It should be noted that if the procedure outlined in Section B.1 were applied to the best regression lines of all months and stations considered together, the pooled slope would be given by the same equation (B.16), written in a slightly different form; the same can be said about the variance of the pooled slope and the variance about the pooled slope regression, which therefore would be given by equations (B.18) and (B.17) respectively. The F-ratio would be given by an expression similar to equation (B.1).

APPENDIX C

The f_oE data used in the statistical analysis of the 2nd, 3rd and 4th chapters are taken from 47 world-wide ionospheric stations, which are listed in Table C.1 and illustrated in Fig. C.1. For those stations marked * the period of data indicated in Table C.1 has been used only in the statistical analysis of Chapter 2, since a different period of f_oE data has been used in the statistical analysis of Chapter 3 and 4. Stations marked ** have only been used in the analysis described in the 2nd Chapter.

TABLE C.1

Station	Code	Geog. Lat. θ^o	Geog. Long. λ^o	Geom. Lat. θ^o_G	Geom. Long. λ^o_G	Magn. Lat. θ^o_M	Period of Data
Resolute Bay	RB	74.7	265.1	82.9	289.3	88	1954 - 1964
Tromso	TR	69.7	19.0	67.2	116.8	67	1951 - 1961
Kiruna	KI	67.8	20.4	65.3	115.9	65	1956 - 1967
Oslo	OS	60.0	11.1	60.0	100.2	59	1949 - 1958
Churchill	CH	58.8	265.8	68.7	322.7	78	1954 - 1964
Inverness	IN	57.5	355.7	60.6	83.3	56	1952 - 1962
De Bilt	DB	52.1	5.2	53.8	89.4	50	1951 - 1961
Adak	AD	51.9	183.4	47.3	240.0	45	1954 - 1964
Lindau	LI	51.6	10.1	52.4	93.9	50	1953 - 1963
*Slough	SL	51.5	359.4	54.3	84.1	50	1947 - 1968
Sottens	SO	46.7	6.7	48.3	88.2	45	1954 - 1964
Ottawa	OT	45.4	284.1	56.9	351.3	62	1954 - 1964
Wakkanai	WA	45.4	141.7	35.3	206.0	40	1958 - 1968
Genova	GE	44.6	9.0	45.8	89.6	42	1956 - 1966
Rome	RO	41.9	12.5	42.5	92.0	39	1957 - 1967

TABLE C.1 continued

Station	Code	Geog. Lat. θ^o	Geog. Long. λ^o	Geom. Lat. θ^o_G	Geom. Long. λ^o_G	Magn. Lat. θ^o_M	Period of Data
Akita	AK	39.7	140.1	29.5	205.4	33	1958 - 1968
*Washington	WAS	38.7	282.9	50.1	350.1	56	1947 - 1967
San Francisco	SF	37.4	237.8	43.7	298.4	43	1948 - 1958
*Tokyo	TO	35.7	139.5	25.4	205.4	30	1948 - 1967
Casablanca	CA	33.6	352.4	38.5	69.0	29	1951 - 1958
*White Sands	WS	32.3	253.5	41.0	316.4	41	1948 - 1968
Yamagawa	YA	31.2	130.6	20.3	197.8	25	1958 - 1968
Okinawa	OK	26.3	127.8	15.3	196.0	20	1950 - 1960
**Maui	MA	20.8	203.5	20.8	268.1	23	1948 - 1967
Puerto Rico	PR	18.5	292.8	30.0	2.0	32	1948 - 1958
Baguio	BA	16.4	120.6	5.1	189.3	10	1952 - 1962
Dakar	DA	14.7	342.6	21.8	54.6	9	1952 - 1962
Panama Canal	PC	9.4	280.1	20.6	348.3	21	1951 - 1958
Ibadan	IB	7.4	3.9	10.6	74.6	- 3	1954 - 1964
Singapore	SI	1.3	103.8	-10.0	172.7	- 9	1954 - 1964
Leopoldville	LE	-4.4	15.2	- 3.1	83.5	-18	1952 - 1962
Talara	TA	-4.6	278.7	6.6	347.7	7	1955 - 1965
Huancayo	HU	-12.0	284.7	- 0.6	353.8	1	1958 - 1968
Townsville	TW	-19.3	146.7	-28.5	218.8	-29	1954 - 1964
**Rarotonga	RA	-21.2	200.2	-20.9	273.7	-23	1948 - 1958
Johannesburg	JO	-26.2	28.0	-26.9	91.3	-43	1949 - 1959
Brisbane	BR	-27.5	152.9	-35.8	226.9	-38	1949 - 1959
Watheroo	W T	-30.3	115.9	-41.7	185.8	-47	1948 - 1958
Capetown	CT	-34.1	18.3	-32.9	79.8	-46	1949 - 1959
Canberra	CN	-35.3	149.0	-43.8	223.7	-47	1949 - 1959

TABLE C.1 continued

Station	Code	Geog. Lat. θ^o	Geog. Long. λ^o	Geom. Lat. θ^o_G	Geom. Long. λ^o_G	Magn. Lat. θ^o_M	Period of Data
Conception	CO	-36.6	287.0	-25.3	356.5	-20	1957 - 1966
Hobart	HO	-42.9	147.2	-51.7	224.6	-59	1947 - 1957
Godleyhead	GO	-43.6	172.8	-48.1	252.8	-51	1958 - 1968
*Port Stanley	PS	-51.7	302.2	-40.4	9.0	-27	1948 - 1967
Campbell Is.	CI	-52.5	169.2	-57.4	253.1	-62	1948 - 1958
Port Lockroy	PL	-64.8	296.5	-53.4	3.9	-39	1954 - 1964
Halley Bay	HB	-75.5	333.4	-65.8	24.3	-47	1957 - 1965

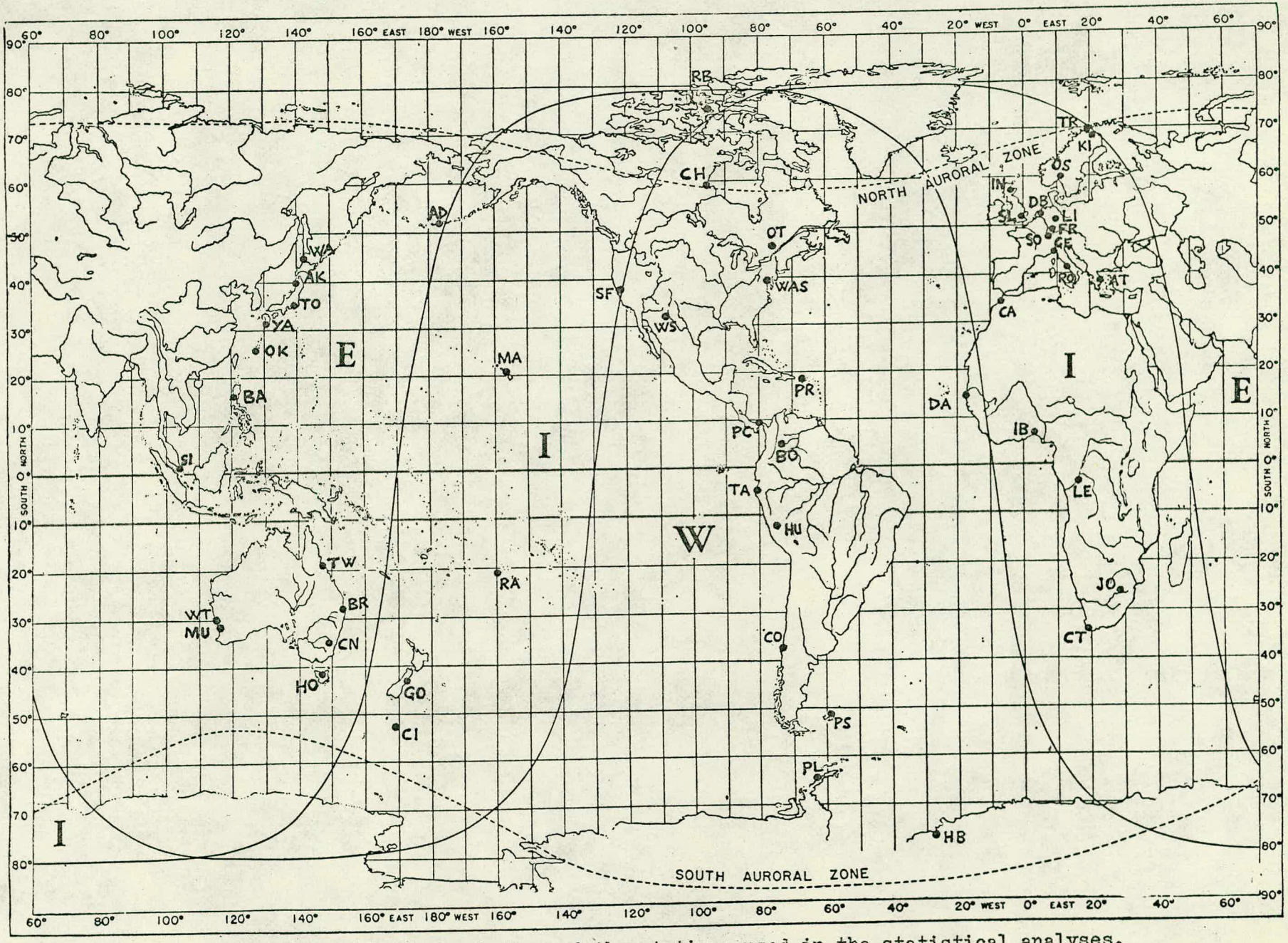

Fig. C.1 Distribution of the stations used in the statistical analyses.

REFERENCES

1. Chapman, S. — Proc. Phys. Soc., 43, 1931, 26.
2. Chapman, S. — Proc. Phys. Soc., 43, 1931, 483.
3. Nicolet, M. — J. Atmos. Terr. Phys., 1, 1951, 141.
4. Appleton, E.V. and Lyon, A.J. — Physics of the Ionosphere, Phys. Soc., 1955, p.20.
5. Appleton, E.V. and Lyon, A.J. — J. Atmos, Terr. Phys., 10, 1957, 1.
6. Robinson, B.J. — Rep. Progr. Phys., 22, 1959, 241.
7. Shimazaki, T. — J. Radio Res. Lab., 4, 1957, 37.
8. Shimazaki, T. — J. Radio Res. Lab., 6, 1959, 107.
9. Beynon, W.J.G. and Brown, G.M. — J. Atmos. Terr. Phys., 14, 1959, 138.
10. Appleton, E.V. and Lyon, A.J. — J. Atmos. Terr. Phys., 21, 1961, 73.
11. Appleton, E.V. — J. Atmos. Terr. Phys., 25, 1963, 577.
12. Landmark, B. — The Ionosphere, in Radio Wave Propagation, AGARD, Lecture series XXIX, 1968.
13. Muggleton, L.M. — J. Atmos. Terr. Phys., 33, 1971, 1291.
14. Harnischmacher, E., — C.R. Acad. Sci., Paris, 230, 1950, 1301.
15. Davies, K. — Ionospheric Radio Propagation, Dover Publications, 1966.
16. Van Zandt, T.E. — The Neutral Atmosphere and the Quiet Ionosphere, in Physics of Geomagnetic Phenomena, Ed. S. Matsushita and W.H. Campbell, Academic Press, Vol. I. 1967.
17. Swenson, G.G. — Proc. I.R.E.E. (Australia), 30, 1969, 1.
18. Ratcliffe, J.A. and Weekes, K. — The Ionosphere, in Physics of the Upper Atmosphere, Ed. J.A. Ratcliffe, Academic Press, 1960.
19. Rishbeth, H. and Garriott, O.K. — Introduction to Ionospheric Physics, Academic Press, 1969.
20. Van Zandt, T.E. and Knecht, R.W. — The Structure and Physics of the Upper Atmosphere, in Space Physics, Ed. D.P. Le Galley and A. Rosen, John Wiley and Sons, 1964.

21. Wilkes, M.V. — Proc. Phys. Soc. B 67, 1954, 304.

22. Muggleton, L.M. — To be published.

23. Horowitz, R.and La Gow, H.E. — J. Geophys. Res.,62, 1957, 57.

24. Robinson, B.J. — J. Atmos. Terr. Phys., 18, 1960, 215.

25. Appleton, E.V. and Piggott, W.R. — J. Atmos. Terr. Phys., 5, 1954, 141.

26. Appleton, E.V. — J. Atmos. Terr. Phys., 26, 1964, 633.

27. Singer, S.F., Maple, E. and Bowen, W.A. — J. Geophys. Res., 56, 1951, 265.

28. Cahill, L.J. — J. Geophys. Res., 64, 1959, 489.

29. Burrows, K. and Hall, S.H. — J. Geophys. Res. 70, 1965, 2149.

30. Maynard, N.C., Cahill, L.J. and Sastry, T.S.G. — J. Geophys. Res., 70, 1965, 1241.

31. Davis, T.N., Stolarik, J.D. and Heppner, J.P. — J. Geophys. Res., 70, 1965, 5883.

32. Maynard, N.C. and Cahill, L.J. — J. Geophys. Res. 70, 1965, 5923.

33. Davis, T.N., Burrows, K. and Stolarik, J.D. — J. Geophys. Res., 72, 1967, 1845.

34. Maynard, N.C. — J. Geophys. Res., 72, 1967, 1863.

35. Cloutier, P.A. and Haymes, R.C. — J. Geophys. Res.,73, 1968, 1771.

36. Sastry, T.S.G. — J. Geophys. Res., 73, 1968, 1789.

37. Shuman, B.M. — J. Geophys. Res., 75, 1970, 3889.

38. Martyn, D.F. — Proc. Roy. Soc. A 189, 1947, 241.

39. Martyn, D.F. — Proc. Roy. Soc. A 190, 1947, 273.

40. Martyn, D.F. — Proc. Roy. Soc. A 194, 1948, 429.

41. Martyn, D.F. — Proc. Roy. Soc. A 194, 1948, 445.

42. Fejer, J.A. — J. Atmos. Terr. Phys., 4, 1953, 184.

43. Duncan, R.A. — J. Atmos. Terr. Phys., 18, 1960, 89.

44. Maeda, K.and Kato, S. — Space Sci. Rev., 5, 1966, 57.

45. Rishbeth, H. — Nature, 226, 1970, 1099.

46. Fejer, J.A. — Motions of Ionization, in Physics of the Earth's Upper Atmosphere, Ed. C.O. Hines et al., Prentice-Hall, Inc., 1965.

47. Appleton, E.V. — Proc. Mixed Comm. on the Ionosphere, 4th Meeting, 1955, p.14.

48. Appleton, E.V., Lyon, A.J. and Turnbull, A.G. — Nature, 176, 1955, 897.

49. Appleton, E.V., Lyon, A.J. and Pritchard, A.G. — J. Atmos. Terr. Phys., 7, 1955, 292.

50. Beynon, W.J.G. and Brown, G.M. — Nature, 177, 1956, 583.

51. Beynon, W.J.G. — J. Atmos. Terr. Phys., 15, 1959, 13.

52. Shimazaki, T. — J. Radio Res. Lab., 5, 1958, 35.

53. Shimazaki, T. — J. Atmos. Terr. Phys., 15, 1959, 77.

54. Shimazaki, T. — J. Radio Res. Lab., 7, 1960, 95.

55. Hibberd, F.H. and Henderson, T.L.E. — J. Atmos. Terr. Phys., 29, 1967, 477.

56. Brown, G.M., Beynon, W.J.G. and Morgan, A.D. — Proc. Intern. Conf. Ionosphere; the Institute of Physics and the Physical Society; 1963, p.177.

57. Brown, G.M. and Wynne, R. — J. Atmos. Terr. Phys., 29, 1967, 1595.

58. Kirkpatrick, C.B. — Austr. J. Sci. Res., A1, 1948, 423.

59. Rastogi, R.G. — Geofis. Pur. Appl., 40, 1958, 145.

60. Beynon, W.J.G. and Brown, G.M. — J. Atmos. Terr. Phys., 15, 1959, 168.

61. Rao, M.K. and Malhotra, P.L. — J. Inst. Telecom. Engrs., (India), 12, 1966, 577.

62. Appleton, E.V. — Proc. Inst. Radio Engrs. 47, 1959, 155.

63. Muggleton, L.M. — J. Atmos. Terr. Phys., 33, 1971, 1307.

64. Allen, C.W. — Terrest. Magn. Atmos. Elect., 51, 1946, 1.

65. Allen, C.W. — Terrest. Magn. Atmos. Elect., 53, 1948, 433.

66. Schwentek, H. — Zeitschrift für Geophysik, 34, 1968, 123.

67. Waldmeier, M. — Helv. Phys. Acta, 17, 1944, 168.

68. Tremellen, K.W. and Cox, J.W. — J. Inst. Elect. Engrs., 94, 1947, 200.

69. Scott, J.C.W. — J. Geophys. Res., 57, 1952, 369.

70. Saha, A.K. — Indian J. Phys., 27, 1953, 431.

71. Noonkester, V.R. — J. Atmos. Terr. Phys., 26, 1964, 965.

72. Denisse, J.F. and Kundu, M.R. — C.R. Acad. Sci., Paris, 244, 1957, 45.

73. Kundu, M.R. and Denisse, J.F. — J. Atmos. Terr. Phys., 13, 1958, 176.

74. Minnis, C.M. and Bazzard, G.H. — Nature, 181, 1958, 1796.

75. Eyfrig, R. — Nature, 196, 1962, 758.

76. Smith, P.A. — J. Atmos. Terr. Phys., 30, 1968, 177.

77. Appleton, E.V. and Beynon, W.J.G. — Intern. Dictionary of Geophysics, Ed. S.K. Runcorn, Pergamon Press, 1967, p. 276.

78. Covington, A.E. — J. Roy. Astron. Soc., Canada, 63, 1969, 125.

79. Volk, W. — Applied Statistics for Engineers, McGraw-Hill, Inc. N.Y., 1958.

80. Weatherburn, C.E. — Mathematical Statistics, Cambridge Univ. Press, 1952.

81. Brookes, B.C. and Dick, W.F.L. — Introduction to Statistical Method, Heinemann, London, 1966.

82. Ionospheric Data, — C.R.P.L. - Series F, Part A; National Bureau of Standards, Boulder, Colorado.

83. Ionospheric Data, — R.S.R.S., Slough, England, U.K.

84. Waldmeier, M. — The Sunspot-Activity in the years 1610 - 1960, Zürich Schulthess and Co., 1961.

85. Quarterly Bulletin on Solar Activity, — International Astronomical Union, (ed. M. Waldmeier), Schulthess and Co., Zürich.

86. Appleton, E.V. and Piggott, W.R. — The Physics of the Ionosphere, Physical Society, 1955, p. 219.

87. Snedecor, G.W. — Statistical Methods, 3rd ed., Iowa State College Press, 1940.

88. Appleton, E.V. and Naismith, R. — Proc. Phys. Soc., 52, 1940, 402.

89. Muggleton, L.M. J. Atmos. Terr. Phys., 31, 1969, 1413.

90. Muggleton, L.M. Telecommunication Journal, 38, 1971, 646.

91. Solar Geophysical Data - Descriptive Text, Feb. 1971.

92. Minnis, C.M. Advances in Radio Research, Ed. J.A. Saxton, Academic Press, Vol. 2, 1964, p.1.

93. Friedman, H. Progress in Radio Science 1960-63, Ed. G.M. Brown, Elsevier Co., Vol. III, 1965, p. 167.

94. Whitten, R.C. and Poppoff, I.G. Physics of the Lower Ionosphere; Prentice-Hall, Inc., 1965.

95. Nicolet, M. International Dictionary of Geophysics, Ed. S.K. Runcorn, Pergamon Press, 1967, p. 281.

96. Friedman, H. Proc. Intern. Conf. Ionosphere, The Institute of Physics and the Physical Society, 1963, p.3 and p.94.

97. Covington, A.E. Proc. Inst. Radio Engrs. N.Y,, 36, 1948, 454.

98. Minnis, C.M. and Bazzard, G.H. J. Atmos. Terr. Phys., 18, 1960, 297.

99. Kiepenheuer, K.O. Solar Activity, in the Sun, Ed. G.P. Kuiper, Univ. of Chicago Press, 1953, p.323.

100. Medd, W.J. and Covington, A.E. Proc. Inst. Radio Engrs. N.Y., 46, 1958, 112.

101. Bennington, T.W. Wireless World, 64, 1958, 472.

102. Gladden, S.C. NBS Report 8734, Boulder, Colorado, 1965.

103. Minnis, C.M. and Bazzard, G.H. J. Atmos. Terr. Phys., 14, 1959, 213.

104. Barclay, L.W. J. Atmos. Terr. Phys., 24, 1962, 547.

105. Joachim, M. Nature, 210, 1966, 289.

106. Muggleton, L.M. and Kouris, S.S. Radio Science, 3, 1968, 1109.

107. Appleton, E.V. and Naismith, R. Phil. Mag., 27, 1939, 144.

108. Mitra, S.K. The Upper Atmosphere, R. Asiatic Soc. of Bengal, 1948.

109. Rawer, K. — The Ionosphere, Frederick Ungar Publishing Co., N.Y., 1956.

110. Shibata, H. and Watanabe, S. — J. Radio Res. Lab., 7, 1960, 621.

111. Naismith, R., Bevan, H.C. and Smith, P.A. — J. Atmos. Terr. Phys., 21, 1961, 167.

112. Naismith, R. and Smith, P.A. — J. Atmos. Terr. Phys., 22, 1961, 270.

113. Minnis, C.M. — J. Atmos. Terr. Phys., 12, 1958, 266.

114. Minnis, C.M. — The Observatory, 77, 1957, 94.

115. Allen, C.W. — The Observatory, 77, 1957, 98.

116. Minnis, C.M. — J. Atmos. Terr. Phys., 12, 1958, 272.

117. Das Gupta, M.K. and Basu, D. — J. Atmos. Terr. Phys., 26, 1964, 135.

118. Appleton, E.V. — Nature, 197, 1963, 1239.

119. Friedman, H. — Astronautics, 8, 1962, 14.

120. Watanabe, K. and Hinteregger, H.E. — J. Geophys. Res., 67, 1962, 999.

121. Bourdeau, R.E., Aikin, A.C. and Donley, J.L. — J. Geophys. Res., 71, 1966, 727.

122. Norton, R.B., Van Zandt, T.E. and Denison, J.S. — Proc. Intern. Conf. Ionosphere, The Institute of Physics and the Physical Society, 1963, p.26.

123. Smith, L.G., Accardo, C.A., Weeks, L.H. and McKinnon, P.J. — J. Atmos. Terr. Phys., 27, 1965, 803.

124. Sengupta, P.R. — J. Atmos. Terr. Phys., 32, 1970, 1273.

125. Bomke, H.A., Blake, H.A., Harris, A.K. and Sheppard, D.J. — J. Geophys. Res. 75, 1970, 6980.

126. Minnis, C.M. and Bazzard, G.H. — J. Atmos. Terr. Phys., 18, 1960, 306.

127. Beynon, W.J.G. and Brown, G.M. — J. Atmos. Terr. Phys., 11, 1957, 128.

128. Minnis, C.M. — J. Atmos. Terr. Phys., 7, 1955, 310.

129. URSI, — Ionospheric Stations Manual, Edited by E.Herbays, W.J.G. Beynon, G.M. Brown, 1958.

130. Bibl, K. — Ann. Géophys., 7, 1951, 208.

131. URSI , Ionospheric Stations Manual Supplement, Edited by G.M. Brown, 1964.

132. Lindley, D.V. Probability and Statistics, Part 2, Cambridge Univ. Press, 1965.

133. Menzel, D.H. and Wolbach, J.G. Scientific Report No. 19, Harvard Univ., 1954.

134. Menzel, D.H. and Wolbach, J.G. Proc. Mixed Comm. on Ionosphere, Fourth Meeting, 1955, p.27.

135. Eyfrig, R. Geofis. Pur. Appl., 45, 1960, 179.

136. Piggott, W.R. and Thrane, E.V. J. Atmos. Terr. Phys., 28, 1966, 467.

137. Menzel, D.H., Wolbach, J.G. and Glazer, H. J. Atmos. Terr. Phys., Special Suppl., 6, 1956, 282.

138. Haubert, A. Mixed Comm. on the Ionosphere, New York Meeting, 1957.

139. Shimazaki, T. J. Atmos. Terr. Phys., 25, 1963, 331.

140. Bellchambers, W.H. and Piggott, W.R. Proc. Roy. Soc., A 256, 1960, 200.

141. Belrose, J.S. The lower ionospheric regions, in Physics of the Earth's Upper Atmosphere, Ed. Hines et al., Prentice-Hall, Inc., 1965.

142. Grace, C.H. J. Geophys. Res., 56, 1951, 452.

143. Matsushita, S. and Maeda, H. J. Geophys. Res., 70, 1965, 2535.

144. Matsushita, S. Solar quiet and lunar daily variation fields, in Physics of Geomagnetic Phenomena, Ed. S. Matsushita and W.H. Campbell, Academic Press, 1967.

145. Matsushita, S. J. Atmos. Terr. Phys., 27, 1965, 1317.

146. Molina, F. and Battelli, O. Atti Convegno Annu. Assoc. Geofis. Ital., 1960, p. 85.

147. Fatkullin, M.N. and Fel'dshteyn, Ya.I. Geomagn. and Aeronomy, 5, 1965, 667.

148. Hutton, R. J. Atmos. Terr. Phys., 29, 1967, 1411.

149. Appleton, E.V. J. Atmos. Terr. Phys., 15, 1959, 9.

150. Shimazaki, T. Nature, 205, 1965, 889.

151. Muggleton, L.M. J. Atmos. Terr. Phys., 33, 1971, 1299.

152. Bishoff, K. — Geomagn. and Aeronomy, 4, 1964, 739.

153. Minnis, C.M. — Nature, 202, 1964, 170.

154. Chapman, S. and Bartels, J. — Geomagnetism, Oxford Univ. Press, 1940.

155. Chapman, S. — Nuovo Cimento, 4, Supplemento, 1956, 1385.

156. Vestine, E.H. — The Upper Atmosphere and Geomagnetism, in Physics of the Upper Atmosphere, Ed. J.A. Ratcliffe, Academic Press, 1960.

157. Onwumechilli, A. — Geomagnetic Variations in the Equatorial Zone, in Physics of Geomagnetic Phenomena, Ed. S. Matsushita and W.H. Campbell, Academic Press, Vol. I, 1967.

158. Hasegawa, M. — J.Geophys.Res., 65, 1960, 1437.

159. Van Sabben, D. — J. Atmos. Terr. Phys., 26, 1964, 1187.

160. Jones, W.B., Graham, R.P. and Leftin, M. — NBS, Technical Note No. 337, Boulder, Colorado, 1966.

ACKNOWLEDGEMENTS

I am indebted to my supervisors Professor W.E.J. Farvis and Dr. L.M. Muggleton for their constant guidance throughout this work.

I would like to thank the University of Edinburgh for the financial support during the entire period of study.

I am grateful to all who helped me in the realization of this work and, in particular, to my parents.